NEW LIGANDS FOR EARLY METAL ACTIVATION OF MOLECULAR NITROGEN

by

GABRIEL MÉNARD

B.Sc., University of Ottawa, 2006

A thesis submitted in partial fulfillment of
the requirements for the degree of

MASTER OF SCIENCE

in

THE FACULTY OF GRADUATE STUDIES

(CHEMISTRY)

THE UNIVERSITY OF BRITISH COLUMBIA

May 2008

ABSTRACT

The synthesis of two new proligands for early metal activation of dinitrogen is reported. The new diamidophosphine $[NPN]^SH_2$ ($[NPN]^SH_2$ = {*N*-(2,4,6-$Me_3C_6H_2$)(3-NH-SC_4H_2)}$_2$PPh) proligand features a bridging thiophene ring between the phosphine and amide donors and was synthesized as a variation to other recent aryl bridged NPN ligands. The potentially dianionic linear-linked aryloxide proligand $[OOO]H_2$ ($[OOO]H_2$ = 2,6-bis(3-adamantyl-5-*t*-butyl-2-hydroxybenzyl)-4-*t*-butylanisole) was also synthesized as a variation to other similar known compounds.

The precursor to the proligand $[NPN]^SH_2$ was successfully synthesized by a high yielding *N*-aryl amination reaction. The second step in the synthesis produces the $[NPN]^SH_2$ compound; however, the product has an unexpected regiochemistry. Detailed mechanistic investigations suggest a possible mechanism involving competitive lithium-halogen and deprotonation reactions.

Zr and Ti complexes of the [OOO] ligand could not be synthesized; however, a new "half-on" $[OOO(H)]TaCl_4$ complex was synthesized and features a pendant phenol with the ligand locked in an S-conformation. Attempts to "close" this ligand to the U-conformation and form the desired $[OOO]TaCl_3$ complex have thus far failed. In contrast, Zr complexes of the $[NPN]^S$ ligand could be readily synthesized and were fully characterized. These include: $[NPN]^SZr(NMe_2)_2$, $[NPN]^SZrCl_2$ and $[NPN]^SZrI_2$. Attempts to reduce $[NPN]^SZrCl_2$ to form a dinitrogen complex have thus far failed; however, reduction of $[NPN]^SZrI_2$ in Et_2O using KC_8 as reducing agent shows promising signs of a dinitrogen complex similar to a previously reported case in our laboratory.

TABLE OF CONTENTS

CHAPTER 2: Ligand Design and Synthesis for Early Metal Complexes

CHAPTER 3: Synthesis of Group 4 or 5 $[NPN]^S$ or [OOO] Complexes for the Activation of Dinitrogen

CHAPTER 4: Thesis Summary and Future Work

APPENDIX: X-ray Crystal Structure Data and Analysis

LIST OF TABLES

LIST OF FIGURES

GLOSSARY

The following abbreviations, most of which are commonly found in the literature, were used in this thesis. Symbols are shown at the end.

Ad	adamantyl
Anal.	analysis
Ar	aryl group or Argon
atm	atmosphere
9-BBN	9-borabicyclo[3.3.1]nonane
^{t}Boc	*tert*-butoxycarbonyl
b.p.	boiling point
bs	broad singlet
^{n}Bu	normal butyl group ($-CH_2CH_2CH_2CH_3$)
^{t}Bu	tertiary butyl group ($-C(CH_3)_3$)
ca.	approximately
Calcd.	calculated
CN	coordination number
Cp	cyclopentadienyl group ($[C_5H_5]^-$)
Cp*	pentamethylcyclopentadienyl group ($[C_5Me_5]^-$)
d	doublet
D	deuterium
DCM	dichloromethane
dppp	1,3-bis(diphenylphosphino)propane
EA	elemental analysis
EI-MS	electron impact-mass spectrometry
Et	ethyl group ($-CH_2CH_3$)
Et_2O	diethyl ether

FW	formula weight
g	gram(s)
GC-MS	gas chromatography-mass spectrometry
gof	goodness of fit
h	hour(s)
^{1}H	proton
$\{^{1}H\}$	proton decoupled
HIPT	hexa-iso-propyl-terphenyl
HMBC	heteronuclear multiple bond correlation
HMQC	heteronuclear multiple quantum correlation
HOMO	highest occupied molecular orbital
Hz	Hertz
$^{n}J_{A\text{-}B}$	n-bond scalar coupling constant between nuclei A and B
K	Kelvin
kJ	kilojoules
L	neutral two-electron donor
LUMO	lowest unoccupied molecular orbital
LutH	2,6-lutidinium
m	multiplet
m-	*meta* position of aryl ring
M	metal (or molar if referring to concentration)
M^{+}	parent ion
MALDI-TOF	matrix assisted laser desorption/ionization – time-of-flight
Me	methyl group ($-CH_3$)
m/e	mass/charge (mass spectrometry unit)
Mes or mesityl	2,4,6-trimethylphenyl
MHz	megahertz
mol	mole(s)

Mt	megatonne (10^9 kg)
MW	molecular weight
NMR	nuclear magnetic resonance
NO_x	nitrogen oxides
[NPN]	$[PhP(CH_2SiMe_2NPh)_2]^{2-}$ unless referring to the family of NPN ligands
[NPN]'	$[\{N\text{-}(2,4,6\text{-}Me_3C_6H_2)(2\text{-}N\text{-}C_6H_4)\}_2PPh]^{2-}$
$[NPN]^*$	$[\{N\text{-}(2,4,6\text{-}Me_3C_6H_2)(2\text{-}N\text{-}5\text{-}MeC_6H_3)\}_2PPh]^{2-}$
$[NPN]^S$	$[\{N\text{-}(2,4,6\text{-}Me_3C_6H_2)(3\text{-}N\text{-}SC_4H_2)\}_2PPh]^{2-}$
o-	*ortho* position of aryl ring
OBu	butoxide
ORTEP	Oakridge thermal ellipsoid plotting program
OTs	tosylate (*para*-toluenesulfonate)
p-	*para* position of aryl ring
Ph	phenyl ring ($-C_6H_5$)
pH	negative logarithm of the proton concentration ($-\log [H^+]$)
pK_a	negative logarithm of the acidity constant ($-\log K_a$)
$^R[PNP]$	$[N(SiMe_2CH_2PR_2)_2]^-$, R = Me, ^{i}Pr, ^{t}Bu, Ph
$[P_2N_2]$	$[PhP(CH_2SiMe_2NSiMe_2CH_2)_2PPh]^{2-}$
ppm	parts per million
ppmv	parts per million by volume
^{i}Pr	isopropyl group ($-CH(CH_3)_2$)
Py	pyridine
R	alkyl or aryl group
reflns	reflections
Rf	retention factor
rt	room temperature
s	singlet

SIPr	*N,N'*-bis(2,6-diisopropylphenyl)4,5-dihydroimidazol-2-ylidene
SO_x	sulfur oxides
t	triplet
T	temperature
THF	tetrahydrofuran
THT	tetrahydrothiophene
TLC	thin layer chromatography
TMS	trimethylsilyl group ($-Si(CH_3)_3$)
tol	tolyl group ($-C_6H_4CH_3$)
V	unit cell volume
X	halide substituent, unless specified otherwise
yr	year
Z	number of formula units in the unit cell
Å	Angström
δ	chemical shift in ppm
Δ	heat
η^n	hapticity of order n
λ	wavelength
μ	bridging
ρ_{calc}	calculated density

ACKNOWLEDGEMENTS

First and foremost, I would like to thank my supervisor Professor Michael Fryzuk for all of his support, guidance and, most importantly, patience. Thanks Mike for always keeping your door open and always answering my questions, even at the busiest of times. Thanks also for allowing me to freely explore chemistry, even when it did not necessarily involve dinitrogen.

I am extremely grateful to the members of the Fryzuk group for creating such a pleasant environment to work in. A very special thanks goes to Dr. Maria João Ferreira. I could not possibly have done this without your endless encouragement, guidance, patience and help MJ. You are both a superb chemist and an excellent friend. Special thanks also to Howie Jong for being my crystal man. Thanks so much for the countless hours you spent playing around with my crystals. Thanks also to Kyle Parker for being a terrific friend both in and out of the lab. I shall definitely miss our countless nights out and our gossip-ridden coffee times. Many thanks to past and present members Bryan Shaw, Rosa Park, Fiona Hess, Nathan Halcovitch, Dr. Owen Summerscales, Dr. Jörg Schachner, Dr. Jörg Sundermeyer and Dr. Yasuhiro Ohki.

A very special thanks goes to all my great friends in Vancouver. I am too afraid to miss anyone, so you all know who you are. I could not possibly have had such a great time here without you. You'll always be welcome to visit wherever I end up.

I am deeply indebted to UBC Chemistry's terrific support staff. A very special thanks to Ken Love and the mechanical shop for their excellent help in dealing with every problem imaginable in the lab. I am also very grateful to the NMR team Dr. Nick Burlinson, Dr. Maria Ezhova and Zorana Danilovic for their friendly help with the

instruments. I also appreciate the help of Marshall Lapawa (MS), David Wong (EA) and Brian Ditchburn (glassblower). I would also like to thank Dr. Subramanian Iyer for being a great supervisor for the inorganic undergraduate labs.

Finally, I would like to thank my dearest mother for always being there as well as my family, Zach, Anik, Josée, and my in-laws for their constant encouragement and support with my academic endeavours. Thank you also for bringing me my two favourite babies, Liam and Zoë. Finally, I would like to thank my most special friend, Joey, for her unwavering friendship, constant support, guidance, encouragement, and most of all, understanding. Tu m'es très chère.

STATEMENT OF CO-AUTHORSHIP

This thesis was written by Gabriel Ménard under the supervision of Professor Michael D. Fryzuk. All research was performed by Gabriel Ménard. All X-ray crystal structures were processed and solved by Howie Jong.

CHAPTER 1

Dinitrogen Activation and Ligand Design

1.1 Dinitrogen, the Haber-Bosch Process and the Environment

Nitrogen, sulfur and carbon are three of the main elements on the planet that are involved in biogeochemical cycles. Since the dawn of the industrial revolution, humans have been able to significantly alter the natural patterns of these cycles. In the 1970s and 1980s, attention was specifically placed on the nitrogen and sulfur cycles due to the increased occurrence of acid rain caused by rising emissions in the oxides of these elements (commonly referred to as NO_x and SO_x gases, respectively).[1] Both NO_x and SO_x gases are by-products of fossil fuel combustion, with SO_x also emanating from the metal smelting industry. Various international protocols such as the *1985 Helsinki Protocol* and the *1994 Oslo Protocol* have contributed significantly to reducing SO_x emissions, whereas current efforts are also putting the focus on NO_x reduction strategies.[2]

Presently, carbon and its cycle are being widely investigated with the advent of global warming leading to climate change. Since carbon dioxide (CO_2) levels never exceeded 300 ppmv (parts per million by volume) in the 650,000 years preceding the industrial revolution,[3] our present atmospheric concentration of approximately 384 ppmv[4] as well as ever increasing carbon emissions are likely to cause perturbations in global temperature and climate. Being a strong greenhouse gas, CO_2 levels significantly contribute to global warming and climate change; however, its impacts will not be discussed here but can be consulted elsewhere.[5]

References begin on p.20

It is interesting to note that humans have actually had a much more significant impact on the amount of nitrogen compounds released in the atmosphere with respect to its natural cycle than in the sulfur and carbon cycles. In fact, while sulfur and carbon levels have gone up 25% and 30% respectively above preindustrial levels, reactive nitrogen levels have approximately doubled.[6] Reactive nitrogen species include NO, NO_2, NH_3 and N_2O and are formed as a result of the chemical transformation of dinitrogen (N_2), a process commonly referred to as fixation. A recent study estimated that without anthropogenic interference, approximately 130-135 Mt N yr^{-1} is fixed (1 Mt = 10^9 kg).[7] The vast majority of this fixation occurs in some bacteria which contain the nitrogenase enzyme capable of transforming N_2 to ammonia (NH_3).[8] In contrast, the same study showed that anthropogenic N_2 fixation is estimated to be approximately 156 Mt N yr^{-1}.

While the combustion of fossil fuels releases NO_x gases as a by-product and thus contributes to the overall anthropogenic N_2 fixation, the Haber-Bosch process contributes far more consuming 98 Mt N yr^{-1} in the mid-1990s alone.[9] This process, developed by Fritz Haber and Carl Bosch, involves reacting N_2 with dihydrogen (H_2) on a metal surface catalyst, usually iron or ruthenium, at high temperatures and pressures (Equation 1.1).[10] To this date, the Haber-Bosch process is the only industrial process to synthesize ammonia in large quantities.

$$N_2\,(g) + 3\,H_2\,(g) \xrightarrow[\substack{400 - 550\ ^\circ C \\ 100 - 300\ atm}]{\text{metal catalyst}} 2\,NH_3\,(g)$$

Equation 1.1

Although this reaction is favourable under ambient conditions, high pressures and temperatures are needed to yield modest reaction rates in order to make this process

References begin on p.20

industrially viable. The process also consumes large quantities of natural gas since the hydrogen needed is obtained through steam reforming, also done at very high temperatures (ca. 1000°C). Given the extreme temperatures and pressure (for ammonia) used in these reactions, it is of little surprise that the overall process is very energy intensive. Since 5% of all natural gas in the mid-1990s was used to make ammonia in the world, and since 25% of energy production worldwide was supplied by natural gas, the Haber-Bosch process is said to consume approximately 1.3% of the total global annual energy output.[9] Altogether, the environmental impacts of the process produce approximately 0.7 tonnes of carbon, in the form of CO_2, for every tonne of ammonia produced. This number rises to one tonne of carbon per tonne of ammonia if poorer fuels such as oil or coal are used to power the plant. In 1996, this total amounted to approximately 1% of total global industrial carbon output.[9]

Considering the rising global population coupled with the need for food and the apparent need for nitrogen fertilizers to sustain current agricultural practices, the Haber-Bosch process is essential in today's world. However, growing concerns over the state of the environment and the pressing need to mitigate the release of climate changing greenhouse gases require us to investigate alternatives to the Haber-Bosch process for ammonia synthesis. Recent advances in the organometallic chemistry of dinitrogen activation, described below, may well pave the way for these new alternatives.

1.2 Dinitrogen as a Ligand

Molecular nitrogen is an extremely stable molecule. Nitrogen fixation (or "activation") involves the chemical transformation of N_2, with its bond length of 1.0975Å,[11] into a different and typically more reactive unit. The process of activating N_2

References begin on p.20

involves changing its structure and bonding. This is typically done by coordinating the molecule onto a highly reduced metal complex, which then serves to add electrons to the π^* orbital of N_2, thus changing its bond order. Reaction of this activated N_2 with various substrates can then serve to change its overall structure.[12,13,14] Typical bonding modes of activated dinitrogen are shown in Table 1.1.

Table 1.1. Typical bonding modes for N_2 in mononuclear and dinuclear complexes.

Coordination Mode	Weak Activation	Strong Activation
End-on mononuclear	M—N≡N	
End-on dinuclear	M—N≡N—M	M=N—N=M
Side-on dinuclear	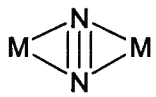	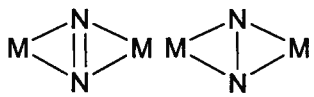
End-on-side-on dinuclear		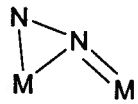

The extreme stability of dinitrogen renders it difficult to activate. Not only does N_2 have no dipole moment, a strong triple bond (945 kJ mol^{-1}) and a large HOMO-LUMO gap, but it is also a poor σ-bond donor and a weak π-acceptor.[15] Thus, N_2 is only activated by a relatively small window of inorganic complexes. Although the enzyme nitrogenase activates N_2 at ambient temperature and pressure using ATP as its energy source, conventional industrial or laboratory conditions for activating N_2 typically require much harsher conditions such as high temperatures and pressures, as described for the Haber-Bosch process above, or the use of strong reducing agents such as Na, K, or Mg.

References begin on p.20

1.3 Short History of Dinitrogen Activation

1.3.1 Dinitrogen–Metal Complexes

The first dinitrogen-metal complex isolated and characterized was $[Ru(NH_3)_5(N_2)]^{2+}$ (**1**) reported in 1965.[16] The coordination mode in this complex is that of end-on mononuclear (Table 1.1). Since then, transition metal complexes of N_2 have been synthesized for nearly every metal.[17] Of these, end-on bonding is the most common type and remains that way to this day. In 1988, the first clear example of the previously speculated[18] side-on bonding mode emerged.[19] The synthesized complex was the side-on Sm_2-N_2 complex (**2**) and was crystallographically characterized. Since this new discovery, the field of N_2 activation has undergone a resurgence.[20]

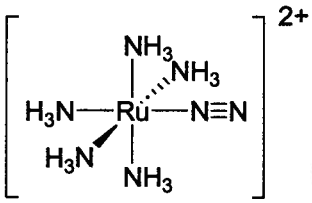

1

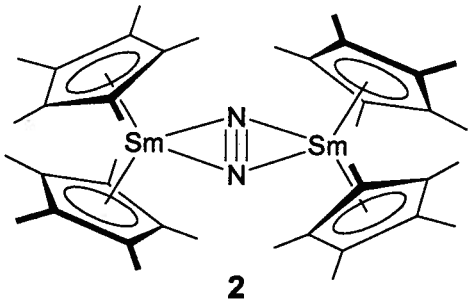

2

Although **2** represents the first unequivocal bimetallic example of a planar side-on metal-N_2 complex, the N-N bond distance was reported to be 1.088(12)Å,[19] thus slightly shorter than the 1.0975Å of free N_2.[11] This is therefore an example of a weak side-on activation of N_2 as shown in Table 1.1. The first strongly activated side-on N_2 complex was reported by the Fryzuk group in 1990.[21] This Zr_2-N_2 complex was formed via reduction of $ZrCl_3[N(SiMe_2CH_2P^iPr_2)_2]$ under an atmosphere of N_2 using two equivalents of Na/Hg amalgam (Scheme 1.1).

References begin on p.20

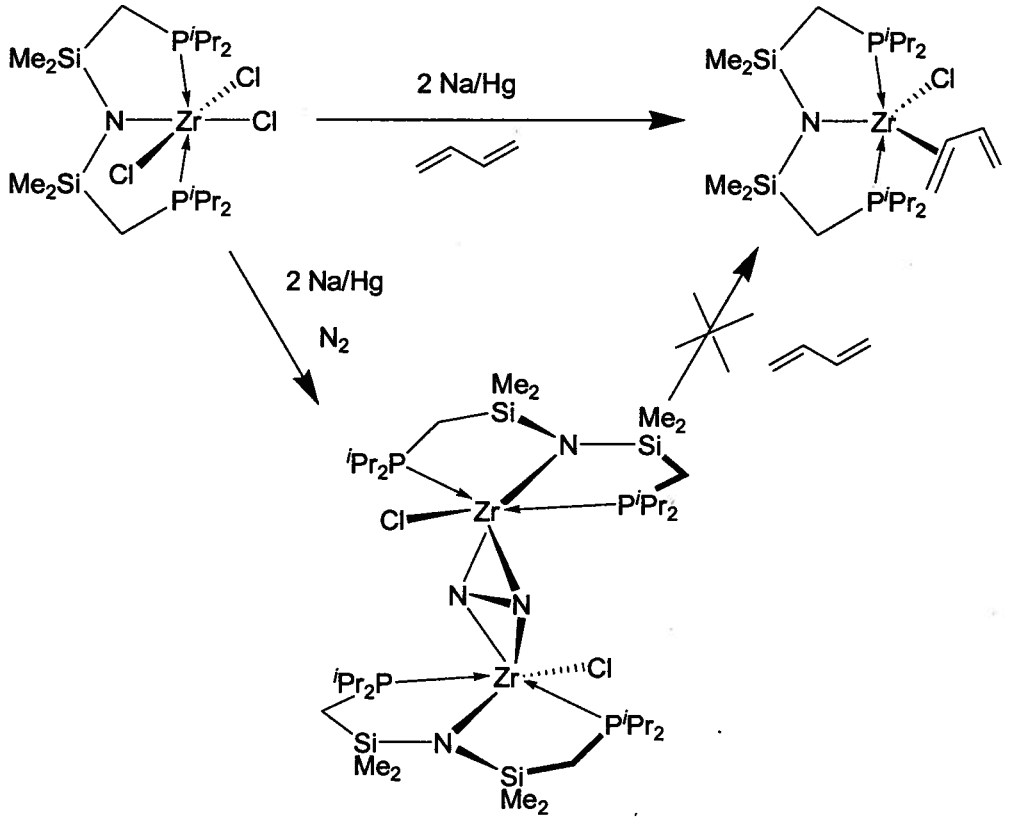

Scheme 1.1

Contrary to the reduction of the starting material in the presence of 1,3-butadiene, the N_2 complex does not add the diene. Thus, the Zr_2-N_2 complex irreversibly binds N_2 unlike the Sm_2-N_2 complex shown above. As a result, the Zr centres were each assigned +4 oxidation states with the N_2 moiety designated a hydrazido or N_2^{4-} unit. This was until recently[22] the longest N-N bond distance ever recorded of 1.548(7)Å.[21] Since the discovery of side-on N_2 complexes, many more examples have been published.[23,24,25,26]

In 1998, a new bonding mode for N_2 was discovered. A Ta_2-N_2 complex was formed in which the N_2 unit was bound in both an end-on and a side-on fashion (Table 1.1).[27] The complex was synthesized, as shown in Scheme 1.2, starting from [NPN]$TaMe_3$ (where [NPN] = $PhP(CH_2SiMe_2NPh)_2^{2-}$) which upon hydrogenation yields the bridging hydride species $([NPN]Ta)_2(\mu\text{-}H)_4$. In the presence of a mixed N_2:H_2 (9:1)

References begin on p.20

atmosphere, this compound spontaneously reduced N_2 with concomitant reductive elimination of H_2 to produce the ([NPN]Ta(μ-H))$_2$(μ-η^1:η^2-N_2). The N_2 bond length in this complex was established to be 1.319(4)Å and the Ta centres were assigned formal oxidation states of +5. The N_2 moiety was established to be the highly activated hydrazido (N_2^{4-}) unit.[27]

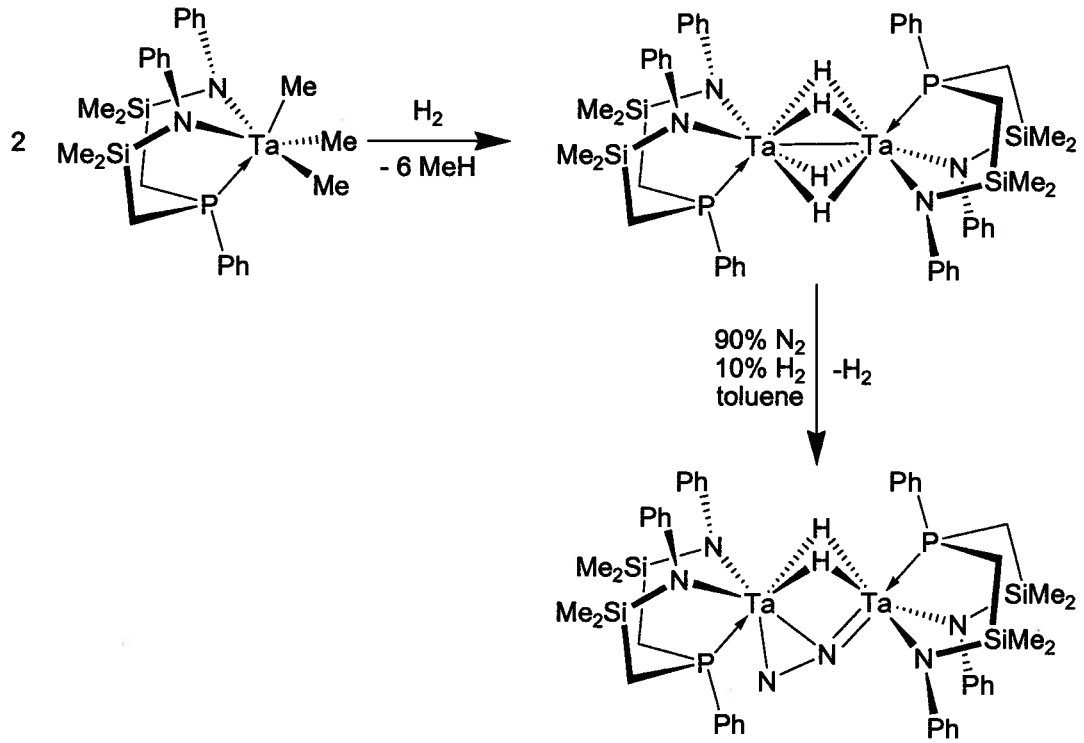

Scheme 1.2

Although N_2 activation can lead to coordinated and lengthened N-N units, highly activated forms lead to N_2 bond scission. The first such clear example to occur homogeneously at a metal centre was reported in 1995 by the Cummins group.[28] The Mo(III) species, Mo(NRAr)$_3$ (where R = C(CD$_3$)$_2$CH$_3$ and Ar = 3,5-C$_6$H$_3$Me$_2$), spontaneously reduces and cleaves N_2 to form the Mo(VI) nitride species NMo(NRAr)$_3$ (Scheme 1.3).

References begin on p.20

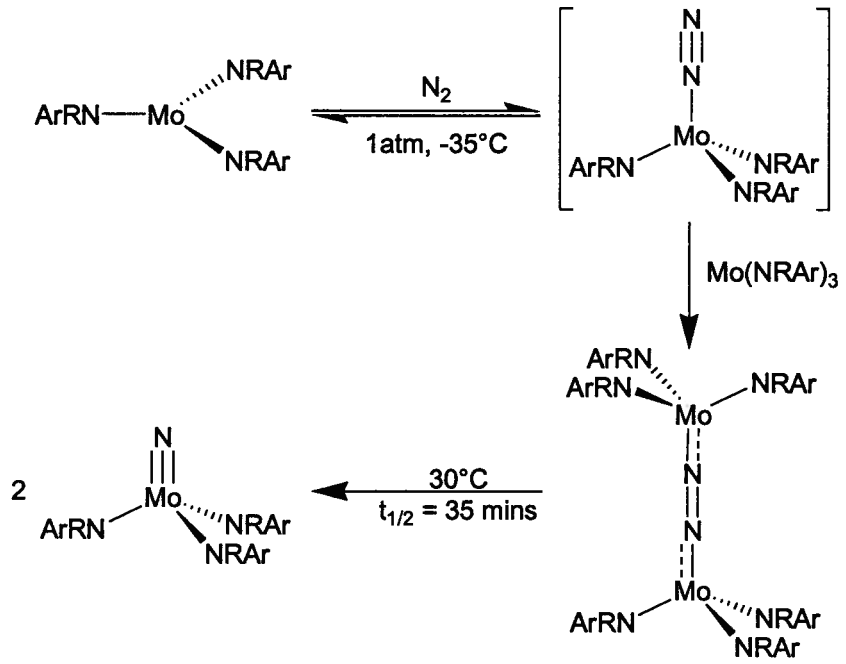

Scheme 1.3

Spectroscopic evidence suggests that the intermediate species is likely the end-on ($[ArRN]_3Mo)_2(\mu\text{-}\eta^1\text{:}\eta^1\text{-}N_2)$ species as shown in Scheme 1.3. This dinuclear intermediate was shown by NMR spectroscopy to follow first order kinetics at 30°C in its dissociation by N-N bond cleavage to the monomeric Mo-nitride product.

1.3.2 Reactivity at the Dinitrogen Centre Leading to NH_3

One of the major goals in N_2 activation chemistry is the addition of H_2 to a fixed N-N moiety in order to ultimately produce NH_3 homogeneously at near ambient conditions, thus improving or ultimately replacing the Haber-Bosch process. Major advances have been accomplished to address this issue. The first such example was reported by the Fryzuk group. The $ZrCl_2[P_2N_2]$ ($[P_2N_2]$ = $[PhP(CH_2SiMe_2NSiMe_2CH_2)_2PPh]^{2-}$)[29] species, formed by the metathesis reaction of *syn*-$Li_2(THF)[P_2N_2]$ (THF = tetrahydrofuran) and $ZrCl_4(THT)$ (THT = tetrahydrothiophene), was shown to activate N_2 via reduction with KC_8 under an atmosphere of N_2.[12] The

References begin on p.20

reduction yields the $\{[P_2N_2]Zr\}_2(\mu\text{-}\eta^2\text{:}\eta^2\text{-}N_2)$ species with an N-N bond length of 1.465(19)Å (Scheme 1.4).[30] Remarkably, unlike typical displacement reactions of the N_2 unit in the presence of H_2,[31,32] this particular Zr_2-N_2 species heterolytically binds H_2 to form an N-H bond and a bridging hydride. Though additional H_2 did not yield NH_3 or hydrazine (N_2H_4), this was nevertheless the first example of the addition of H_2 to a coordinated N_2 moiety.

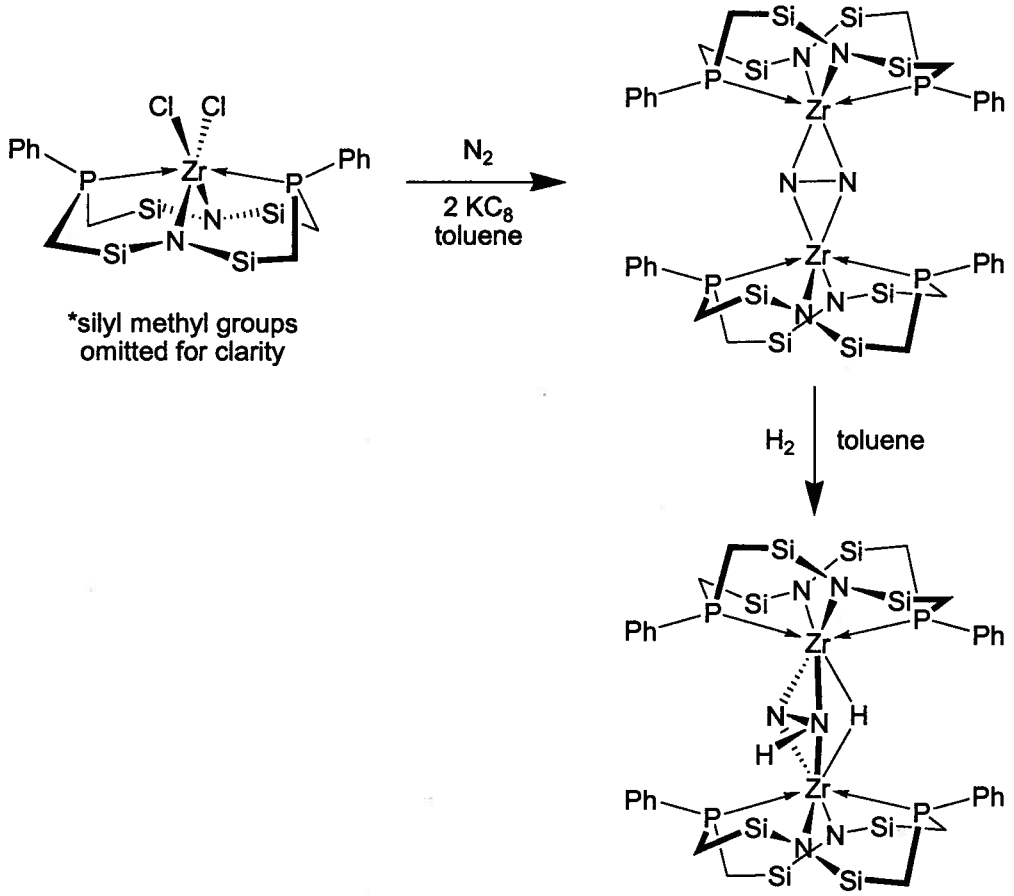

Scheme 1.4

Similar side-on Zr_2-N_2 reactivity is seen with zirconocene complexes. In one particular case, a tetramethylcyclopentadienyl zirconium chloride complex, $(\eta^5\text{-}C_5Me_4H)_2ZrCl_2$, is reduced with Na/Hg amalgam in an atmosphere of N_2 to yield the bridged N_2 species $[(\eta^5\text{-}C_5Me_4H)_2Zr]_2(\mu\text{-}\eta^2\text{:}\eta^2\text{-}N_2)$ (Scheme 1.5).[33] In the presence of 1

References begin on p.20

atm of H_2, this complex also adds H_2 but rather forms two N-H bonds and two Zr-H bonds, $[(\eta^5\text{-}C_5Me_4H)_2ZrH]_2(\mu\text{-}\eta^2\text{:}\eta^2\text{-}N_2H_2)$, with no bridging hydrides. Gentle heating (85°C) of a heptane solution of this complex in the presence of 1 atm of H_2 remarkably yields NH_3, albeit in low yield (10-15%), and Zr(IV) hydride species (60%). This is the first clear example of NH_3 production at a well-defined Zr complex.

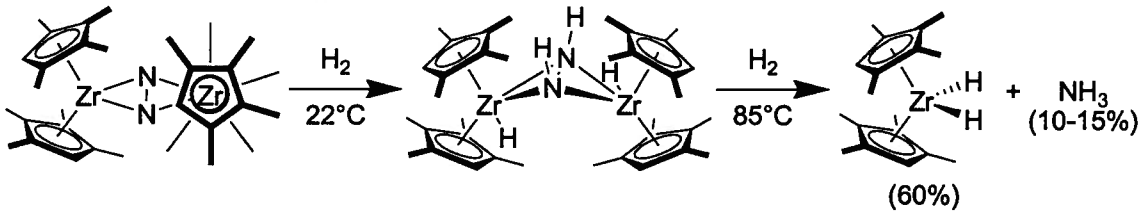

Scheme 1.5

An alternate route to synthesize NH_3 from metal-N_2 complexes is by protonation procedures largely developed by Chatt and co-workers in the 1970s.[17] While this is a viable route to NH_3 synthesis, this process has only ever been done catalytically by electrochemistry.[34] Shortly after the discovery of the formation of an N-H bond using H_2 by the Fryzuk group, the Hidai group developed a reaction that involves both protonation and H_2 in a system capable of producing NH_3 in a non-catalytic fashion.[35]

Extensive work on the $M(N_2)_2(L)_4$ (M = Mo or W; L = phosphine) family of complexes has shown that protonation experiments using inorganic acids can liberate NH_3 in some cases.[36,37,38] These experiments were recently expanded in attempts to protonate the N_2 units using acidic metal-H_2 complexes as the proton sources (Scheme 1.6).[35] Furthermore, these H_2 complexes were synthesized using H_2[39] and not inorganic acids as previously done.[40] This allowed the Hidai group to form NH_3 circuitously by forming a metal-H_2 complex which then serves to protonate the coordinated N_2 unit.

References begin on p.20

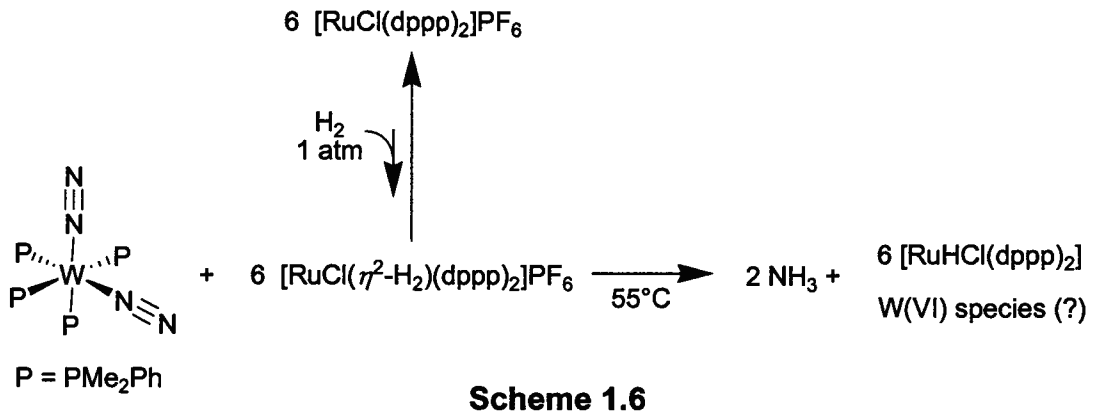

Scheme 1.6

The acidic Ru species (*trans*-[RuCl(η^2-H_2)(dppp)$_2$]PF_6) (dppp = 1,3-bis(diphenylphosphino)propane),[39] easily formed in an atmosphere of H_2 and having a pK_a of 4.4, was used as the proton source. The Ru-H_2 source is prepared in a 1:9 ratio with its Ru precursor [RuCl(dppp)$_2$]PF_6 beforehand. It then readily protonates the *cis*-[W(N_2)$_2$(PMe_2Ph)$_4$] species in an atmosphere of H_2 at 55°C to yield NH_3 in a 55% yield after subsequent base distillation. Although this is an example of NH_3 synthesis using strictly H_2 and N_2 as feedstocks, [RuHCl(dppp)$_2$] and intractable W(VI) species remain.[35] Therefore, this is an example of an incomplete catalytic cycle.

The first example of a catalytic cycle to reduce N_2 to NH_3 at a single metal site was reported by Schrock in 2003.[41] Although the N-H bonds were formed using H^+ rather than H_2, along with a sacrificial reducing agent, this is nonetheless the first example of a well defined catalytic system to reduce N_2 to NH_3 at a metal centre. The [HIPTN_3N]Mo(N_2) (**3**) (where HIPT (hexa-iso-propyl-terphenyl) is 3,5-(2,4,6-^{i}Pr$_3$C$_6$H$_2$)$_2$C$_6$H$_3$ and HIPTN_3N is [((HIPT)NCH$_2$CH$_2$)$_3$N]$^{3-}$) species is slowly reduced with the mild reducing agent decamethylchromocene, [Cr(η^5-C$_5$Me$_5$)$_2$], in a 36-fold excess and protonated with a 48-fold excess of {LutH}{BAr$_4$} (where {LutH} is 2,6-lutidinium and where Ar is 3,5-(CF$_3$)$_2$C$_6$H$_3$).

References begin on p.20

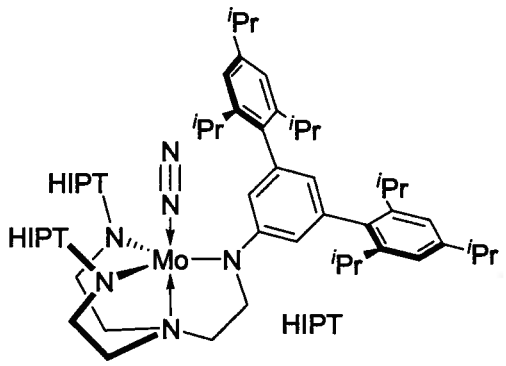

3

Slow addition of the reducing agent was necessary in order to avoid any side reactions. The source of N in NH_3 was confirmed to come from the N_2 unit of **3** by ^{15}N labelling and ^{15}N NMR spectroscopy. This system was shown to produce, via a well defined series of intermediates, a 66% NH_3 yield with respect to reducing equivalents, second only to nitrogenase which has an average 75% yield. Furthermore, this 1 atmosphere, room temperature system was also shown to form a catalytic cycle with 4 turnovers.[41]

1.3.3 Ligand Effects on the Activation of Dinitrogen

Small modifications to ancillary ligands in metal complexes have often been shown to have potentially dramatic effects on their coordination chemistry and reactivity. Some notable recent examples in the context of N_2 activation will be presented in this section.

Ligand design has been shown to play a very important role in some linear-linked aryloxide ligand systems. For example, minor ligand modifications done on a bridged Nb-Nb dimer led to remarkably different chemistry (Scheme 1.7).[42] Reductions of the very similar complexes containing either R = Me or R = ^{t}Bu ligand systems with $LiBHEt_3$ yield different results as shown in the scheme. Whereas N_2 activation and cleavage

References begin on p.20

occurs with the ^{t}Bu-type ligand, a bridged hydride-chloride Nb-Nb complex, with no N_2 activation, is produced with the Me ligand version. This is a clear example of how a seemingly small modification to the ancillary ligand, that of changing a Me for a ^{t}Bu group relatively far from the metal centre, can have a significant impact on the overall reactivity of a metal complex.

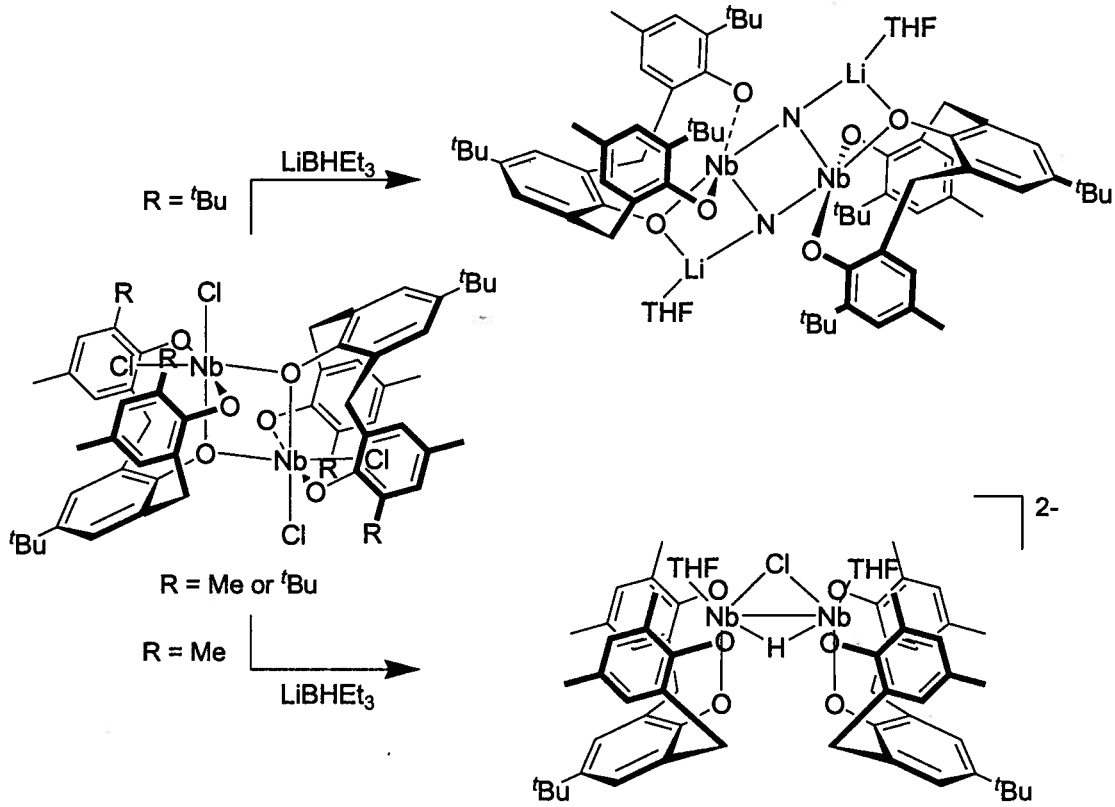

Scheme 1.7

Perhaps one of the best known recent examples of the role ancillary ligands play in the overall reactivity of metal complexes is in the zirconocene system, briefly outlined in Scheme 1.5. Three decades earlier, the Bercaw group had published a result showing the weak activation of N_2 by reducing the $Cp^*_2ZrCl_2$ complex (where $Cp^* = \eta^5\text{-}C_5Me_5$) with Na/Hg amalgam to produce the end-on $[Cp^*_2Zr(\eta^1\text{-}N_2)]_2(\mu\text{-}\eta^1\text{:}\eta^1\text{-}N_2)$ species as shown in Scheme 1.8.[43] It was later shown that a slight modification to the Cp^* ligands,

References begin on p.20

that of removing a Me group on each ring, has a pronounced effect on the reactivity of the complex towards N_2 activation.[33] Following an analogous procedure to Bercaw's reported reduction, the reduction of the modified $(\eta^5\text{-}C_5Me_4H)_2ZrCl_2$ species instead produces the strongly activated, side-on complex $[(\eta^5\text{-}C_5Me_4H)_2Zr]_2(\mu\text{-}\eta^2\text{:}\eta^2\text{-}N_2)$.

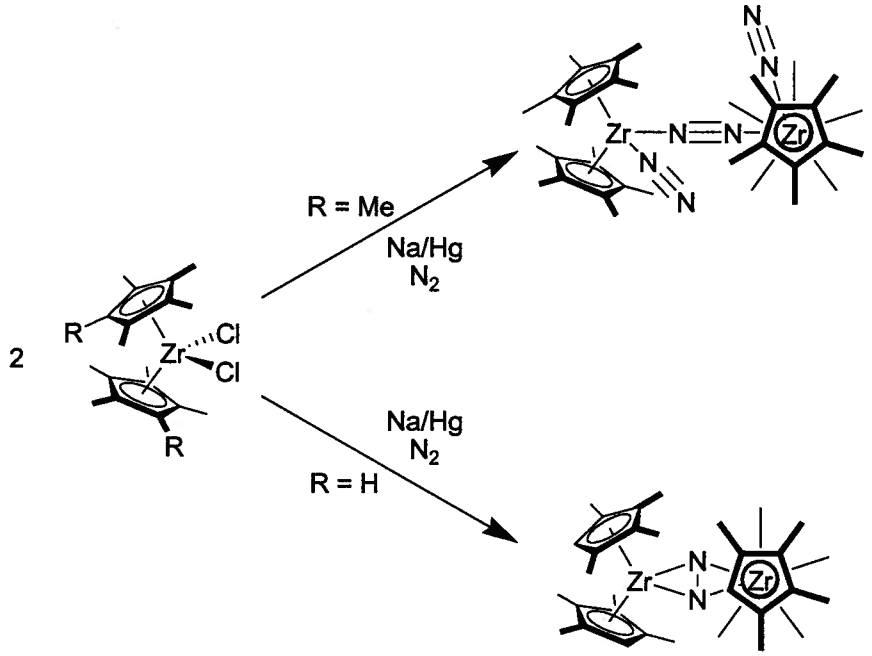

Scheme 1.8

It was also shown that mixed Cp rings can change the equilibrium of N_2 binding from mostly side-on, as seen for $[(\eta^5\text{-}C_5Me_4H)_2Zr]_2(\mu\text{-}\eta^2\text{:}\eta^2\text{-}N_2)$, to mostly end-on, as seen for $[Cp^*_2Zr(\eta^1\text{-}N_2)]_2(\mu\text{-}\eta^1\text{:}\eta^1\text{-}N_2)$. This was accomplished by synthesizing the mixed Cp ring system $(\eta^5\text{-}C_5Me_5)(\eta^5\text{-}C_5Me_4H)ZrI_2$. Reduction of this complex with KC_8 under an atmosphere of N_2 afforded the all end-on complex $[(\eta^5\text{-}C_5Me_5)(\eta^5\text{-}C_5Me_4H)Zr(\eta^1\text{-}N_2)]_2(\mu\text{-}\eta^1\text{:}\eta^1\text{-}N_2)$.[44] Thus, it was concluded that the removal of one methyl group – not two as initially speculated[33] – from $(\eta^5\text{-}C_5Me_5)(\eta^5\text{-}C_5Me_4H)ZrI_2$ to $(\eta^5\text{-}C_5Me_4H)_2ZrCl_2$ results in the drastic change in N_2 activation and coordination.

References begin on p.20

1.4 Ligand Design and Activation of Dinitrogen in the Fryzuk Group

1.4.1 The [PNP] Hybrid Ligand

Ligand design in the Fryzuk group has traditionally always focused on "hybrid" multidentate ligand systems, combining both hard amide donors (NR_2^-) with soft phosphine donors (PR_3). The rationale for combining these two seemingly very different donor types is to allow for coordination of these ligands to either early or late transition metals as well as the lanthanides and actinides. In fact, the amide donor is well suited to coordinate to high-valent, electron-poor early metals, whereas the phosphine donor is well suited to coordinate to low-valent, electron-rich late metal centres.[45]

The first example of these ligands to be synthesized was the ^{Ph}[PNP] ligand (where ^{Ph}[PNP] = $[N(SiMe_2CH_2PPh_2)_2]^-$).[46] Alkyl substituted phosphines, ^{R}[PNP] (where R = Me, ^{i}Pr, ^{t}Bu) can also be readily synthesized.[47] Both alkyl and aryl derivatives are synthesized starting from the commercially available disilazane $HN(SiMe_2CH_2Cl)_2$ (see Scheme 1.9). Salt metathesis using two equivalents of $LiPR_2$ readily forms the [PNP] derivative. The lithiated [PNP] is obtained using an extra equivalent of $LiPR_2$ (when R = alkyl) or an equivalent of *n*-butyl lithium (^{n}BuLi) (when R = Ph). Both alkyl and aryl lithiated [PNP] ligands are synthesized in high yields and are shown in Scheme 1.9.

References begin on p.20

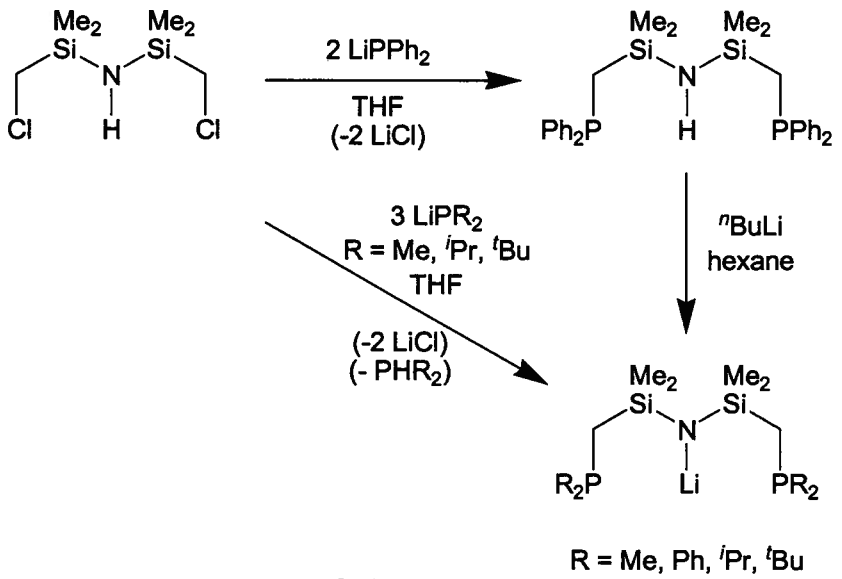

Scheme 1.9

Although the [PNP] ligand is extremely versatile being able to bind to both early and late transition metals,[47] and is able to activate N_2 with early metals, as shown in Scheme 1.1,[21] a common problem faced with early transition metal complexes of this ligand is phosphine dissociation.[48] This can potentially have adverse effects in subsequent reactions of N_2 complexes. A macrocyclic P_2N_2-type ligand was therefore synthesized to remedy this situation by preventing phosphine dissociation.

1.4.2 The [P_2N_2] Ligand

The next generation hybrid ligand to be developed in the Fryzuk group was the [P_2N_2] ([P_2N_2] = $[PhP(CH_2SiMe_2NSiMe_2CH_2)_2PPh]^{2-}$) ligand. This ligand is easily synthesized in a similar fashion to the [PNP] ligand, however an extra equivalent of the disilazane and a primary rather than a secondary phosphine are used as shown in Scheme 1.10.[29]

References begin on p.20

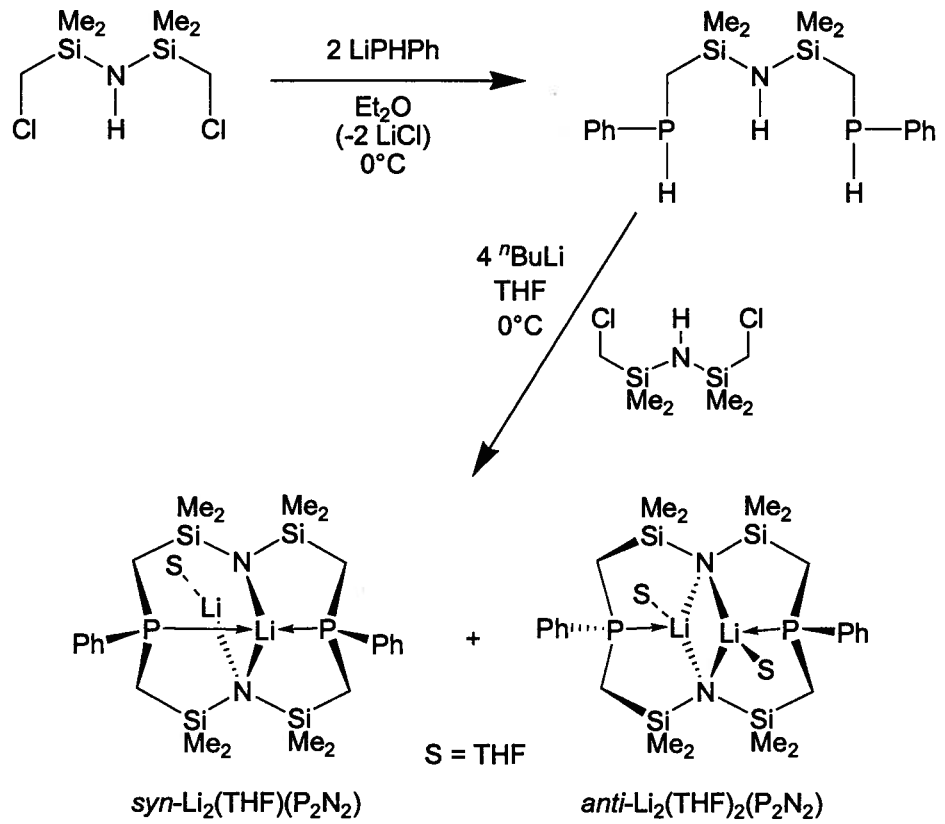

Scheme 1.10

Remarkably, unlike in conventional macrocyle synthesis,[49] high dilution is not necessary for the synthesis of this ligand. This is attributed to both the role of lithium templating as well as the Thorpe-Ingold effect, due to the $SiMe_2$ groups, in the synthesis. Furthermore, as shown in Scheme 1.10, two diastereomers (*syn* and *anti*) can be synthesized. The ratio of these two species produced is largely temperature dependant, the *anti* configuration being the major product at lower temperatures. The ratios are also significantly altered by the choice of solvents used. Whereas both *syn* and *anti* are synthesized using THF as the solvent, the *syn* product can be obtained quantitatively using diethyl ether (Et_2O) as the solvent.

The transition metal chemistry of this ligand has already been highlighted in Scheme 1.4. In addition to this system, group 5 metal chemistry and N_2 activation has

References begin on p.20

been explored. For example, both $V[P_2N_2]$ and $Nb[P_2N_2]$-type complexes have been synthesized; however, under reducing conditions, both form the less reactive end-on dinuclear complexes (Table 1.1).[50,51] Although the $[P_2N_2]$ ligand has shown remarkable transition metal chemistry, the macrocyclic tetradentate nature of this ligand can make the metal centre coordinatively and electronically saturated and, thus, render it less reactive. In order to prevent phosphine dissociation, as discussed in the [PNP] ligand system above, and open up a coordination site of $[P_2N_2]$, an [NPN]-type ligand was synthesized.

1.4.3 The [NPN] Ligand

The tridentate dianionic [NPN] ([NPN] = $[PhP(CH_2SiMe_2NPh)_2]^{2-}$) ligand can be synthesized as shown in Scheme 1.11.[52]

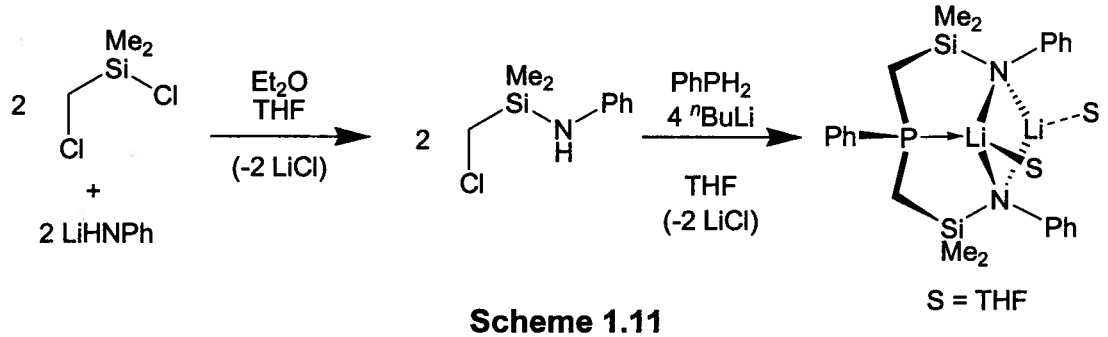

Scheme 1.11

This ligand has proven to be very versatile for N_2 activation using group 4 and 5 metals.[27,53] A new bonding mode for coordinated N_2, that of end-on-side-on, was also discovered using a Ta[NPN] complex as shown in Scheme 1.2.[27] While this ligand has been proven to be very versatile, it is however prone to ligand decomposition specifically at the labile N-Si bond.[54] In order to remedy this situation, a more robust type of [NPN] containing an aryl group instead of the $-CH_2SiMe_2-$ linker, was recently synthesized.[55]

The new ligand, denoted $[NPN]^*$ ($[NPN]^*$ = $\{[N\text{-}(2,4,6\text{-}Me_3C_6H_2)(2\text{-}N\text{-}5\text{-}MeC_6H_3)]_2PPh\}^{2-}$) was synthesized in a two step procedure beginning with the

References begin on p.20

bromination of mesityltolylamine. This brominated diarylamine is then treated with ^{n}BuLi (2.0 eq). Dichlorophenylphosphine ($PhPCl_2$ (0.5eq)) is then added dropwise very slowly to this solution (Scheme 1.12). The dioxane or THF adduct of this dilithiated $[NPN]^*$ ligand can then be isolated.

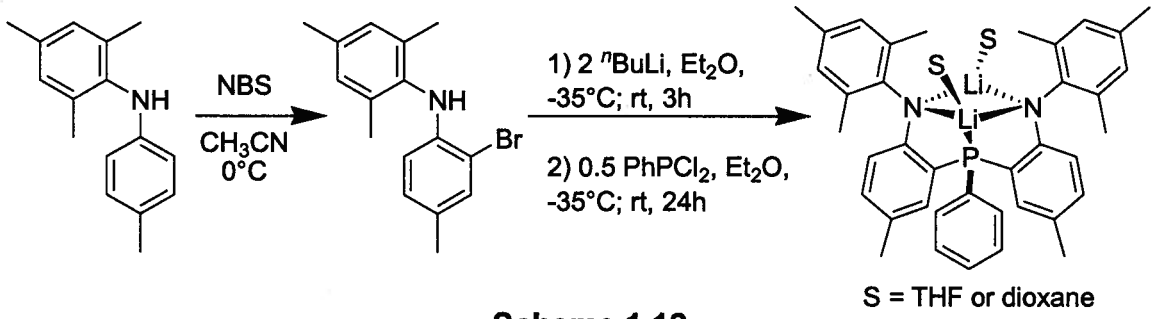

Scheme 1.12

The $[NPN]^*ZrCl_2$ complex was recently synthesized and was shown to activate N_2 to form the side-on bridged $\{[NPN]^*Zr(THF)\}_2(\mu\text{-}\eta^2\text{:}\eta^2\text{-}N_2)$.[56] The PMe_3 and PMe_2Ph adducts of this complex were also shown to add H_2 to form an N-H bond and a bridging hydride, in the form of $\{[NPN]^*Zr(PMe_2R)\}(\mu\text{-}H)(\mu\text{-}NNH)\{Zr[NPN]^*\}$ (where R = Me or Ph), analogous to the bonding seen in Scheme 1.4. Current studies are underway to determine this complex's reactivity towards a variety of reagents in an effort to functionalise the coordinated N_2 unit.

1.5 Scope of Thesis

Chapter two details the synthesis and characterization of two new proligands. The first is a new [NPN]-type system, denoted $[NPN]^SH_2$ ($[NPN]^SH_2$ = $\{N\text{-}(2,4,6\text{-}Me_3C_6H_2)(3\text{-}NH\text{-}SC_4H_2)\}_2PPh$), containing a bridging thiophene as the arene linker, similar to the $[NPN]^*$. The initial *N*-aryl amination reaction to yield the $[NPN]^SH_2$ precursor is discussed as well as the unexpected regiochemistry in the final $[NPN]^SH_2$ product. Mechanistic studies into this unexpected regiochemistry are also presented. The

References begin on p.20

second proligand is a new linear-linker aryloxide, denoted $[OOO]H_2$ ($[OOO]H_2$ = 2,6-bis(3-adamantyl-5-*t*-butyl-2-hydroxybenzyl)-4-*t*-butylanisole), similar to the one shown in Scheme 1.7. It features bulky adamantyl groups in the *ortho* positions of the outer phenyl rings and a methoxy group on the central phenyl ring.

Chapter three of this thesis deals with the attempted syntheses of Ti and Zr complexes of [OOO]. The successful synthesis of a new "half-on" $[OOO(H)]TaCl_4$ complex is reported. The attempted synthesis of a Ta complex of the $[NPN]^S$ ligand is also presented. A very unusual oxidative ring-closing rearrangement of the $[NPN]^S$ ligand, while trying to synthesize a $[NPN]^STaCl_3$, was observed. The successful syntheses of $[NPN]^SZr(NMe_2)_2$, $[NPN]^SZrCl_2$ and $[NPN]^SZrI_2$ are reported. Finally, all attempts to synthesize a Zr_2-N_2 complex from $[NPN]^SZrCl_2$ or from $[NPN]^SZrI_2$ using KC_8, sodium naphthalenide or Mg powder in THF or other solvents will be outlined. Preliminary evidence for a Zr_2-N_2 complex is also presented.

In chapter four, the conclusions obtained as well as the future work that can be undertaken with these ligand systems and complexes are presented.

References begin on p.21

1.6 References

[1] *Acid Deposition Causes and Effects*; Green, A. E. S, Smith, W. H., Eds.; Government Institutes, Inc.: Maryland, 1983.

[2] Environment Canada. (2002). "What's Being Done? What is the UN-ECE Doing?" http://www.ec.gc.ca/acidrain/done-europe.html. (Accessed February 17, 2008).

[3] Siegenthaler, U.; Stocker, T. F.; Monnin, E.; Lüthi, D.; Schwander, J.; Stauffer, B.; Raynaud, D.; Barnola, J-M.; Fischer, H.; Masson-Delmotte, V.; Jouzel, J. *Science*. **2005**, *310*, 1313.

[4] Earth System Research Laboratory, National Oceanic and Atmospheric Administration. (2008). "Recent Global Monthly Mean CO_2." http://www.esrl.noaa.gov/gmd/webdata/ccgg/trends/co2_trend_gl.pdf. (Accessed February 17, 2008)

[5] IPCC Fourth Assessment Report. (2007). "Working Group II Report 'Impacts, Adaptation and Vulnerability.'" http://www.ipcc.ch/ipccreports/ar4-wg2.htm. (Accessed February 17, 2008).

[6] Smil, V. *Enriching the Earth*; MIT Press: Cambridge, MA, 2001.

[7] Galloway, J. N.; Dentener, F. J.; Capone, D. J.; Boyer, E. W.; Howarth, R. W.; Seitzinger, S. P.; Asner, G. P.; Cleveland, C. C.; Green, P. A.; Holland, E. A.; Karl, D. M.; Michaels, A. F.; Porter, J. H.; Townsend, A. R.; Vörösmarty, C. J. *Biogeochemistry*. **2004**, *70*, 153.

[8] Thorneley, R. N. F.; Lowe, D. J. *J. Biol. Inorg. Chem.* **1996**, *1*, 576.

[9] Jenkinson, D. S. *Plant and Soil*. **2001**, *228*, 3.

References begin on p.21

[10] Tamaru, K.; Ertl, G. In *Catalytic Ammonia Synthesis*; Jennings, J. R., Ed.; Plenum Press: New York, 1991.

[11] Sutton, L. E. *Tables of Interatomic Distances and Configuration in Molecules and Ions*; Chemical Society Special Publications No. 11, Chemical Society: London, 1958.

[12] Fryzuk, M. D.; Love, J. B.; Rettig, S. J.; Young, V. G. *Science*. **1997**, *275*, 1445.

[13] Morello, L.; Love, J. B.; Patrick, B. O.; Fryzuk, M. D. *J. Am. Chem. Soc.* **2004**, *126*, 9480.

[14] Bernskoetter, W. H.; Pool, J. A.; Lobkovsky, E.; Chirik, P. J. *J. Am. Chem. Soc.* **2005**, *127*, 7901.

[15] Yamabe, T.; Hori, K.; Minato, T.; Fukui, K. *Inorg. Chem.* **1980**, *19*, 2154.

[16] Allen, A. D.; Senoff, C. V. *Chem. Comm.* **1965**, 621.

[17] Chatt, J.; Dilworth, J. D.; Richards, R. L. *Chem. Rev.* **1978**, *78*, 589.

[18] Orgel, L. E. *An Introduction to Transition Metal Chemistry*; Methuen: London, 1960.

[19] Evans, W. J.; Ulibarri, T. A.; Ziller, J. W. *J. Am. Chem. Soc.* **1988**, *110*, 6877.

[20] MacLachlan, E. A.; Fryzuk, M. D. *Organometallics*. **2006**, *25*, 1530.

[21] Fryzuk, M. D.; Haddad, T. S.; Rettig, S. J. *J. Am. Chem. Soc.* **1990**, *112*, 8185.

[22] Hirotsu, M.; Fontaine, P. P.; Zavalij, P. Y.; Sita, L. R. *J. Am. Chem. Soc.* **2007**, *129*, 12690.

[23] Evans, W. J.; Allen, N. T.; Ziller, J. W. *J. Am. Chem. Soc.* **2001**, *123*, 7927.

[24] Cloke, F. G. N.; Hitchcock, P. B. *J. Am. Chem. Soc.* **2002**, *124*, 9352.

[25] Duchateau, R.; Gambarotta, S.; Beydoun, N.; Benzimon, C. *J. Am. Chem. Soc.* **1991**, *113*, 8986.

References begin on p.21

[26] Cohen, J. D.; Fryzuk, M. D.; Loehr, T. M.; Mylvaganam, M.; Rettig, S. J. *Inorg. Chem.* **1998**, *37*, 112.

[27] Fryzuk, M. D.; Johnson, S. A.; Rettig, S. J. *J. Am. Chem. Soc.* **1998**, *120*, 11024.

[28] Laplaza, C. E.; Cummins, C. C. *Science.* **1995**, *268*, 861.

[29] Fryzuk, M. D.; Love, J. B.; Rettig, S. J. *Chem. Commun.* **1996**, 2783.

[30] Morello, L.; Ferreira, M. J.; Patrick, B. O.; Fryzuk, M. D. *Inorg. Chem.* **2008**, *47*, 1319.

[31] Manriquez, J. M.; McAlister, D. R.; Sanner, R. D.; Bercaw, J. E. *J. Am. Chem. Soc.* **1978**, *100*, 2716.

[32] George, T. A.; Tisdale, R. C. *Inorg. Chem.* **1988**, *27*, 2909.

[33] Pool, J. A.; Lobkovsky, E.; Chirik, P. J. *Nature*, **2004**, *427*, 527.

[34] Pickett, C. J.; Talarmin, J. *Nature*, **1985**, *317*, 652.

[35] Nishibayashi, Y.; Iwai, S.; Hidai, M. *Science.* **1998**, *279*, 540.

[36] Chatt, J.; Pearman, A. J.; Richards, R. L. *J. Chem. Soc. Dalton Trans.* **1977**, 1852.

[37] Takahashi, T.; Mizobe, Y.; Sato, M.; Uchida, Y.; Hidai, M. *J. Am. Chem. Soc.* **1980**, *102*, 7461.

[38] Hidai, M.; Mizobe, Y. *Chem. Rev.* **1995**, *95*, 1115.

[39] Rocchini, E.; Mezzetti, A.; Rulegger, H.; Burckhardt, U.; Gramlich, V.; Del Zotto, A.; Martinuzzi, P.; Rigo, P. *Inorg. Chem.* **1997**, *36*, 711.

[40] Jia, G.; Morris, R. H.; Schweitzer, C. T. *Inorg. Chem.* **1991**, *30*, 593.

[41] Yandulov, D. V.; Schrock, R. R. *Science*, **2003**, *301*, 76.

[42] Kawaguchi, H.; Matsuo, T. *Angew. Chem. Int. Ed.* **2002**, *41*, 2792.

[43] Manriquez, J. M.; Bercaw, J. E. *J. Am. Chem. Soc.* **1974**, *96*, 6229.

[44] Pool, J. A.; Bernskoetter, W. H.; Chirik, P. J. *J. Am. Chem. Soc.* **2004**, *126*, 14326.

References begin on p.21

[45] Pearson, R. G. *J. Chem. Ed.* **1968**, *45*, 581.

[46] Fryzuk, M. D.; MacNeil, P. A.; Rettig, S. J.; Secco, A. S.; Trotter, J. *Organometallics*. **1982**, *1*, 918.

[47] Fryzuk, M. D. *Can. J. Chem.* **1992**, *70*, 2839.

[48] Fryzuk, M. D.; Carter, A.; Rettig, S. J. *Organometallics*, **1992**, *11*, 469.

[49] Lindoy, L. F. *The Chemistry of Macrocyclic Ligand Complexes*; Cambridge University Press: Cambridge, 1989.

[50] Giesbrecht, G. R. *Amidophosphine Complexes of Electron-Poor Metals*; PhD thesis, University of British Columbia: Vancouver, 1998.

[51] Fryzuk, M. D.; Kozak, C. M.; Bowdridge, M. R.; Patrick, B. O.; Rettig, S. J. *J. Am. Chem. Soc.* **2002**, *124*, 8389.

[52] Fryzuk, M. D.; Johnson, S. A.; Patrick, B. O.; Albinati, A.; Mason, S. A.; Koetzle, T. F. *J. Am. Chem. Soc.* **2001**, *123*, 3960.

[53] Morello, L.; Yu, P.; Carmichael, C. D.; Patrick, B. O.; Fryzuk, M. D. *J. Am. Chem. Soc.* **2005**, *127*, 12796.

[54] Fryzuk, M. D.; MacKay, B. A.; Johnson, S. A.; Patrick, B. O. *Angew. Chem. Int. Ed.* **2002**, *41*, 3709.

[55] MacLachlan, E. A.; Fryzuk, M. D. *Organometallics*, **2005**, *24*, 1112.

[56] MacLachlan, E. A.; Hess, F. M.; Patrick, B. O.; Fryzuk, M. D. *J. Am. Chem. Soc.* **2007**, *129*, 10895.

References begin on p.21

CHAPTER 2

Ligand Design and Synthesis for Early Metal Complexes

2.1 Introduction*

Modifications to ligands can lead to dramatic changes in the reactivity of metal complexes as was detailed in Chapter 1. In order to expand on the effects of ligand design and modification on the chemistry of early metal activation of N_2, new ligands were synthesized. The design and synthesis of both a new [NPN] proligand, as well as a new linear-linked aryloxide proligand similar to the one shown in Scheme 1.7, are reported in this chapter.

Various ancillary ligands have been developed in our group, including the [PNP], the $[P_2N_2]$ and the [NPN] systems. Markedly different chemistry is obtained using these very different ligands. For example, whereas both Zr[PNP] and $Zr[P_2N_2]$ systems are capable of activating N_2 in a side-on manner, as shown in Schemes 1.1 and 1.4 respectively, the $\{[P_2N_2]Zr\}_2(\mu\text{-}\eta^2\text{:}\eta^2\text{-}N_2)$ product is also capable of adding H_2 to form an N-H bond and a bridging hydride[1] while the $\{[PNP]ZrCl\}_2(\mu\text{-}\eta^2\text{:}\eta^2\text{-}N_2)$ cannot.[2]

Furthermore, modifying the $[P_2N_2]$ ligand by synthesizing its $[As_2N_2]$ analogue ($[As_2N_2] = [PhAs(CH_2SiMe_2NSiMe_2CH_2)_2AsPh]^{2-}$) also leads to very different chemistry. In fact, while the $[As_2N_2]ZrCl_2$ analogue of $[P_2N_2]ZrCl_2$ can be readily synthesized, reduction of this species with either KC_8 (as in Scheme 1.4 for $[P_2N_2]$), Mg(anthracene)$(THF)_3$ or activated Mg did not yield an N_2 complex.[3]

---

* A version of this chapter will be submitted for publication. Co-authors: Gabriel Ménard, Michael D. Fryzuk, Howie Jong.

References begin on p.68

Finally, another minor change that had deleterious effects was with the [NPN] ligand. As previously shown in Scheme 1.2, hydrogenation of $[NPN]TaMe_3$ leads to the tetrahydride species $([NPN]Ta)_2(\mu\text{-}H)_4$. This species spontaneously reacts with N_2 by reductive elimination of H_2 to produce the side-on-end-on species $([NPN]Ta(\mu\text{-}H))_2(\mu\text{-}\eta^1{:}\eta^2\text{-}N_2)$. Subsequent reactions of this compound can lead to ligand decomposition usually caused by the labile N-Si bond in the [NPN] ligand. For example, the reaction of the $([NPN]Ta(\mu\text{-}H))_2(\mu\text{-}\eta^1{:}\eta^2\text{-}N_2)$ species with 9-borabicyclo[3.3.1]nonane (9-BBN) leads to ligand rearrangement promoted by N-Si bond scission.[4] In order to remedy this situation, a new [NPN] ligand containing a $-CH_2CH_2-$ linker instead of the usual $-CH_2SiMe_2-$ linker was synthesized. Although Ta complexes of this new ligand can be synthesized, subsequent hydrogenation to yield the analogous Ta tetrahydride species failed.[5]

The newest generation of ligand in the Fryzuk group is the $[NPN]^*$. This ligand was designed to prevent unwanted side reactions[6,7] by introducing a more robust, less flexible and less labile aryl group to replace the $-CH_2SiMe_2-$ linker traditionally used. Part of the research in this thesis focuses on modifying the $[NPN]^*$ structure and replacing the existing six-membered tolyl linker with a five-membered ring ($[NPN]^X$ - Figure 2.1).

References begin on p.68

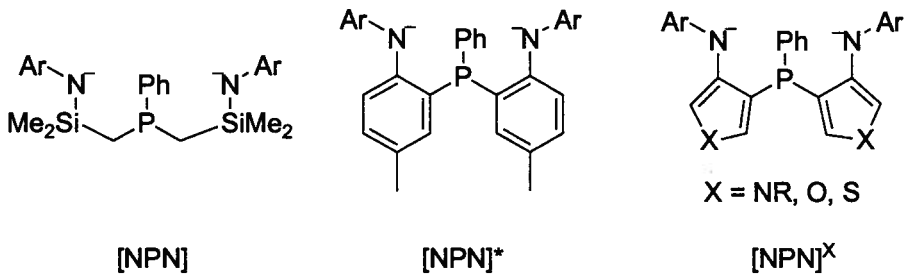

Figure 2.1. Modification introduced from the classic [NPN] to the $[NPN]^*$. The $[NPN]^X$ ligand is presented as a potential new modification to the $[NPN]^*$. Typically, Ar = Ph for [NPN] and Ar = mesityl (2,4,6-trimethylaniline) for $[NPN]^*$ and $[NPN]^X$.

Yet another new type of ligand, not typically used in our laboratory, was also investigated as part of this research. As an extension of the vast array of calixarene chemistry,[8] the Scott group recently reinvestigated a class of linear-linked aryloxide ligands (briefly shown in Scheme 1.7), originally discovered by Koebner in 1933,[9] in an attempt to discover its unexplored coordination chemistry (Figure 2.2 – Kawaguchi's ligands are also shown).[10] These ligands are convenient for probing ancillary ligand effects on reactivity since they can be easily tuned as exemplified in Figure 2.2.

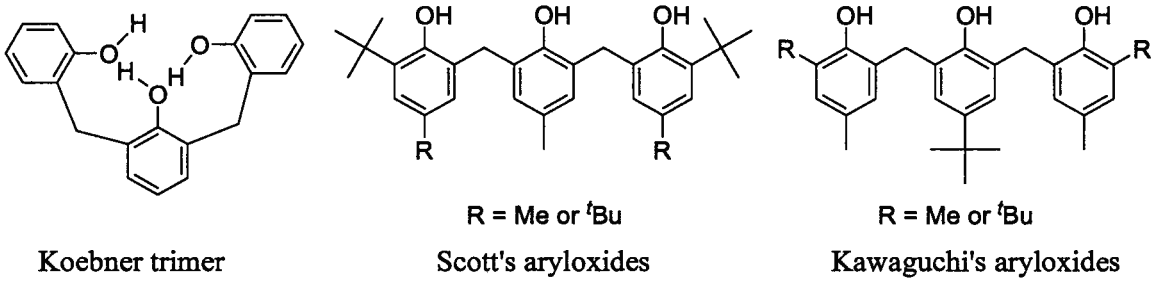

Figure 2.2. General depiction of the original Koebner trimer and two recent modifications.

References begin on p.68

In the past few years, Kawaguchi's group has extensively used this type of ligand for groups 4 and 5 chemistry.[11,12,13] A very recent example features the cleavage of N_2 by a bridged niobium tetrahydride complex using a tripodal aryloxide ancillary ligand.[14] As an extension of aryloxide coordination chemistry, our approach was to synthesize a new ligand, similar to Kawaguchi's shown in Figure 2.2, but incorporating bulkier adamantyl groups in the R positions of the ligand. Unlike the ligands in Figure 2.2, the new ligand synthesized is dianionic as it was mainly designed for group 4 metal activation of N_2. Reduction of a group 4 dihalide complex bearing a dianionic ligand provides the required number of electrons to produce highly activated coordinated N_2 species as shown in many examples in Chapter 1. The proposed modifications were undertaken in an attempt to monitor their effects on the metal reactivity towards N_2.

Although research in the Fryzuk group typically involves mixed-donor ligands, the fairly recent and attractive chemistry of these multidentate aryloxide ligands in early metal chemistry of N_2 was appealing to investigate.[15,16]

2.2 Results and Discussion

2.2.1 Design of a New [NPN] Proligand: General Considerations

Several different synthetic strategies can be undertaken for the synthesis of a new [NPN] ligand with a five-membered aryl linker. Recent work in our group has led to a modified $[NPN]^*$ ligand, denoted [NPN]' ([NPN]' = $\{[N\text{-}(2,4,6\text{-}Me_3C_6H_2)(2\text{-}N\text{-}C_6H_4)]_2PPh\}^{2-}$), which contains a phenyl rather than a tolyl linker as seen for $[NPN]^*$.[17] A similar synthetic protocol to the synthesis of this [NPN]' was undertaken for the new five-membered aryl-bridged [NPN]; the retrosynthetic analysis is shown in Scheme 2.1.

References begin on p.68

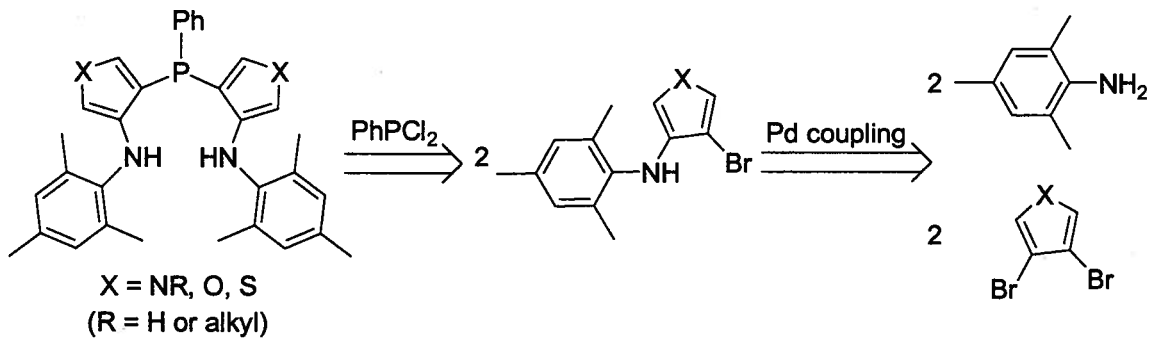

Scheme 2.1

Mesitylaniline was used rather than any other aryl group so as to not over-modify the [NPN]* ligand. As denoted in the scheme, there were three obvious choices of five-membered aromatic linkers that could be used: pyrrole, furan or thiophene. General comparisons can be made with these three rings. Although pyrrole, furan and thiophene are all aromatic with 6 π-electrons, thiophene has the highest degree of aromaticity. The degree of aromaticity of a compound is determined by its resonance energy.† Thiophene's empirical resonance energy of 120 kJ mol^{-1} is closest to benzene's 150 kJ mol^{-1}. The order of increasing aromatic character is: furan < pyrrole < thiophene < benzene.[18] Thus thiophene's similarity to benzene makes it a more attractive target.

The possibility of using furan as the linker was considered but ultimately rejected. Due to its low resonance energy, furan's cyclic conjugation can easily be disrupted. In fact, furan undergoes electrophilic substitution 10^{11} times faster than benzene.[18] Considering much of the metal-N_2 chemistry undertaken in our group involves reactions with electrophiles,[19] this particular characteristic was considered undesirable. Furthermore, furan and its derivatives can be easily protonated by Brönsted acids to yield ring-opened 1,4-dicarbonyls. With strong acids, furan also polymerizes.[18] Since the

† Resonance energy is defined as the "deficiency in the energy content of a system when compared with non-conjugated or aliphatic reference structures."[18]

References begin on p.68

synthesis of the proligand involves protonation (*vide infra*), this was also seen as a negative attribute.

Using pyrrole in the synthesis of a new ligand was also determined to be less desirable. The Pd-catalyzed coupling step, as seen in Scheme 2.1, would be complicated by the possibility of having competing reactions between the pyrrole N-H bond and the mesitylaniline N-H bond for coupling to the C-Br bond of 3,4-dibromopyrrole. Furthermore, the pyrrole N-H is considered acidic with a pK_a of 17.5,[18] thus causing obvious problems in the coordination chemistry of this ligand with proton sensitive metal starting materials. Both these problems could be easily prevented by using an alkyl substituted pyrrole but it still faces many of the same problems as furan by being both acid-sensitive and prone to polymerization. Furthermore, although pyrrole is considered to have more aromatic character, it is 10^5 times more susceptible than furan towards electrophilic attack (10^{16} times more than benzene).[18]

Commercial availability of the heterocycles also played a big role in determining which one to use. Of the three, 3,4-dibromofuran, pyrrole or thiophene, only 3,4-dibromothiophene is readily commercially available. 3,4-dibromofuran can only be purchased from very few sources and at a much higher cost than the thiophene. It can be synthesized; however, the yields are typically low.[20] On the other hand, alkyl substituted 3,4-dibromopyrrole starting materials are not commercially available. Furthermore, there is no clear way of synthesizing them without typically obtaining a mixture of products.[21]

Unlike both furan and pyrrole, thiophene is far less sensitive to acids and less prone to ring-opening reactions.[18] Its chemistry is also very well established[22] and although S-containing groups are often excellent ligands in coordination chemistry, the

References begin on p.68

thiophene S is considered an extremely poor ligand especially with early transition metals.[23] Finally, although thiophene can be oxidized to its 1,1-dioxide form, this reaction is of little concern as it requires strong oxidizing agents.[24]

2.2.2 Synthesis of the $[NPN]^SH_2$ Precursor

The synthesis of $[NPN]^SH_2$ (**2.2**) ($[NPN]^SH_2$ = {*N*-(2,4,6-$Me_3C_6H_2$)(3-NH-SC_4H_2)}$_2$PPh) was undertaken firstly by a Pd-catalyzed Buchwald-Hartwig type *N*-aryl amination[25,26] of mesitylaniline with 3,4-dibromothiophene. The initial cross-coupling reaction to yield the product (**2.1**) was optimized by screening several different Pd catalysts and reagent ratios. The results with the approximate gas chromatography-mass spectrometry (GC-MS) results are shown in Table 2.1.

Table 2.1. Pd catalyst screening reactions for the synthesis of **2.1**.

Entry	Catalyst system	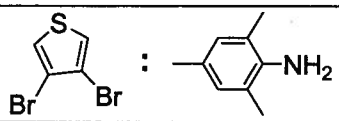	Time (hrs)	Temp. (°C)	GC-MS yield (%)
1	$Pd(PPh_3)_4$ (4%)	1 : 1	15	25	0
2	$Pd(OAc)_2$ (4%) + $P(^tBu)_3$ (4%)	1 : 1	15	25	5
3	(SIPr)Pd(allyl)Cl (1%)	1 : 1	15	25	20
4	(SIPr)Pd(allyl)Cl (2%)	1 : 1	15	25	30
5	(SIPr)Pd(allyl)Cl (5%)	1 : 1	15	25	48
6	(SIPr)Pd(allyl)Cl (5%)	3 : 1	15	25	100

* All reactions were performed in toluene using 1.1 eq. NaO^tBu

The reactions in entries 2[27] and 3-6[28] were performed using modified procedures of known literature. The reactions using the *N*-heterocyclic Pd complex, (SIPr)Pd(allyl)Cl (SIPr = [*N*,*N*'-bis(2,6-diisopropylphenyl)4,5-dihydroimidazol-2-

References begin on p.68

ylidene]), provided some of the most promising initial results. In fact, it was immediately clear that this catalyst proved superior to both $Pd(PPh_3)_4$ (entry 1) and the $Pd(OAc)_2/P(^tBu)_3$ system (entry 2) under identical reaction conditions. The reactions were performed at room temperature since heating these systems could lead to the production of small amounts of the disubstituted N^3,N^4-dimesitylthiophene-3,4-diamine by-product. Increasing the (SIPr)Pd(allyl)Cl catalyst loading from 1% to 5% increased the yield; however, complete conversion could not be obtained with high catalyst loadings. Instead, complete conversion to yield **2.1** could be achieved using an excess (3 equivalents) of 3,4-dibromothiophene with a 5% catalyst loading (with respect to the aniline). The details of the synthesis are outlined in Equation 2.1.

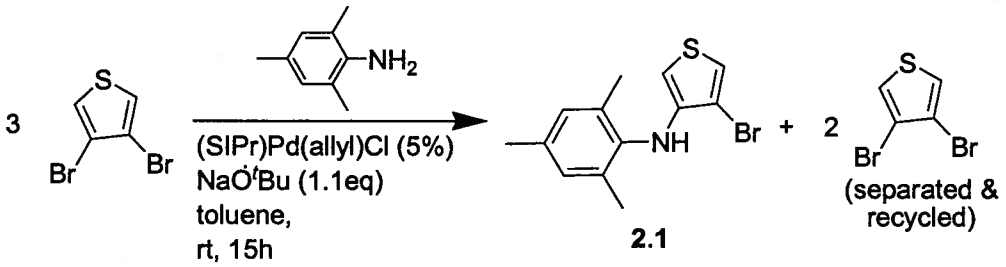

Equation 2.1

The reaction was done under an atmosphere of N_2 in toluene at room temperature, overnight (15 hours). The extraction and purification is done in open air. An aqueous wash seems to play an important role in the overall yield. The removal of the water soluble ^tBuOH and NaO^tBu (NaOH and ^tBuOH in water) by-products, which may otherwise interfere in the chromatography step, may be the reason. Silica gel column chromatography nicely separates the product (**2.1**) from the excess 3,4-dibromothiophene (Rf values of 0.19 and 0.71 in hexanes, respectively). The 3,4-dibromothiophene can be recycled. The isolated yield of product is 74%. It was fully characterized by ^1H and ^{13}C

References begin on p.68

NMR spectroscopy as well as electron impact-mass spectrometry (EI-MS), elemental analysis (EA) and single crystal X-ray diffraction (solid state structure is shown in the appendix). The product seems to be photo and/or thermally sensitive turning red gradually over time in the solid state. It can be stored indefinitely in the dark at -35°C under N_2.

The synthesis of **2.1** presents a marked improvement in reaction conditions, reaction time and overall yield as compared to the analogous reaction performed for the synthesis of the [NPN]' precursor.[17] The synthesis of the [NPN]' precursor (phenyl-bridged analog to **2.1**) requires a harsher 3-day reflux of a 1,4-dioxane (b.p. 101°C) solution and yields a maximum 53% yield. Moreover, the synthesis of **2.1** is, to the best of our knowledge, the first high yielding Pd-catalyzed *N*-aryl amination coupling of 3,4-dibromothiophene to quantitatively yield the mono-substituted product under mild reaction conditions. Although the analogous reaction of diphenyl amine and 3,4-dibromothiophene to yield the mono-substituted product has been reported,[29] this product was not isolated and only a 12% yield, determined by GC-MS, was reported. Similar reactions to produce either C-C bonded species, such as 3-benzyl-4-bromothiophene from 3,4-dibromothiophene,[30] or C-N bonded species, using monobromothiophenes[27,31,32] or polysubstituted monobromothiophenes,[33] have been well documented.

Figure 2.3 displays the typical numbering scheme for thiophenes as well as the very diagnostic coupling constants found for thiophene aromatic protons.[34] The numbering scheme is also applied to **2.1** and will be used throughout this thesis.

References begin on p.68

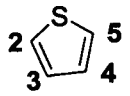

J (2-3) = 4.9-6.2 Hz, typical = 5.4 Hz
J (3-4) = 3.4-5.0 Hz, typical = 4.0 Hz
J (2-4) = 1.2-1.7 Hz, typical = 1.5 Hz
J (2-5) = 3.2-3.7 Hz, typical = 3.4 Hz

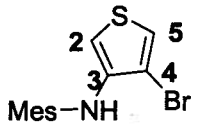

2.1

Figure 2.3. Typical numerical assignments and coupling constants for thiophene shown on the left. On the right, the assignments that will be used for **2.1** (Mes = mesityl).

2.2.3 Synthesis of $[NPN]^SH_2$: Formation of An Unexpected Product

The details for the synthesis of the new $[NPN]^SH_2$ proligand, **2.2**, are shown in Equation 2.2. All steps are done *in situ* beginning with the lithiation reaction using *tert*-butyl lithium (^{t}BuLi), followed by the addition of $PhPCl_2$ and finally protonation using excess trimethylammonium chloride (Me_3NHCl) (yield: 50%). ^{t}BuLi was used rather than ^{n}BuLi since the latter generated lots of unreacted **2.1** and product isolation proved far more problematic. The phosphine, as shown in the retrosynthetic analysis in Scheme 2.1, was expected to be in the 4- positions of the thiophene rings since lithium-bromine exchange should lead to C-Li bonds in those positions. However, this anticipated product was not obtained; instead, the phosphine was bound to the 2- positions of the thiophene rings as shown in Equation 2.2.

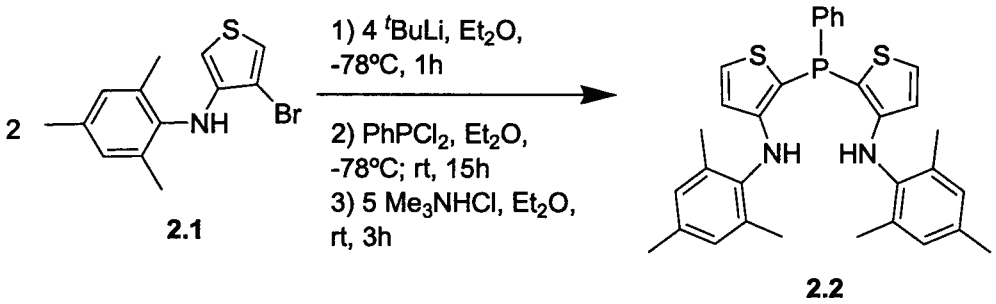

Equation 2.2

References begin on p.68

The $^{31}P\{^1H\}$ NMR spectrum in C_6D_6 shows one singlet at -55.5 ppm. The ^1H and ^{13}C NMR spectra of **2.2** are consistent with the proposed structure. The initial evidence that showed the formation of the 2- substituted product came from the coupling constants for the thiophene protons in the ^1H NMR spectrum (see Figure 2.4).

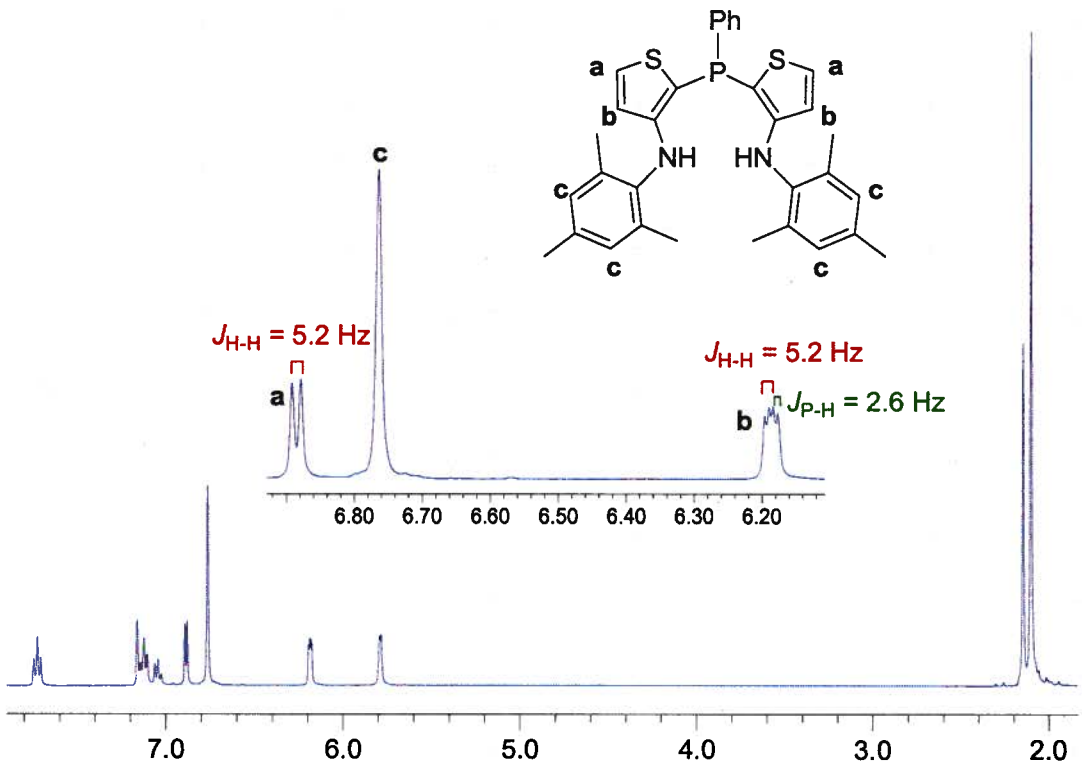

Figure 2.4. 400 MHz ^1H NMR spectrum of **2.2** in C_6D_6.

Two thiophene signals were observed, a doublet at 6.88 ppm and a doublet of doublets at 6.19 ppm (due to coupling to both H and P) with J_{H-H} values of 5.2 Hz (the dd also had J_{P-H} = 2.6 Hz). As shown in Figure 2.3, these values for the coupling constants are indicative of two protons side-by-side in the 4,5- positions of the thiophene rings *and not* at opposite ends of one-another as in the expected 2,5- positions.[34] As will be seen in Chapter 3, several solid state structures of this ligand in metal complexes confirm this

References begin on p.68

finding. Mechanistic investigations to explain this unexpected regiochemistry were performed and the results are given in the following section.

2.2.4 Mechanistic Investigation Into the Synthesis of $[NPN]^SH_2$

The unexpected regiochemistry of **2.2** prompted us to investigate this reaction in more detail. Some possible mechanisms are shown in Figure 2.5.

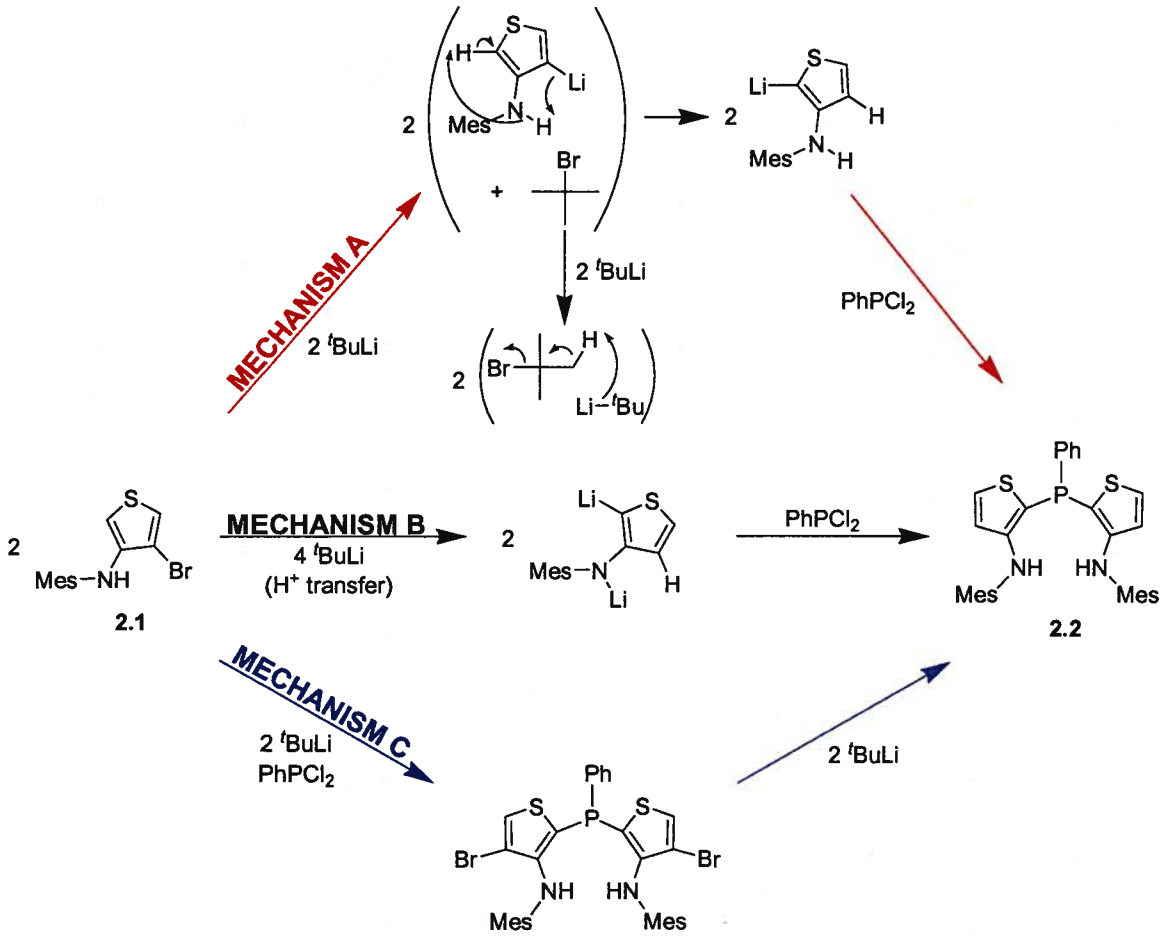

Figure 2.5. Proposed mechanisms for the synthesis of **2.2** using **2.1**, ^tBuLi and $PhPCl_2$. The final protonation step using Me_3NHCl is assumed in each case.

Mechanisms A-C propose three very different reaction pathways for the synthesis of $[NPN]^SH_2$ (**2.2**). The first (A) involves lithium-bromine exchange to yield the 4-

References begin on p.68

lithiated product which intramolecularly rearranges to the 2-lithiated precursor. Concurrent quenching of the *tert*-butyl bromide by the second equivalent of ^{t}BuLi also occurs as expected (*vide infra*). Mechanism B involves the formation of a dilithiated-debrominated version of **2.1** which is proposed to form via intra- or intermolecular proton transfer to the 4- position. This then reacts in the less hindered 2- position with $PhPCl_2$ to yield **2.2**. The final proposed mechanism involves deprotonation in the 2- position followed by reaction with $PhPCl_2$ to form a dibrominated **2.2** precursor. This is then debrominated by subsequent lithium-bromine exchange to yield **2.2**.

Mechanism A is based on the known reactivity of ^{t}BuLi; it is well known that 2 equivalents of ^{t}BuLi are necessary for each aryl-halide that is to be lithiated.[35,36,37] This occurs since the product of lithium-halogen exchange with ^{t}BuLi is *tert*-butyl halide which, in the presence of ^{t}BuLi, easily undergoes elimination to yield isobutane, isobutene and lithium halide (Scheme 2.2).

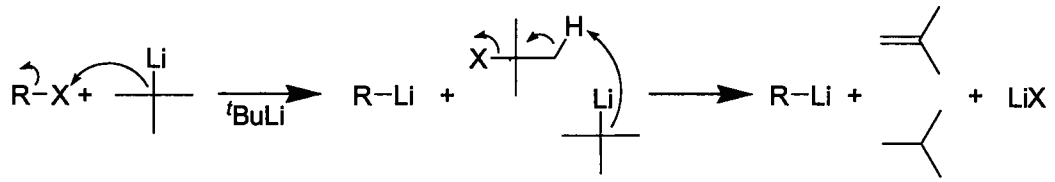

Scheme 2.2

Mechanism A relies on two important assumptions: 1) that lithium-halogen exchange is more rapid than deprotonation of the N-H bond, likely due to the steric protection offered by the adjacent bulky mesityl ring and; 2) that the rearrangement is a result of an intramolecular proton transfer. Steric hindrance must be responsible for the first assumption since previous reports suggest that acidic protons near aryl-bromide bonds, in the presence of ^{n}BuLi, are deprotonated first before subsequent lithium-halogen exchange.[38] The second assumption would require the pK_a values of the thiophene and

References begin on p.68

the N-H aniline protons in **2.1** to be known. No attempts to determine these values were made but, for comparison, reported values for the pK_a of free thiophene are 33.0[39] and 39.0[40] for the 2,5- and 3,4- protons respectively. The pK_a for the N-H of ditolylamine, a similar diarylamine, is 22.95 (other diarylamines are in the same region).[41] Thus, using these approximate values, it is clear that a potential problem arises: the N-H bond is likely more acidic than the neighbouring proton in the 2- position. Nonetheless, this mechanism could not be discounted and needed to be addressed. One way to do so would be to protect the N-H bond with a protecting group. Removal of the N-H proton should therefore give a clue as to whether or not this intramolecular mechanism is plausible.

Several attempts were made to protect the N-H bond of **2.1** with trimethylsilyl chloride (TMSCl), trimethylsilyl iodide (TMSI), di-*tert*-butyldicarbonate ($O(^tBoc)_2$) and methyl chloroformate. Substitution of the N-H bond by a methyl group, using methyl iodide, was also attempted. Although the TMSCl, TMSI and methyl iodide reactions gave mixtures of products, *N*-protected **2.1** could not be isolated from any of these mixtures. Following known procedures, more conventional protecting reagents such as ($O(^tBoc)_2$)[42] and methyl chloroformate[43] did not yield any reaction with **2.1**.

While it is possible that the position of this 2- proton, being adjacent to an amine group as well as the thiophene S, could render it more acidic than in free thiophene and thus make this mechanism more likely, subsequent deuteration experiments seem to disprove this mechanism. Standard experiments using D_2O as the quenching agent did not yield any conclusive results and this was attributed in part to the facile H/D exchange properties of the amine group.[‡] Subsequent reactions attempted with methanol-d_4

[‡] Stirring a solution of **2.1** in pre-dried THF with 10 eq. D_2O for 2 hours yielded at least a 50% decrease in the N-H signal in the ^1H NMR (C_6D_6) spectrum upon removal of solvents.

References begin on p.68

(CD_3OD) also gave inconclusive results as an unknown by-product was formed. However, deuteration experiments were successful using trifluoroacetic acid-d (CF_3COOD) as the quenching agent. The H/D and product ratios were integrated by ^1H NMR spectroscopy; for example, Figure 2.6 gives a typical result for this type of experiment showing a mixture of **2.1(H/D)** and the debrominated **2.3(H/D)** (results from Scheme 2.4 – *vide infra*). The aromatic protons are easily identified and integrated.

References begin on p.68

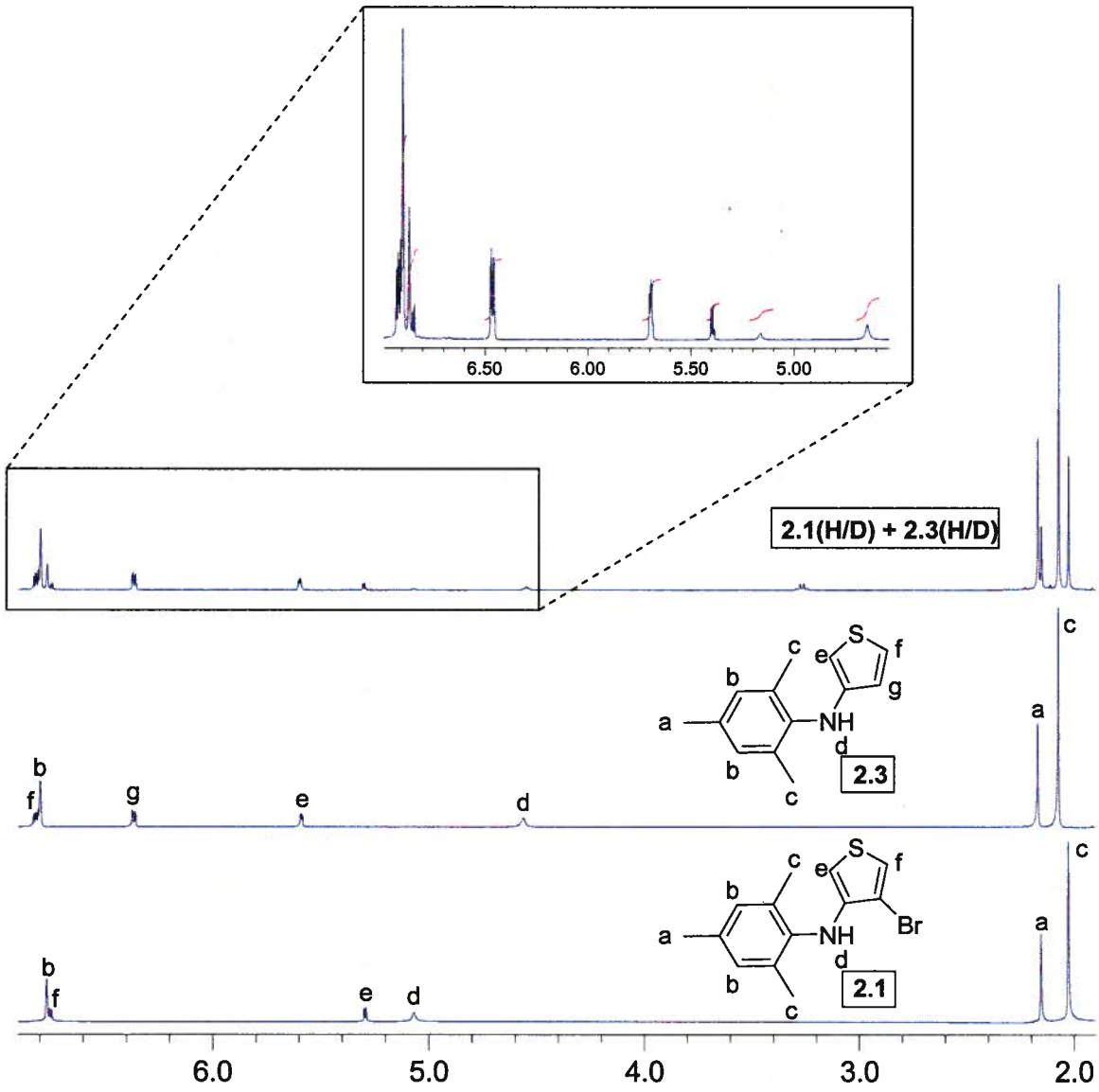

Figure 2.6. ^{1}H NMR spectra of **2.1** and **2.3** in C_6D_6. The result from a deuteration experiment using 1 equivalent ^{t}BuLi and 1 equivalent CF_3COOD is shown as an example **(2.1(H/D) + 2.3(H/D))**. Inset is a typical integration of the N-H, 2-, 4- and 5- (always integrated with the *meta*-mesityl protons) H/D ratios. These results are from the experiment shown in Scheme 2.4 (*vide infra*).

References begin on p.68

An experiment performed using 1 equivalent of **2.1**, 2 equivalents of ^{t}BuLi and 2 equivalents of CF_3COOD as the quenching agent, yielded convincing evidence to disprove Mechanism A. The results were analysed and the ratios integrated by ^{1}H NMR spectroscopy in C_6D_6. The averaged results of two runs are summarized in Scheme 2.3.

Scheme 2.3

These results show that there is complete deprotonation of the N-H moiety as well as lithium-bromine exchange, with no sign of **2.1** or a deuterated analog. The lack of an N-H bond in the product serves to disprove the intramolecular proton transfer mediated by the N-H bond proposed in Mechanism A. Furthermore, these results clearly show that the 2 equivalents of ^{t}BuLi were completely consumed by **2.1** since there is an approximate 200% deuterium count in the product, indicating two lithiations occured. Therefore, the process from Scheme 2.2, where 2 equivalents of ^{t}BuLi are needed per halide, does not seem to be applicable since this would be expected to produce an approximate 100% total deuterium count in the product as a result of only one lithiation. Instead, the approximate 200% deuterium count in the product suggests that 1 equivalent of ^{t}BuLi was used for lithium-bromine exchange and 1 equivalent used for deprotonation.

Further evidence to discount the reaction in Scheme 2.2 was obtained in a test reaction of **2.1** using 3 equivalents of ^{t}BuLi and 1 equivalent of chlorodiphenylphosphine (Ph_2PCl). The product distribution is shown in Equation 2.3. The *tert-*

References begin on p.68

butyldiphenylphosphine (Ph_2P^tBu) formed was characterized by comparison to its known $^{31}P\{^1H\}$ and ^1H NMR spectra.[44] The formation of significant amounts of both this compound and **2.3** suggests that both unconsumed ^tBuLi and lithiated **2.3** react competitively with Ph_2PCl before the Me_3NHCl quench. This experiment suggests that the reaction in Scheme 2.2 does not occur here since lithium-bromine exchange and N-H deprotonation using ^tBuLi would be expected to consume all 3 equivalents of the reagent in the reaction mixture, and no excess ^tBuLi would remain to react with Ph_2PCl and form the Ph_2P^tBu species.

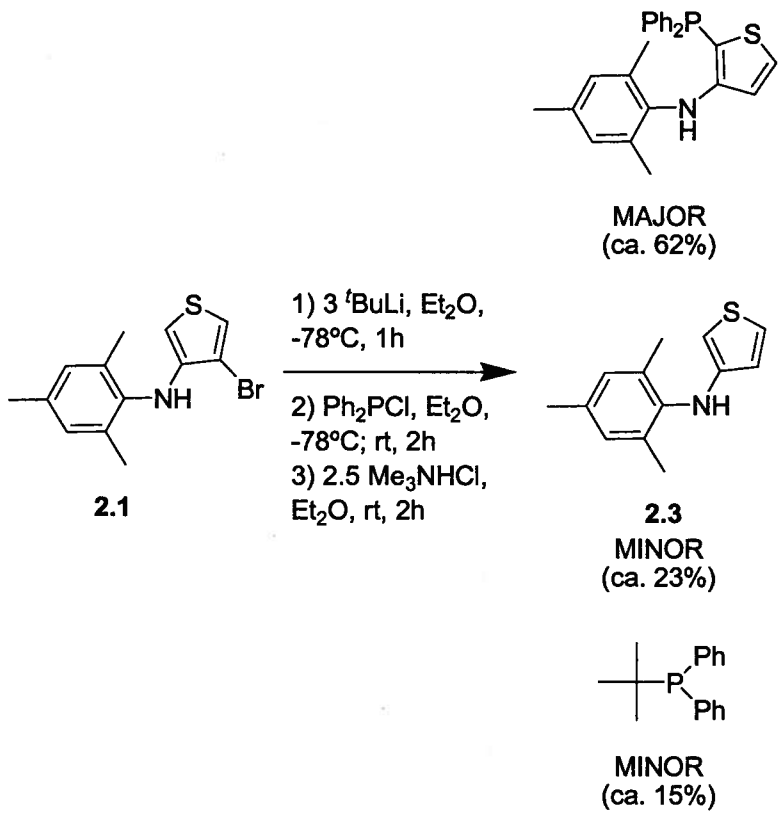

Equation 2.3

Scheme 2.3, shown above, gives convincing evidence for the presence of a dilithiated species of **2.3** similar to the proposed intermediate in Mechanism B but containing a mixture of 2- and 4- lithiation. Thus, it would be expected that in the

References begin on p.68

synthesis of **2.2**, there should also be some product with the phosphine in the 4- positions of the thiophene rings. The results from the crude, integrated ^{1}H NMR analysis of this reaction prior to purification is shown in Equation 2.4. Both $^{31}P\{^{1}H\}$ and ^{1}H NMR spectra do not indicate the presence of a 4-bonded phosphine product.

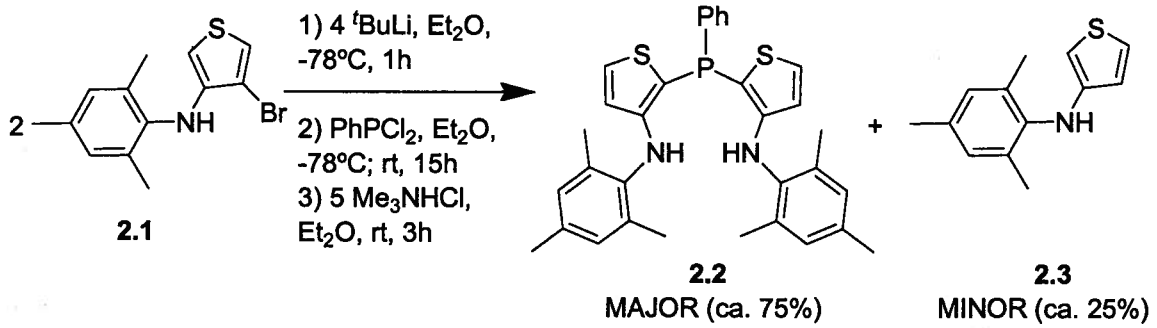

Equation 2.4

Only minor impurities, none of which indicate the presence of 4- substitution, are present in the $^{31}P\{^{1}H\}$ and ^{1}H NMR spectra. Thus, it would seem that although quenching by a small electrophile such as deuterium can lead to substitution in the 4- position, larger electrophiles such as $PhPCl_2$ or Ph_2PCl do not seem to react at this position.

Mechanism C was suggested from the results of a test reaction analogous to the synthesis of $[NPN]^{S}H_2$ (Equation 2.4), but using only 1 equivalent of $^{t}BuLi$. The details of this reaction, with approximate ratios integrated from the ^{1}H NMR spectrum, are shown in Equation 2.5.

References begin on p.68

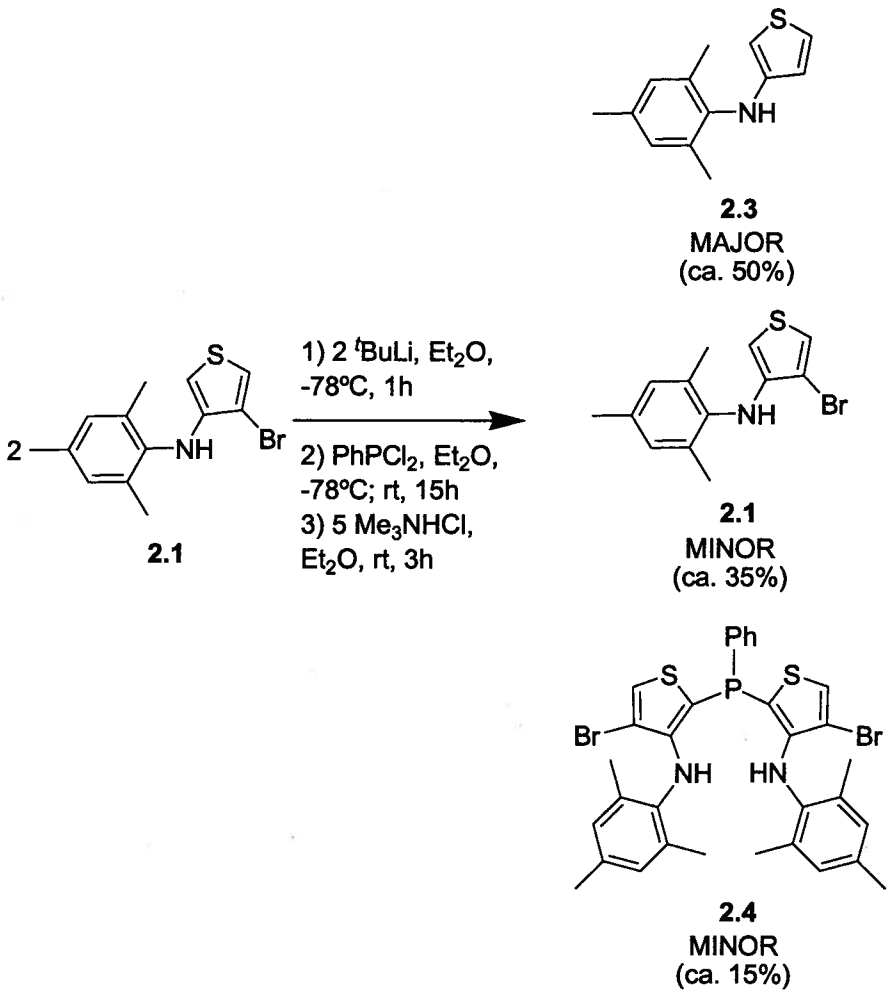

Equation 2.5

Crude $^{31}P\{^1H\}$ and ^1H NMR analysis indicate the presence of a new species, denoted **2.4**. Upon workup and isolation, EI-MS helped to identify this species since a 1:2:1 dibromo signal was obtained for the molecular ion peak and had the correct molecular weight for **2.4**, the dibrominated version of $[NPN]^SH_2$. This was unambiguously confirmed by single crystal X-ray diffraction studies of **2.4**. The solid state structure is shown in Figure 2.7.

References begin on p.68

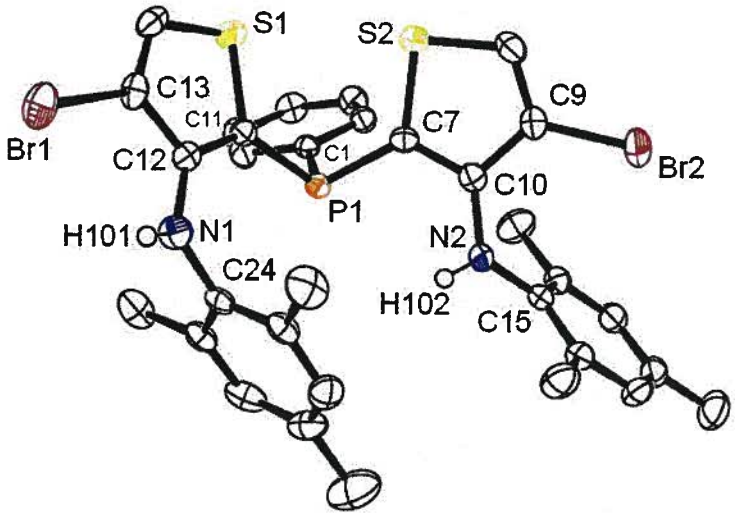

Figure 2.7. ORTEP drawing of the solid-state molecular structure of **2.4** (ellipsoids drawn at the 50% probability level). All hydrogen atoms, except the N-H bonds, have been omitted for clarity. Selected bond lengths (Å) and angles(°): C1-P1 1.847(2), C7-P1 1.807(3), C11-P1 1.811(3), C9-Br2 1.888(3), C10-N2 1.386(3), C15-N2 1.431(3), N2-H102 0.75(3), C13-Br1 1.892(3), C12-N1 1.376(3), C24-N1 1.418(4), N1-H101 0.75(3), C1-P1-C7 101.40(11), C1-P1-C11 99.71(11), C7-P1-C11 104.71(12), C10-C9-Br2 126.0(2), C10-N2-C15 126.0(2), C10-N2-H102 112(2), C15-N2-H102 116(2), C12-C13-Br1 121.0(2), C12-N1-C24 124.3(2), C12-N1-H101 116(2), C24-N1-H101 119(2).

This result can suggest a reaction pathway such as Mechanism C. Deuteration experiments were performed in order to obtain more insight into this reaction; the results of two averaged experiments using 1:1 equivalent ratios of ^{t}BuLi and CF_3COOD are summarized in Scheme 2.4. The ratios were integrated by ^{1}H NMR spectroscopy in C_6D_6.

References begin on p.68

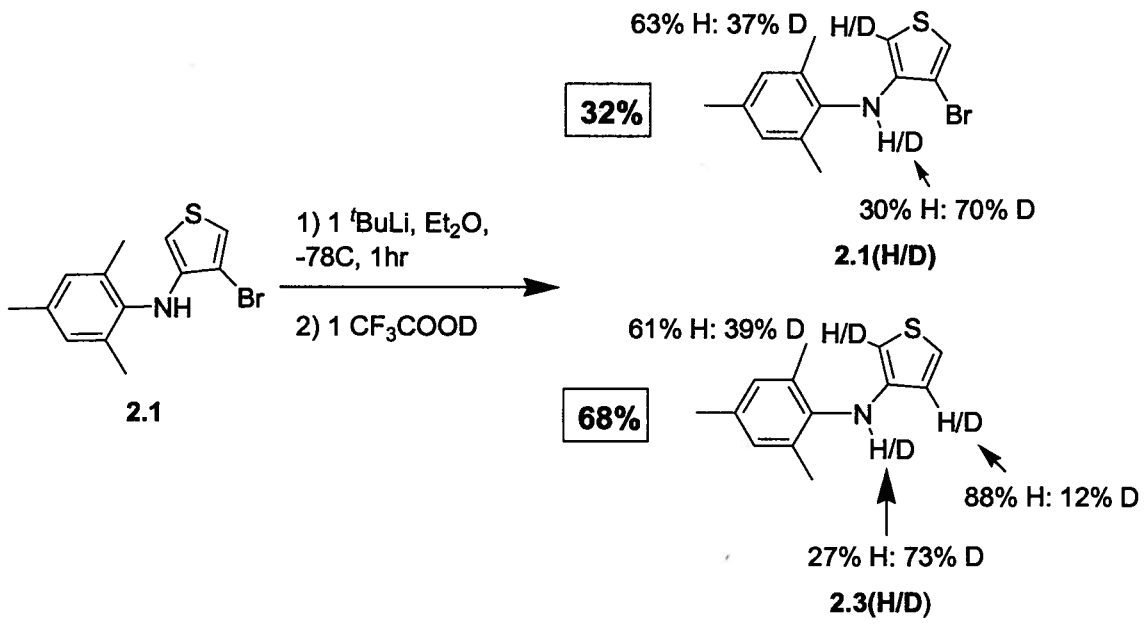

Scheme 2.4

Lithium-bromine exchange seems to be the most favourable reaction since 68% of the products no longer contain a bromine atom (**2.3(H/D)**). Furthermore, deprotonation either at the 2- or the N- position, also plays a very significant role as can be seen by the H/D ratios in both **2.1(H/D)** and **2.3(H/D)**. Closer inspection of these results reveals additional information. For example, the high proton ratio in the 4- position of **2.3(H/D)** could suggest rapid proton transfer, either intermolecularly or intramolecularly (as in Mechanism A). Also, the very similar H/D ratios in the 2- and N- positions of both **2.1(H/D)** and **2.3(H/D)** could suggest that there is a proton in equilibrium between these two positions. This is more clearly shown in Figure 2.8.

References begin on p.68

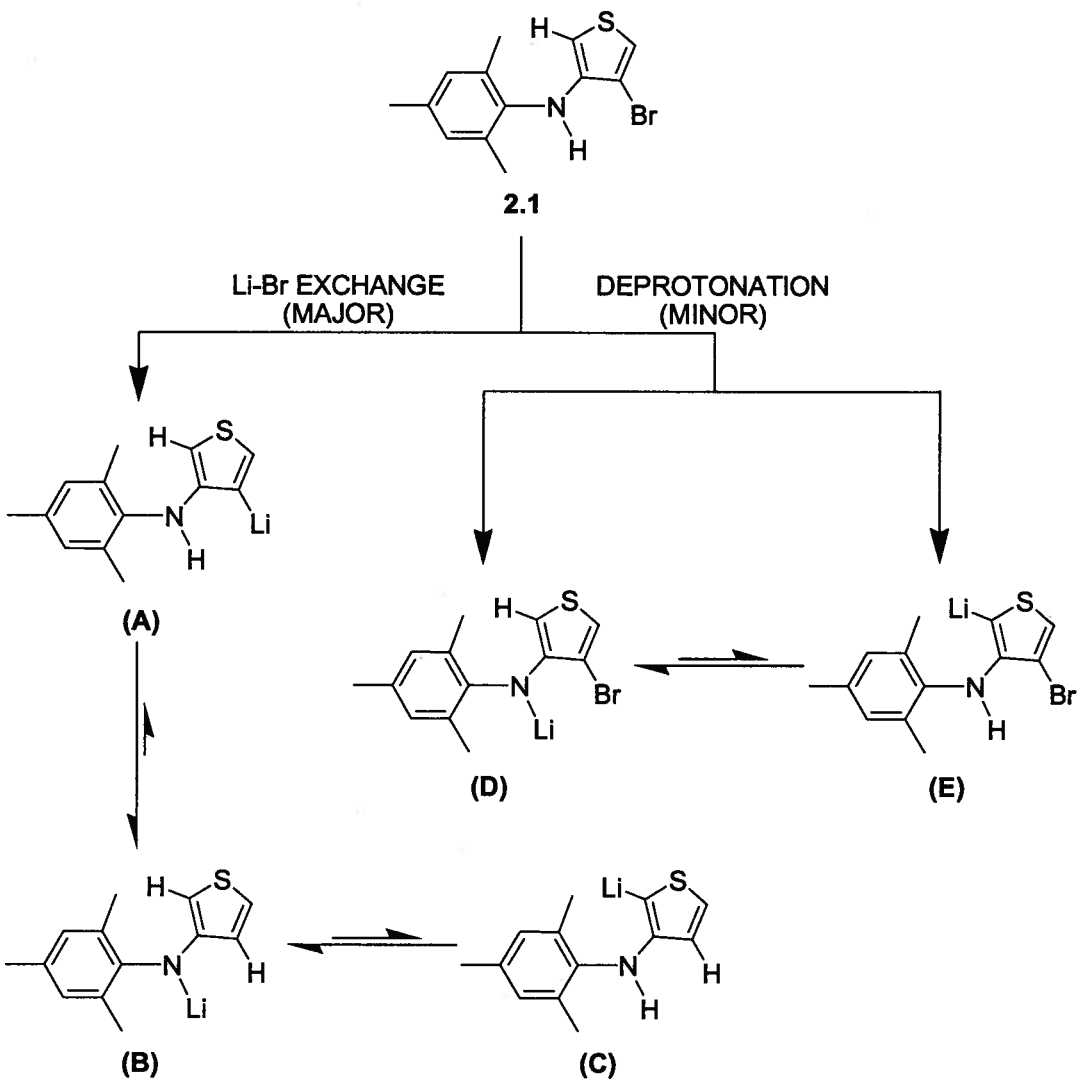

Figure 2.8. Competitive lithium-bromine exchange and deprotonation reactions can lead to the proposed equilibriums when 1 equivalent of ^{t}BuLi is used with **2.1**. Intermolecular interactions have been omitted here for simplicity.

Both the intramolecular proton transfer (**A** to **B**) along with the possible equilibrium products **B-C** and **D-E** are shown here. Both equilibriums are shifted with the Li at the N- centre. This reflects the results from Scheme 2.4 and is consistent with the proposed higher acidity of the N- centre versus the 2-C centre (*vide supra*). Although

References begin on p.68

intermolecular interactions likely play a factor in these reactions, they have been omitted here for simplicity.

What remains most important from this figure is that lithium-bromine exchange is the most favourable reaction, as seen in Scheme 2.4. In the reaction pathway proposed by Mechanism C, it is implied that 1 equivalent of ^{t}BuLi reacts with 1 equivalent of **2.1** to form the 2-lithiated **2.1** species (compound **E** in Figure 2.8). While the formation of **E** is likely to occur based on the deuteration experiments (Scheme 2.4), and while **2.4**, an essential intermediate for Mechanism C, does occur as shown in Equation 2.5, it is very unlikely that **2.2** is ultimately produced from **2.4**. Part of the reason lies in the yield of **2.4** in Equation 2.5 being only 15%. The crude reaction mixture also displays no sign of **2.2** by $^{31}P\{^{1}H\}$ and ^{1}H NMR analysis. Furthermore, as shown in both Equation 2.5 and Scheme 2.4, the major product in the reaction of **2.1** with 1 equivalent of ^{t}BuLi is the debrominated species **2.3**, the opposite of what would be expected if Mechanism C were correct. Moreover, it was previously shown that in the presence of 2 equivalents of ^{t}BuLi (as in the synthesis of **2.2**), **2.1** undergoes complete lithium-bromine exchange (see Scheme 2.3). For these reasons, Mechanism C was deemed to be unlikely.

Evidence gathered thus far suggests that Mechanism B is the most likely reaction pathway. Since the reaction of **2.1** with 1 equivalent of ^{t}BuLi and 0.5 equivalent $PhPCl_2$ shows no sign of the $[NPN]^{S}H_2$ (**2.2**) proligand, it is hypothesized that the formation of a dilithiated, as in Mechanism B, rather than monolithiated species is necessary in order to promote the reaction at the 2- position. Further evidence in the following section also suggests that the 4- position is ultimately unreactive toward $PhPCl_2$. This evidence will help to formulate a final proposed mechanism for this reaction.

References begin on p.68

2.2.5 Attempt to Promote Phosphine Incorporation in the 4- Position of Thiophene

In order to probe the reactivity at the 4- position and "force" the phosphine in these positions of the thiophene rings, a new ligand precursor with methylated 2,5-positions, denoted **2.5**, was synthesized as shown in Equation 2.6.

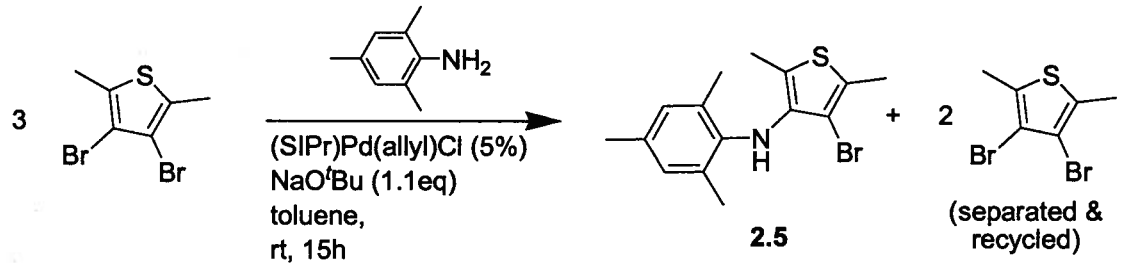

Equation 2.6

The synthesis of **2.5** is analogous to the synthesis of **2.1**; however, a slightly more arduous workup is required and the isolated yield is lower (55%) due to the apparent sensitivity of this compound to silica gel chromatography. This compound was fully characterized by ^{1}H and ^{13}C NMR spectroscopy, as well as EI-MS and EA.

The attempted synthesis of a new [NPN]^S-type proligand, denoted ^{Me2}[NPN]^{S}H$_2$ (**4**), with the phosphine in the 4- positions of the thiophene rings was unsuccessful. The synthesis was attempted using 3, 2 or 1 equivalents of ^{t}BuLi.

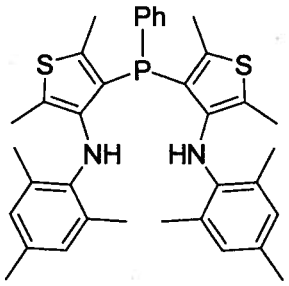

4

None of these reactions produced any evidence of the formation of **4** on the basis of ^{31}P{^{1}H} and ^{1}H NMR spectroscopy. In fact, similar to the reactions with **2.1**, significant amounts of the bromine-free material, denoted **2.6**, could be seen in the ^{1}H

References begin on p.68

NMR spectrum; this material could be separated and was characterized by ^{1}H and ^{13}C NMR spectroscopy, as well as EI-MS. The results of the reactions of **2.5** with different equivalents of $^{t}BuLi$ and with 0.5 equivalents of $PhPCl_2$ are shown in Scheme 2.5. The product ratios were integrated by ^{1}H NMR spectroscopy. Identical reaction conditions to the synthesis of **2.2** were used but are abbreviated here for clarity.

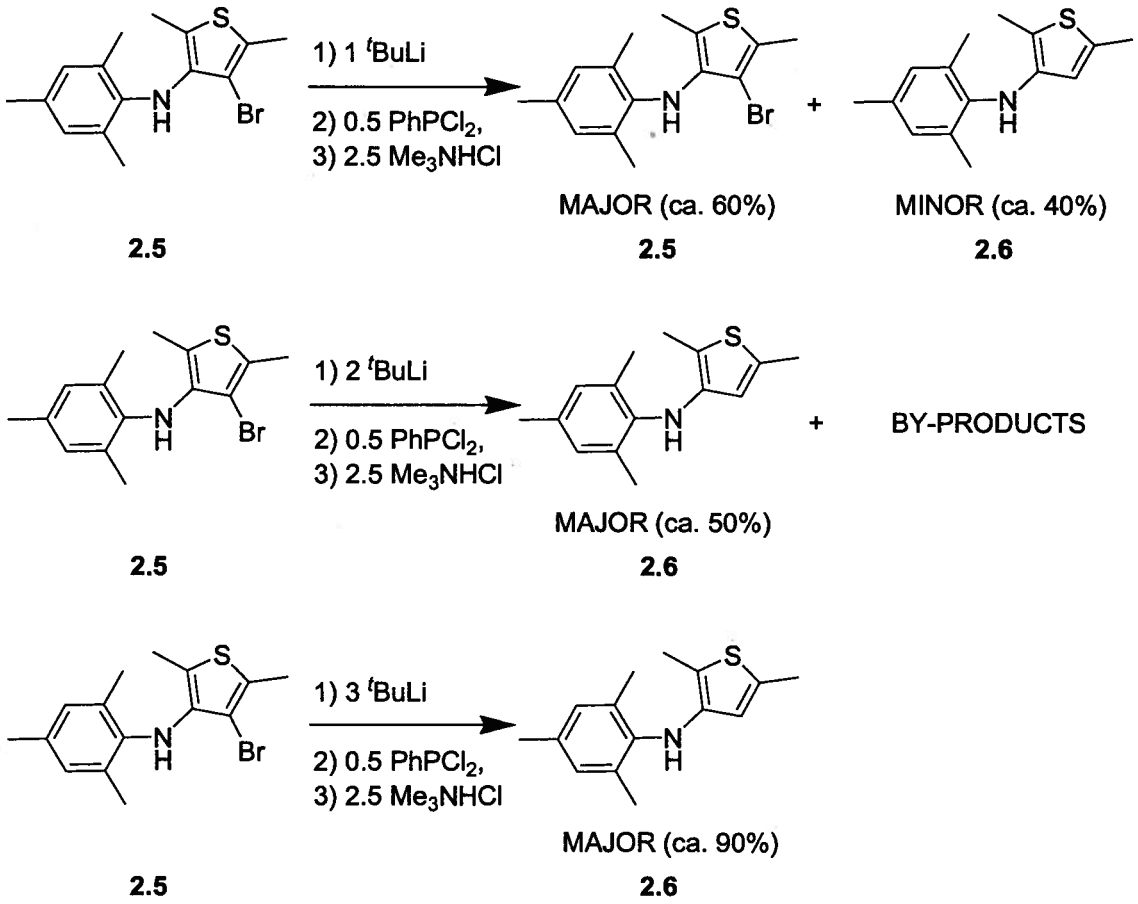

Scheme 2.5

All crude $^{31}P\{^{1}H\}$ NMR spectra for these reactions showed multiple signals due to mixtures of products – none showed any clear signs of a major product being formed. Furthermore, none of the peaks from the $^{31}P\{^{1}H\}$ NMR spectra of the 1 equivalent reaction matched the 2 equivalent reaction. One unknown peak from the 2 equivalent reaction was also seen in the 3 equivalent reaction, at -41.5 ppm; however, this last

References begin on p.68

spectrum displayed extremely weak ^{31}P signals even with a concentrated sample. Given the observation that the phosphorus-free derivative **2.6** is the major product, this lack of phosphorus-containing materials is not surprising.

The 2 equivalents reaction, as shown in Scheme 2.5, is the only one that could possibly contain **4**. However, the $^{31}P\{^{1}H\}$ NMR spectrum contains many products and the ^{1}H NMR spectrum shows large quantities of **2.6**. Attempts to separate the compounds in this mixture failed. Regardless, no clear evidence for **4** was observed in this mixture.

Deuteration experiments, analogous to those performed on **2.1**, were also performed with **2.5**. The results from these experiments are summarized in Scheme 2.6.

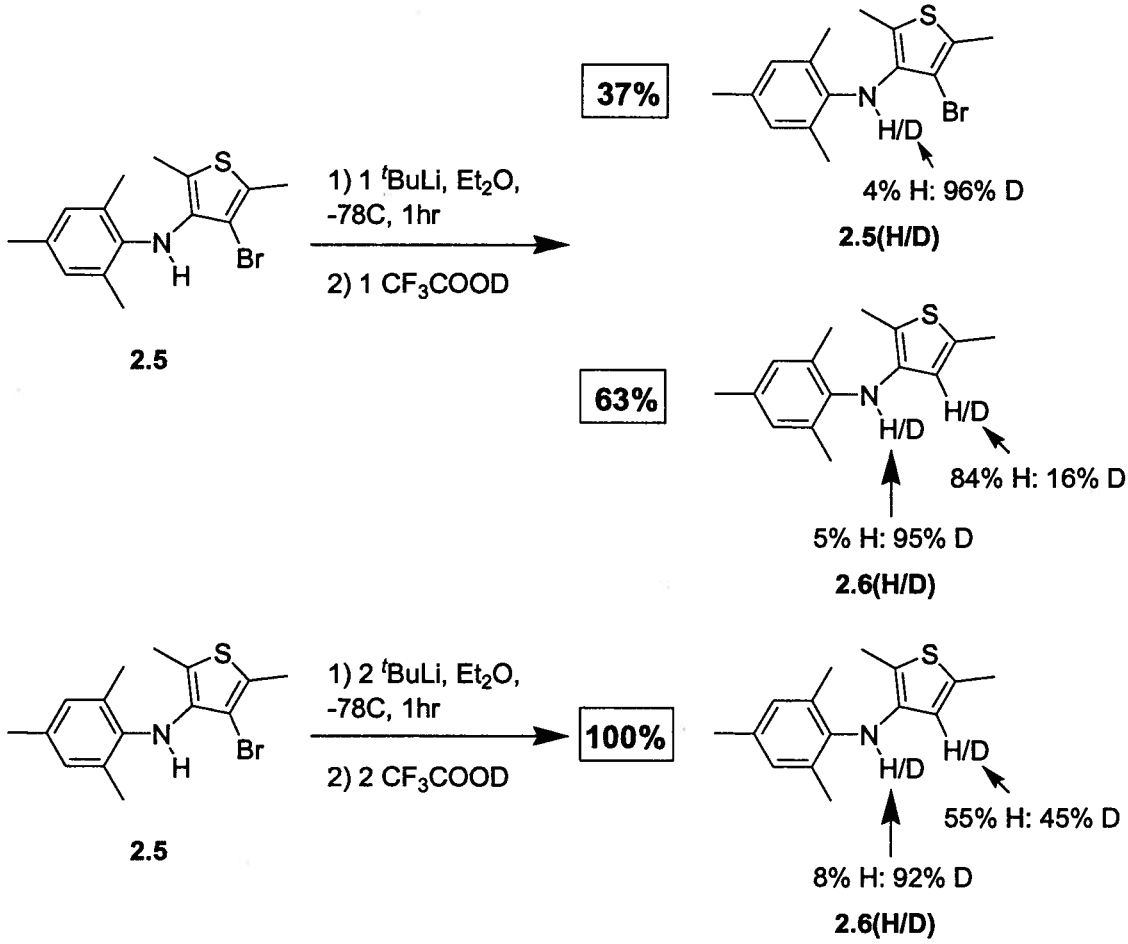

Scheme 2.6

References begin on p.68

The results using 1 equivalent of ^{t}BuLi again show a very high ratio of H in the 4-position of **2.6(H/D)**. This result can also help to explain the results from Scheme 2.5 using 1 equivalent of ^{t}BuLi. Here, only **2.5** and **2.6** were present and their yields were estimated. Considering the high H ratio at the 4- position of **2.6(H/D)** in the analogous reaction in Scheme 2.6, it would seem that the lithiated 4- position is rapidly quenched, either intramolecularly from the adjacent N-H bond or intermolecularly, and thus unavailable for further reaction with electrophiles, such as $PhPCl_2$ (Scheme 2.5) or CF_3COOD (Scheme 2.6). It should be noted that, as with **2.1** and **2.3**, it is believed that the N-Li bonds formed with either **2.5** or **2.6** are too sterically crowded to participate in any reactions with $PhPCl_2$.

Also notable from Scheme 2.6 is the significant incorporation of deuterium in the 4- position when using 2 equivalents of ^{t}BuLi. The reason for the slightly lower H count in the 4- position, as compared with the 1 equivalent reaction, is explained more clearly in Figure 2.9.

References begin on p.68

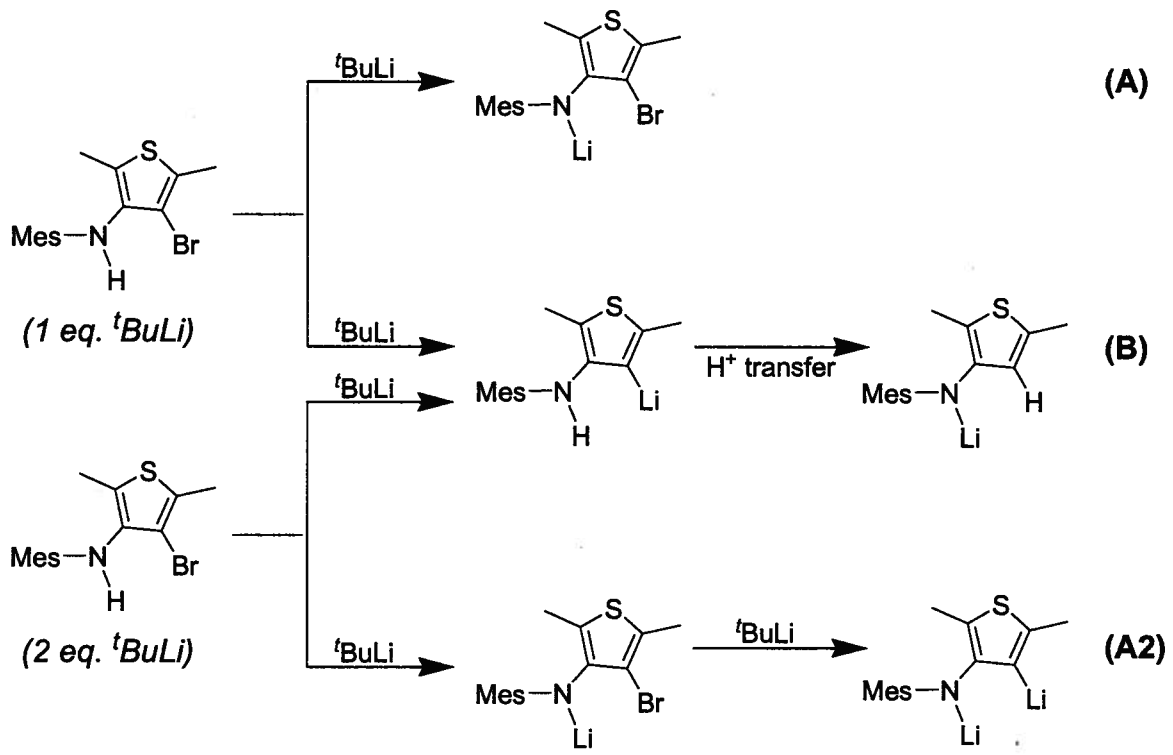

Figure 2.9. Possible proposed reactions of **2.5** when 1 or 2 equivalents of ^{t}BuLi are used.

From Figure 2.9, reaction B is speculated to be common to both reaction mixtures and the major reaction since it involves initial lithium-bromine exchange (see Scheme 2.6). Reaction B explains the high H ratios in the 4- positions (also seen in the deuteration reactions with **2.1**). Reaction A2 represents the next step to reaction A1 which, as expected, would be more common when higher concentrations of ^{t}BuLi are used. However, as opposed to Reaction B, Reaction A2 leads to a C-Li bond in the 4-position. Quenching of this bond with CF_3COOD would lead to a C-D bond. Reaction A2 is expected to be more prevalent with higher ^{t}BuLi concentrations. It is also likely what causes the higher deuterium count in the 4- position when 2 equivalents of ^{t}BuLi are used as opposed to only 1 equivalent.

References begin on p.68

Although a C-Li bond seems to form in the 4- position of **2.5** (and also with **2.1**), it does not seem to react favourably with $PhPCl_2$ to produce the desired proligand (**4**). The lack of reactivity in the 4- position, for both **2.1** and **2.5**, is likely what explains the unexpected regiochemistry obtained in the synthesis of the $[NPN]^SH_2$ proligand (**2.2**). Thus, both **2.1** and **2.5** display the same trend in that the C-Li bond forms in the 4-position but does not react with $PhPCl_2$; however, it can be deuterated with smaller electrophiles such as deuterium.

In conclusion, various experiments using **2.1** and **2.5** with $PhPCl_2$, Ph_2PCl or CF_3COOD seem to support that lithium-bromine exchange occurs predominantly in these reactions, but is in competition with the deprotonation of the N-H and/or the 2- position (for **2.1**) protons. Through extensive reactivity studies on **2.1** and **2.5** using either CF_3COOD or $PhPCl_2$, it is believed that the 4- position C-Li bond that initially forms via lithium-bromine exchange does not favourably react with $PhPCl_2$. Part of the reason likely has to do with inter- or intramolecular proton transfer quenching this 4- position. In the case of **2.1**, it is believed that this, along with competitive deprotonation in the 2-position, leads to the formation of the required 2,N-dilithiated species which ultimately forms the $[NPN]^SH_2$ proligand (**2.2**). Finally, it should be noted that longer reaction times at -78°C prior to deuteration or changing the reaction temperature to room temperature prior to deuteration did not produce any significantly different results.

2.2.6 Synthesis of a New $[OOO]H_2$ Proligand

The synthesis of a new linear-linked aryloxide proligand $[OOO]H_2$ ($[OOO]H_2$ = 2,6-bis(3-adamantyl-5-*t*-butyl-2-hydroxybenzyl)-4-*t*-butylanisole) was initiated in order to see if any differences could be observed in its reactivity and coordination chemistry

References begin on p.68

compared to known examples.[16] The new proligand (**2.9**), similar to both those from Scott and Kawaguchi's groups shown in Figure 2.2, features bulky adamantyl groups on the outer *ortho* positions of the phenyl side-arms and *tert*-butyl groups in all three *para* positions of the phenyl rings. The details of this three step synthesis are shown in Scheme 2.7.

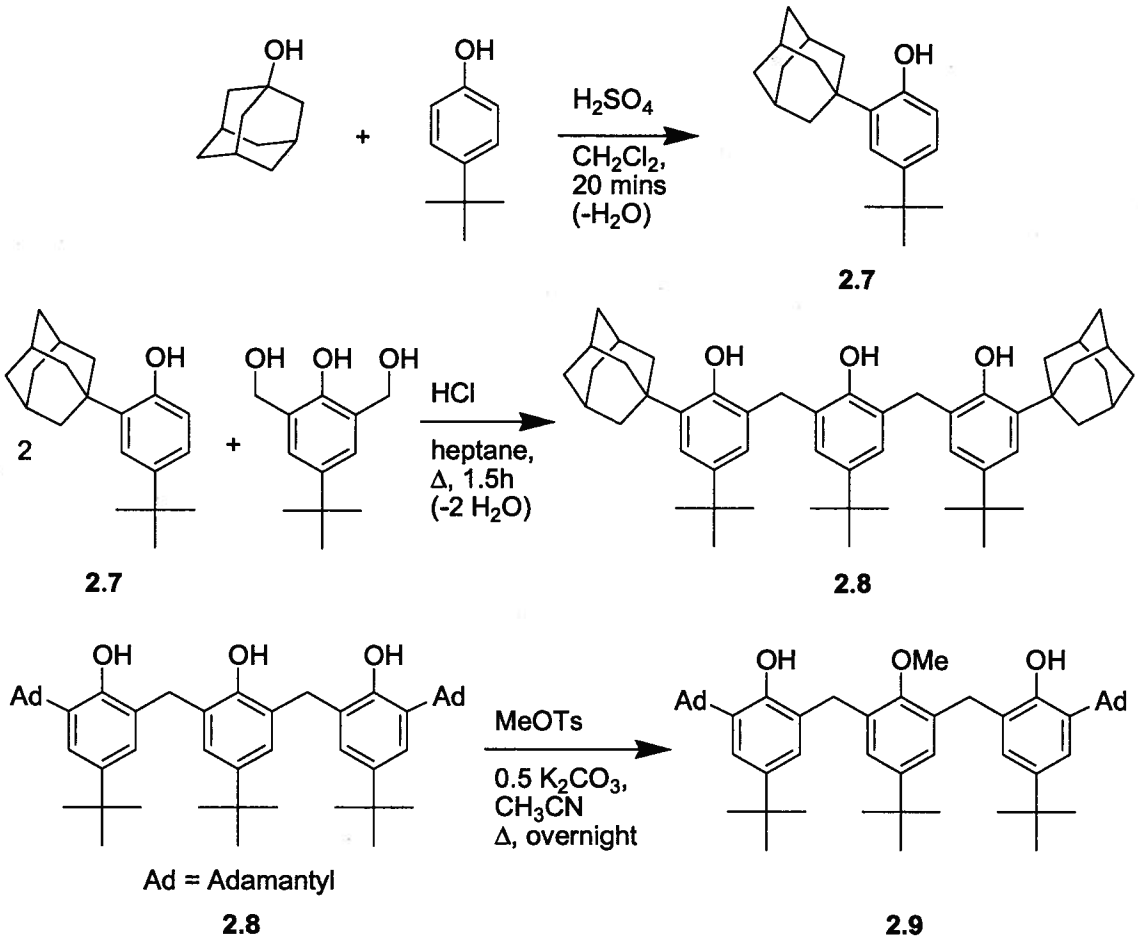

Scheme 2.7

The initial condensation step to produce **2.7** follows a known procedure (for the *para*-methyl analog) with minor modifications.[45] It should be noted that **2.7** is commercially available but only in milligram quantities and only from very few suppliers. The yield for this reaction is 67% on a 20g scale.

References begin on p.68

The next step in the synthesis involves another condensation reaction using 2.2 equivalents of **2.7** with one equivalent of 2,6-bis(hydroxymethyl)-4-*t*-butylphenol (synthesized by a known procedure)[46] to produce **2.8** following a similar literature preparation.[10] The procedure that was followed for this reaction to form an analogous compound required the use of a 7:1 ratio of the phenol:triol. We discovered that equally good yields could be obtained using only 2.2 equivalents of **2.7** instead of 7. This makes the workup procedure much easier. The final yield for the synthesis of **2.8** is 63%. It was characterized by ^{1}H and ^{13}C NMR and EI-MS. The results are consistent with the proposed structure. Unfortunately, no EA has yet been obtained for this compound since this species seems to display a very strong affinity for residual solvents such as pentane, hexane, dichloromethane and toluene. Thus, even heating this compound under high vacuum for extended periods of time did not yield the solvent free compound.

The final reaction to form the new $[OOO]H_2$ proligand (**2.9**) involves a methylation reaction to selectively methylate the central phenol using methyl *para*-toluenesulfonate (MeOTs). This was done following the exact procedure of a similar previously reported synthesis.[47] Compound **2.9** is obtained in 75% yield. It was fully characterized by ^{1}H and ^{13}C NMR, EI-MS and EA and the results are consistent with the proposed structure. The new methyl peak can be easily seen as a sharp singlet in the ^{1}H NMR (C_6D_6) spectrum at 3.31 ppm. The chemistry of this new, air-stable, proligand has been explored and is presented in the following chapter.

2.3 Conclusions

In this chapter, the syntheses of new [NPN] and [OOO]-type proligands are reported. The new $[NPN]^{S}H_2$ proligand features a bridging five-membered thiophene

References begin on p.68

ring, the first of its kind in our laboratory. The precursor to this proligand was successfully synthesized by a high yielding *N*-aryl amination reaction using 3,4-dibromothiophene and mesitylaniline. To the best of our knowledge, there are no known high-yielding *N*-aryl amination reactions using 3,4-dibromothiophene to exclusively produce the singly substituted product. The final step in the synthesis of the $[NPN]^{S}H_2$ proligand is a salt metathesis reaction using the lithiated ligand precursor and $PhPCl_2$. The product of this reaction has an unexpected regiochemistry since the phosphine was expected to be attached in the 4- positions of the thiophene rings, where lithium-bromine exchange reactions occur, rather than the resulting 2- positions. Detailed mechanistic investigations suggest that lithium-bromine exchange is the predominant reaction, but is in competition with the deprotonation of the N-H and/or the 2- position protons. Lithium-bromine exchange produces the 4- position C-Li bond; however, evidence suggests that this bond does not react favourably with $PhPCl_2$ to produce the expected regiochemistry in the product. Moreover, this C-Li centre is believed to be significantly quenched inter- or intramolecularly by proton transfer, thus making it unavailable for further reactivity. This, along with the competitive deprotonation reaction in the 2-position, may serve to promote the formation of the required 2,N-dilithiated species which ultimately reacts predominantly with $PhPCl_2$ to form the $[NPN]^{S}H_2$ proligand.

As a further exploration in ligand design for early transition metal activation of N_2, a new dianionic linear-linked aryloxide proligand, denoted $[OOO]H_2$, was successfully synthesized. The proligand can be synthesized by an easy three step procedure to yield the final product in moderate yield. The synthesis of this compound can be readily done on a multi-gram scale. Chapter 3 will explore the coordination

References begin on p.68

chemistry of both the [OOO] and $[NPN]^S$ ligands with group 4 and group 5 metals. Efforts into the activation of N_2 using new $Zr[NPN]^S$ complexes are also discussed.

2.4 Experimental Section

2.4.1 General Considerations

Unless otherwise stated, all manipulations were performed under an atmosphere of dry, oxygen-free N_2 or Ar by means of standard Schlenk or glovebox techniques (Innovative Technology glovebox equipped with a –35 °C freezer). Hexanes, toluene, tetrahydrofuran, pentane, benzene, and diethyl ether were purchased anhydrous from Aldrich, sparged with N_2, and passed through columns containing activated alumina and Ridox catalyst. Dichloromethane (DCM), heptane and acetonitrile, all for the synthesis of **2.7-2.9**, were purchased anhydrous and used without further purification. $CDCl_3$ and C_6D_6 were dried on activated 5Å molecular sieves and freeze-pump-thaw degassed three times. The high vacuum line was equipped with a Hg diffusion pump and could attain a maximum vacuum of 1 millitorr. ^1H, $^{31}P\{^1H\}$, and $^{13}C\{^1H\}$ NMR spectra were recorded on a Bruker AV-300, a Bruker AV-400, or a Bruker AV-400inv spectrometer, operating at 300.1, 400.0, and 400.0 MHz for ^1H spectra, respectively. All spectra were recorded at room temperature. ^1H NMR spectra were referenced to residual protons in the deuterated solvent: C_6D_6 (7.16 ppm), $CDCl_3$ (7.24 ppm). $^{31}P\{^1H\}$ NMR spectra were referenced to external $P(OMe)_3$ (141.0 ppm with respect to 85% H_3PO_4 at 0.0 ppm). $^{13}C\{^1H\}$ NMR spectra are referenced to residual solvent: C_6D_6 (128.0 ppm) or $CDCl_3$ (77.23 ppm). Chemical shifts (δ) listed are in ppm, and absolute values of the coupling constants are in Hz. GC-MS spectra were recorded on an Agilent series 6890 GC system with a 5973 mass selective detector. Mass spectrometry (EI-MS), elemental analysis (C, H, N) and

References begin on p.68

X-ray crystallography were all performed at the Department of Chemistry of the University of British Columbia.

2.4.2 Starting Materials and Reagents

Mesitylaniline and $PhPCl_2$ (Aldrich) were both distilled prior to use. 3,4-dibromothiophene (Alfa) was degassed by freeze-pump-thaw and mixed with activated molecular sieves (5Å). CF_3COOD, purchased in sealed glass ampoules, Me_3NHCl and MeOTs (Aldrich) were used without further purification. 3,4-dibromo-2,5-dimethylthiophene,[48] (SIPr)Pd(allyl)Cl,[49] and 2,6-bis(hydroxymethyl)-4-*t*-butylphenol[46] were prepared by literature methods. ^{t}BuLi (~1.7 M in pentane) was doubly titrated using a known literature procedure.[50] All other compounds were purchased from commercial suppliers and were used as received.

Synthesis of 2.1. A 500 mL round bottom Schlenk flask equipped with a magnetic stir bar, was charged with (SIPr)Pd(allyl)Cl (1.17 g, 2 mmol), NaO^{t}Bu (4.33 g, 45 mmol) and toluene (300 mL). The reaction mixture was stirred for 5 minutes then 3,4-dibromothiophene (13.7 mL, 124 mmol) and mesitylaniline (5.8 mL, 41 mmol) were added all at once. The solution quickly turned dark green/brown and was allowed to stir overnight (15 hrs). The mixture was then poured on 300 mL water in open air. The organic phase was separated and washed with another 2 x 300 mL water. The combined aqueous extracts were washed with 2 x 100 mL toluene. The organics were combined and dried with $MgSO_4$. The mixture was filtered and the toluene was removed by roto-evaporation (rotovap). Column chromatography using silica gel of the resulting black crude liquid separated the excess 3,4-dibromothiophene (Rf = 0.71) from the desired product (Rf = 0.19) using hexanes as the solvent. Once the 3,4-dibromothiophene is

References begin on p.68

separated, the polarity of the eluent can be increased to 2% Et_2O in hexanes. The total weight of the pure white product is 9.0 g (74% yield). Slow evaporation of a hexanes solution of the compound yielded single crystals suitable for X-ray crystallography.

^{1}H NMR (400 MHz, C_6D_6): δ 6.77 (s, 2H), 6.75 (d, J = 3.6 Hz, 1H), 5.29 (d, J = 3.6 Hz, 1H), 5.07 (bs, 1H), 2.16 (s, 3H), 2.03 (s, 6H).

^{13}C NMR (100 MHz, C_6D_6): δ 143.3, 137.2, 135.4, 135.2, 129.6, 122.4, 102.8, 96.8, 21.0, 17.9.

Anal. Calcd for $C_{13}H_{14}BrNS$: C, 52.71; H, 4.76; N, 4.73. Found: C, 53.00; H, 4.95; N, 4.96.

EI-MS (m/z): 297 $[M]^+$, 216 $[M - Br]^+$.

Synthesis of $[NPN]^SH_2$ (2.2). A 1 L, 2-neck round bottom Schlenk flask was equipped with a magnetic stirbar and 2 dropping funnels. One was charged with 2.04 eq. ^{t}BuLi (1.74 M in pentane, 60 mL, 104 mmol) and the other with a dilute solution of 0.5 eq. $PhPCl_2$ (3.38 mL, 25 mmol) in 250 mL Et_2O. The round bottom was loaded with 15 g (50 mmol) of **2.1** in 300 mL Et_2O. The solution was stirred and was cooled to -78°C (dry ice/acetone bath) on the Schlenk line. The ^{t}BuLi solution was added dropwise to the solution. The pale yellow solution was kept at -78°C while stirring for 1 hour following the addition. The $PhPCl_2$ solution was then added dropwise at -78°C over 5 hours. The solution gradually went from pale yellow to dark orange/brown. The solution was allowed to warm to room temperature overnight. The following morning, an excess of Me_3NHCl (11.95 g, 125 mmol) was added all at once to the stirring solution. The solution was stirred for 3 hours after which time the Et_2O was removed *in vacuo*. The brown residue was dissolved in ca. 200 mL toluene and was filtered on a glass frit with

References begin on p.68

celite. The celite was then washed with toluene. The toluene was thoroughly removed *in vacuo* to obtain a viscous dark brown/blackish residue. The residue was mixed with ca. 200 mL hexanes. A pale beige solid nicely crashed out of this and was filtered on a glass frit. Repeated trituration using hexanes yielded 6.8 g (50% yield) of pure product.

^{1}H NMR (400 MHz, C_6D_6): δ 7.75-7.71 (m, 2H), 7.14-7.11 (m, 2H), 7.06-7.02 (m, 1H), 6.88 (d, J = 5.2 Hz, 2H), 6.76 (s, 4H), 6.19 (dd, J_{H-H} = 5.2 Hz, J_{P-H} = 2.6 Hz, 2H), 5.79 (*N-H*) (d, J_{P-H} = 3.2 Hz, 2H), 2.15 (s, 6H), 2.10 (s, 12H).

^{31}P{^{1}H} NMR (161 MHz, C_6D_6): δ -55.5.

^{13}C NMR (100 MHz, C_6D_6): δ 153.7 (d, J = 74.4 Hz), 138.0, 137.8, 135.6, 135.2, 132.2 (d, J = 70.8 Hz), 131.3 (d, J = 11.2 Hz), 129.5, 128.8 (d, J = 25.6), 128.4, 119.3 (d, J = 14.8 Hz), 103.8 (d, J = 61.2 Hz), 20.9, 18.4.

Anal. Calcd for $C_{32}H_{33}N_2PS_2$: C, 71.08; H, 6.15; N, 5.18. Found: C, 71.31; H, 6.29; N, 5.51.

EI-MS (m/z): 540 $[M]^+$, 525 $[M - CH_3]^+$.

Isolation of 2.3. This air-sensitive compound was extracted from the crude reaction mixture in the attempted synthesis of **2.2** using 3 equivalents of ^{t}BuLi (analogous to Synthesis of $[NPN]^SH_2$ (**2.2**) but using 3 eq. ^{t}BuLi). Once the viscous dark brown/blackish residue is obtained after the celite filtration, the Schlenk flask containing the residue was fitted with a distillation bridge attached to a flask submerged in liquid N_2. The apparatus was attached to the high vacuum line and the pressure was reduced to 10 millitorr. The oily compound was distilled off by heating the flask to 125-135°C.

References begin on p.68

^{1}H NMR (400 MHz, C_6D_6): δ 6.82 (dd, J = 3.2 Hz, J = 5.2 Hz, 1H), 6.80 (s, 2H), 6.37 (dd, J = 1.6 Hz, J = 5.2 Hz, 1H), 5.59 (dd, J = 1.6 Hz, J = 3.2 Hz, 1H), 4.56 (bs, 1H), 2.17 (s, 3H), 2.07 (s, 6H).

^{13}C NMR (100 MHz, C_6D_6): δ 146.9, 138.3, 134.7 (2 overlapping carbons), 129.6, 125.2, 120.0, 98.3, 20.9, 18.1.

Anal. Calcd for $C_{13}H_{15}NS$: C, 71.84; H, 6.96; N, 6.44. Found: C, 72.22; H, 7.02; N, 6.38.

EI-MS (m/z): 217 $[M]^+$, 202 $[M - CH_3]^+$.

Synthesis of 2.4. A 250 mL, 2-neck round bottom Schlenk flask was equipped with a magnetic stirbar and 2 dropping funnels. One was charged with 1.05 eq. ^{t}BuLi (1.62 M in pentane, 3.28 mL, 5.3 mmol) and the other with a dilute solution of 0.5 eq. $PhPCl_2$ (0.34 mL, 2.5 mmol) in 25 mL Et_2O. The round bottom was loaded with 1.5 g (5.0 mmol) of **2.1** in 30 mL Et_2O. The solution was stirred and was cooled to -78°C (dry ice/acetone bath) on the Schlenk line. The ^{t}BuLi solution was added dropwise to the solution. The pale yellow solution was kept at -78°C while stirring for 1 hour following the addition. The $PhPCl_2$ solution was then added dropwise at -78°C over 5 hours. The solution gradually went from pale yellow to beige/orange. The solution was allowed to warm to room temperature overnight. The following morning, an excess of Me_3NHCl (1.50 g, 15.7 mmol) was added all at once to the stirring solution. The solution was stirred for 3 hours after which time the Et_2O was removed *in vacuo*. The brown residue was dissolved in ca. 20 mL toluene and was filtered on a glass frit with celite. The celite was then washed with toluene. The toluene was thoroughly removed *in vacuo* to obtain a viscous dark brown/blackish residue. The black residue was dissolved in minimal toluene and filtered through 10 cm of silica on a glass frit to remove the black impurities.

References begin on p.68

The toluene was removed from the extracts *in vacuo* to yield an oil. Trituration of this oil using hexanes yields a white powder than can be purified by subsequent hexanes and pentane washes. Minimal yield is obtained (11%, 0.200 g). Single crystals suitable for X-ray diffraction can be grown by slow evaporation of a benzene solution.

^{1}H NMR (400 MHz, C_6D_6): δ 7.16-7.12 (m, 2H), 7.00-6.95 (m, 3H), 6.92 (d, J_{H-P} = 1.2 Hz, 2H), 6.66 (bs, 2H), 6.49 (bs, 2H), 5.14 (bs, 2H), 2.10 (s, 6H), 2.02 (s, 6H), 1.89 (s, 6H).

^{31}P{^{1}H} NMR (161 MHz, C_6D_6): δ -41.6.

EI-MS (m/z): 698 $[M]^+$, 683 $[M - CH_3]^+$.

Synthesis of 2.5. A 500mL round bottom Schlenk flask equipped with a magnetic stir bar, was charged with (SIPr)Pd(allyl)Cl (0.704 g, 1.23 mmol), NaO^{t}Bu (2.61 g, 27 mmol) and toluene (200 mL). The reaction mixture was stirred for 5 minutes then 3,4-dibromo-2,5-dimethylthiophene (20.0 g, 74 mmol) and mesitylaniline (3.47 mL, 25 mmol) were added all at once. The solution quickly turned dark green/brown and was allowed to stir overnight. The next morning, the toluene was removed *in vacuo*. The black residue was dissolved in 150 mL DCM and 150 mL water was added to this in open atmosphere. The phases were separated and the organic phase washed with another 2 x 150 mL water. The combined aqueous phases were then washed with another 2 x 150 mL DCM. The organic phases were combined, dried with $MgSO_4$, filtered and rotovaped to yield a black residue. This residue was dissolved in minimal toluene and filtered on 10 cm packed silica on a glass frit. Toluene was added until no more 3,4-dibromo-2,5-dimethylthiophene and no more product were seen by TLC (Rf values of 0.79 and 0.29 respectively using hexanes as solvent). The toluene was removed *in vacuo* from the

References begin on p.68

extracts. A dark brown liquid remained. A portion of the product was obtained by trituration of this liquid by slowly adding ethanol (EtOH). The product is filtered and approximately 1.75 g (22% yield) of pure white product is obtained. The EtOH washings are brought to dryness and further purification is done by flash chromatography on silica using hexanes to separate the 3,4-dibromo-2,5-dimethylthiophene and rapidly increasing to 4% Et_2O in hexanes. Approximately 8 g of pure 3,4-dibromo-2,5-dimethylthiophene is recycled in this step and a further 2.6 g (33% yield) of pure product is obtained. The combined yield is therefore 4.35 g (55% yield).

^{1}H NMR (400 MHz, C_6D_6): δ 6.72 (s, 2H), 4.78 (bs, 1H), 2.14 (s, 3H), 2.10 (s, 3H), 2.02 (s, 6H), 1.59 (s, 3H).

^{13}C NMR (100 MHz, C_6D_6): δ 138.1, 136.5, 133.4, 133.3, 129.3, 128.8, 112.1, 106.7, 20.9, 18.6, 15.1, 12.5.

Anal. Calcd for $C_{15}H_{18}BrNS$: C, 55.56; H, 5.59; N, 4.32. Found: C, 55.92; H, 5.61; N, 4.33.

EI-MS (m/z): 325 $[M]^+$, 244 $[M - Br]^+$.

Isolation of 2.6. This compound was extracted from the crude reaction mixture in the attempted synthesis of **4** using 3 equivalents of ^{t}BuLi (exactly the same procedure as the synthesis of **2.2**). Once the viscous dark brown/blackish residue is obtained after the celite filtration (see synthesis of **2.2** for details), the Schlenk flask containing the residue was fitted with a distillation bridge attached to a flask submerged in liquid N_2. The apparatus was attached to the high vacuum line and the pressure was reduced to 10 millitorr. The solid compound was not distilled off but rather sublimed when heating the flask to 150°C.

References begin on p.68

^{1}H NMR (400 MHz, C_6D_6): δ 6.82 (s, 2H), 6.02 (s, 1H), 4.24 (bs, 1H), 2.19 (s, 3H), 2.11 (s, 6H), 2.06 (s, 3H), 2.01 (s, 3H).

^{13}C NMR (100 MHz, C_6D_6): δ 141.2, 139.7, 134.1, 133.6, 133.5, 129.6, 119.8, 111.1, 20.9, 18.4, 15.3, 11.4.

Satisfactory EA values for this compound could not be obtained due small amounts of inseparable impurities.

EI-MS (m/z): 245 $[M]^+$, 230 $[M - CH_3]^+$, 212 $[M - S]^+$.

Synthesis of 2.7. This compound was synthesized following a similar procedure to previously reported.[45] In a 500 mL single neck round bottom, 15.41 g (103 mmol) of 4-*tert*-butylphenol was dissolved in 90 mL DCM. 16.42 g (108 mmol) 1-adamantanol was then added to the mixture. While stirring the solution vigorously, H_2SO_4 (18 M, 6.0 mL) is added dropwise over 20 minutes. The biphasic mixture is then stirred for another 20 minutes. 100 mL H_2O is then added to the mixture. The solution was brought to a pH of 9.0 with the slow addition of a solution of NaOH (2 M). The mixture was extracted with DCM (3 x 100 mL). The combined organics were washed with 150 mL brine, dried with $MgSO_4$, filtered and rotovaped. The off-white solids are then dissolved in a minimal amount of a warm solution of 25% (v/v) DCM in hexanes. The product is then extracted by flash silica gel chromatography using the same solution as eluent. Minor amounts of 2,6-diadamantyl-4-*tert*-butylphenol elute first but can be easily separated from the main product. Total yield is 19.46 g (67%).

^{1}H NMR (400 MHz, $CDCl_3$): δ 7.33 (d, J = 2.4 Hz, 1H), 7.14 (dd, J = 2.4 Hz, J = 8.0 Hz, 1H), 6.65 (d, J = 8.0 Hz, 1H), 4.65 (s, 1H), 2.22 (bs, 6H), 2.17 (bs, 3H), 1.87 (bs, 6H), 1.38 (s, 9H).

References begin on p.68

^{13}C NMR (100 MHz, $CDCl_3$): δ 152.2, 143.3, 135.8, 124.2, 123.5, 116.4, 40.9, 37.3, 37.1, 34.6, 31.9, 29.3.

Anal. Calcd for $C_{20}H_{28}O$: C, 84.45; H, 9.92. Found: C, 84.28; H, 9.65.

EI-MS (m/z): 284 $[M]^+$, 269 $[M - CH_3]^+$.

Synthesis of 2.8. In a 100mL round bottom flask equipped with a Dean-Stark apparatus was added 6.72g (32mmol) 2,6-bis(hydroxymethyl)-4-*t*-butylphenol and 2.2 eq. (20g, 70mmol) of 2-adamantyl-4-*t*-butylphenol (**2.7**). The solids were dissolved in 30mL hot heptane. Once dissolved, 2mL concentrated HCl (12M) was added dropwise. The solution was refluxed for 2 hours. The solution was then cooled and was washed with 3 x 50mL water. The combined aqueous phases were then washed with another 2 x 50mL DCM. The combined organic extracts were dried with $MgSO_4$, filtered and rotovaped. The product was recrystallized with hexanes and a small amount of DCM at -18°C. The white solid obtained was filtered, washed with minimal cold hexanes and dried thoroughly *in vacuo*. A total of 14.9g (63% yield) of product was obtained.

^1H NMR (400 MHz, $CDCl_3$): δ 8.13 (s, 1H), 7.21 (s, 2H), 7.19 (d, J = 1.6 Hz, 2H), 7.10 (d, J = 1.6 Hz, 2H), 6.70 (s, 2H), 3.89 (s, 4H), 2.11 (bs, 18H), 1.80 (bs, 12H), 1.29 (s, 9H), 1.28 (s, 18H).

^{13}C NMR (100 MHz, $CDCl_3$): δ 149.5, 148.0, 144.2, 143.4, 135.8, 127.6, 127.2, 126.1, 125.5, 122.5, 41.4, 37.2, 37.1, 34.5, 34.2, 32.2, 31.8, 31.7, 29.3.

Satisfactory EA values for this compound could not be obtained due to persistent residual solvents.

EI-MS (m/z): 742 $[M]^+$, 724 $[M - H_2O]^+$.

References begin on p.68

Synthesis of 2.9. The preparation of this compound followed the exact literature preparation for the related compounds.[47] The obtained yield was 75%.

^{1}H NMR (400 MHz, C_6D_6): δ 7.40 (d, J = 2.4 Hz, 2H), 7.22 (d, J = 2.4 Hz, 2H), 7.19 (s, 2H), 6.44 (s, 2H), 3.71 (s, 4H), 3.31 (s, 3H), 2.36 (bs, 12H), 2.10 (bs, 6H), 1.86 (d, ^2J = 12.0 Hz, 6H), 1.77 (d, ^2J = 12.0 Hz, 6H), 1.40 (s, 18H), 1.06 (s, 9H).

^{13}C NMR (100 MHz, C_6D_6): δ 151.6, 151.4, 148.8, 142.5, 137.0, 132.5, 126.7, 126.5, 125.2, 122.7, 62.4, 41.0, 37.7, 37.6, 34.5, 34.3, 32.0, 31.8, 31.2, 29.7.

Anal. Calcd for $C_{53}H_{72}O_3$: C, 84.08; H, 9.59. Found: C, 84.38; H, 9.78.

EI-MS (m/z): 757 $[M]^+$, 725 $[M - CH_3OH]^+$.

2.4.3 Deuteration Experiments

All deuteration experiments were performed on small scales using the exact same procedure. Only the equivalents of ^{t}BuLi and CF_3COOD can change. The example procedure is given for the deuteration of **2.1** using 1 equivalent ^{t}BuLi with 1 equivalent CF_3COOD:

In a 50 mL single-neck round bottom Schlenk flask equipped with a magnetic stirbar was added 0.200 g (0.68 mmol) **2.1**. 10 mL Et_2O was added to the solid. The solution was cooled to -78°C using a dry ice/acetone bath. 1.0 eq. ^{t}BuLi (1.62 M in pentane, 0.42 mL, 0.68 mmol) was added dropwise to the solution. The solution turned yellow and was allowed to stir at the same temperature for 1 hour. 1.0 eq. CF_3COOD (52 μL, 0.68 mmol) was added all at once. The solution was allowed to stir for 15 minutes at -78°C then the bath was removed and the solution was allowed to warm to room temperature and stir for 30 minutes. The Et_2O was removed *in vacuo*. The round bottom was brought inside the

References begin on p.68

glovebox where the oily solid was dissolved in minimal C_6D_6 and filtered through a glass fibre pad in a pipette for NMR analysis.

2.4.4 Substitution Experiments Using $PhPCl_2$ or Ph_2PCl

All experiments with 1, 2 or 3 equivalents of ^{t}BuLi were performed identically to the synthesis of **2.2** described above. The same ratios of reagents and solvents were used except for the ratio of ^{t}BuLi. For the experiment using 3 equivalents of ^{t}BuLi with one equivalent of **2.1** and 0.5 equivalent of a dilute 0.1 M solution of Ph_2PCl, the latter solution could be added more rapidly dropwise rather than over a 5 hour time span. All crude results were analysed by $^{31}P\{^1H\}$ and ^1H NMR spectroscopy following protonation, filtration through celite, and removal of solvents as described in the synthesis of **2.2**.

References begin on p.69

2.5 References

[1] Fryzuk, M. D.; Love, J. B.; Rettig, S. J.; Young, V. G. *Science*. **1997**, *275*, 1445.

[1] Fryzuk, M. D.; Haddad, T. S.; Rettig, S. J. *J. Am. Chem. Soc.* **1990**, *112*, 8185.

[1] Carmichael, C. D.; Fryzuk, M. D. *J. Chem. Soc., Dalton Trans.* **2005**, 452.

[1] Fryzuk, M. D.; MacKay, B. A.; Johnson, S. A.; Patrick, B. O. *Angew. Chem. Int. Ed.* **2002**, *41*, 3709.

[1] Corkin, J. R.; Fryzuk, M. D. *unpublished results*.

[1] MacKay, B. A.; Patrick, B. O.; Fryzuk, M. D. *Organometallics*. **2005**, *24*, 3836.

[1] Morello, L.; Yu, P.; Carmichael, C. D.; Patrick, B. O.; Fryzuk, M. D. *J. Am. Chem. Soc.* **2005**, *127*, 12796

[1] Gutsche, C. D. *Calixarenes*; Royal Society of Chemistry: Cambridge, 1989.

[1] Koebner, Z. M. *Angew. Chem.* **1933**, *46*, 251.

[1] Gordon, B. W. F.; Scott, M. J. *Inorg. Chim. Acta.* **2000**, *297*, 206.

[1] Matsuo, T.; Kawaguchi, H. *Organometallics*. **2003**, *22*, 5379.

[1] Matsuo, T.; Kawaguchi, H. *Inorg. Chem.* **2002**, *41*, 6090.

[1] Kawaguchi, H.; Matsuo, T. *J. Organomet. Chem.* **2005**, *690*, 5333.

[1] Akagi, F.; Matsuo, T.; Kawaguchi, H. *Angew. Chem. Int. Ed.* **2007**, *46*, 8778.

[1] Kawaguchi, H.; Matsuo, T. *J. Organomet. Chem.* **2004**, *689*, 4228.

[1] Matsuo, T.; Kawaguchi, H. *Chem. Lett.* **2004**, *33*, 640.

[1] MacLachlan, E. A. *Group 4 Complexes of an Arene-Bridged Diamidophosphine Ligand for Nitrogen Activation*; PhD thesis, University of British Columbia: Vancouver, 2006.

[1] Eicher, T.; Hauptmann, S. *The Chemistry of Heterocycles*; Wiley-VCH: Weinheim, 2003.

[1] MacLachlan, E. A.; Fryzuk, M. D. *Organometallics*. **2006**, *25*, 1530.

[1] Mee, S. P. H.; Lee, V.; Baldwin, J. E.; Cowley, A. *Tetrahedron*. **2004**, *60*, 3695.

[1] Gilow, H. M.; Burton, D. E. *J. Org. Chem.* **1981**, *46*, 2221.

[1] *The Chemistry of Heterocyclic Compounds, Thiophene and its Derivatives*; Gronowitz, S., Ed.; John Wiley and Sons: New York, 1985; Vol. 44, Parts 1-5.

[1] Angelici, R. J. *Organometallics*. **2001**, *20*, 1259.

[1] Yu, Y.; Lemal, D. M.; Jasinski, J. P. *J. Am. Chem. Soc.* **2000**, *122*, 2440.

[1] Guram, A. S.; Rennels, R. A.; Buchwald, S. L. *Angew. Chem. Int. Ed.* **1995**, *34*, 1348.

[1] Louie, J.; Hartwig, J. F. *Tetrahedron Lett.* **1995**, *36*, 3609.

[1] Hooper, M. W.; Utsunomiya, M.; Hartwig, J. F. *J. Org. Chem.* **2003**, *68*, 2861.

[1] Viciu, M. S.; Navarro, O.; Germaneau, R. F.; Kelly III, R. A.; Sommer, W.; Marion, N.; Stevens, E. D.; Cavallo, L.; Nolan, S. P. *Organometallics*, **2004**, *23*, 1629.

[1] Watanabe, M.; Yamamoto, T.; Nishiyama, M. *Chem. Commun.* **2000**, 133.

[1] Minato, A.; Tamao, K.; Suzuki, K.; Kumada, M. *Tetrahedron Lett.* **1980**, *21*, 4017.

[1] Luker, T. J.; Beaton, H. G.; Whiting, M.; Mete, A.; Cheshire, D. R. *Tetrahedron Lett.* **2000**, *41*, 7731.

[1] Ogawa, K.; Radke, K. R.; Rothstein, S. D.; Rasmussen, S. C. *J. Org. Chem.* **2001**, *66*, 9067.

[1] Begouin, A.; Hesse, S.; Queiroz, M-J. R. P.; Kirsch, G. R. *Synthesis*, **2005**, 2373.

[1] Silverstein, R. M.; Webster, F. X. *Spectrometric Identification of Organic Compounds*, 6th ed.; Wiley: New York, 1998.

[1] Clayden, J.; Greeves, N.; Warren, S; Wothers, P. *Organic Chemistry*; Oxford University Press: Oxford, 2001.

[1] Corey, E. J.; Beames, D. J. *J. Am. Chem. Soc.* **1972**, *94*, 7210.

[1] Bailey, W. F.; Gagnier, R. P.; Patricia, J. J. *J. Org. Chem.* **1984**, *49*, 2098.

[1] Beak, P.; Musick, T. J.; Chen, C. *J. Am. Chem. Soc.* **1988**, *110*, 3538.

[1] Fraser, R. R.; Mansour, T. S.; Savard, S. *Can. J. Chem.* **1985**, *63*, 3505.

[1] Shen, K.; Fu, Y.; Li, J-N.; Liu, L.; Guo, Q-X. *Tetrahedron*. **2007**, *63*, 1568.

[1] Cox, R. A.; Stewart, R. *J. Am. Chem. Soc.* **1976**, *98*, 488.

[1] Chankeshwara, S. V.; Chakraborti, A. K. *Org. Lett.* **2006**, *8*, 3259.

[1] Handy, S. T.; Sabatini, J. J.; Zhang, Y.; Vulfova, I. *Tetrahedron Lett.* **2004**, *45*, 5057.

[1] Russell, G. A.; Khanna, R. K. *Phosphorus, Sulfur Relat. Elem.* **1987**, *29*, 271.

[1] Gademann, K.; Chavez, D. E.; Jacobsen, E. N. *Angew. Chem. Int. Ed.* **2002**, *41*, 3059.

[1] Glaser, T.; Lügger, T. *Inorg. Chim. Acta.* **2002**, *337*, 103.

[1] Matsuo, T.; Kawaguchi, H. *J. Am. Chem. Soc.* **2005**, *127*, 17198.

[1] Peeters, L. D.; Jacobs, S. G.; Eevers, W.; Geise, H. J. *Tetrahedron*. **1994**, *50*, 11533.

[1] Navarro, O.; Nolan, S. P. *Synthesis*. **2006**, 366.

[1] Gilman, H.; Cartledge, F. K. *J. Organomet. Chem.* **1964**, *2*, 447.

CHAPTER 3

Synthesis of Group 4 or 5 [NPN]^S or [OOO] Complexes for the Activation of Dinitrogen

3.1 Introduction*

Various early transition metal complexes bearing a wide range of ancillary ligands have proven successful in the activation of N_2. Such ligands include: tripyrrole (**5**)[1], bulky amides (**6**)[2] or combined pentamethylcyclopentadienyl/amidinate (**7**)[3] ligands as shown in Figure 3.1.

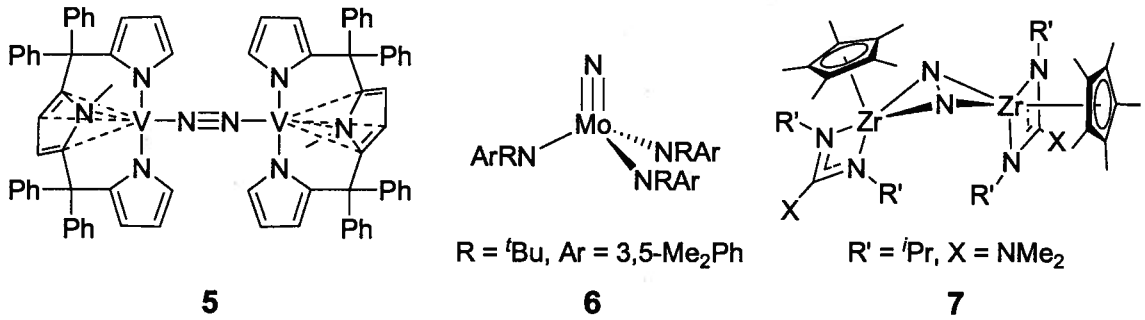

Figure 3.1. Examples of ancillary ligands used in early metal activation of N_2.

In the Fryzuk group, successful activation of N_2 has been accomplished using groups 4 and 5 metal complexes of the mixed donor ligands [PNP], [P_2N_2] or [NPN]. Some of these examples are given in Figure 3.2.

* A version of this chapter will be submitted for publication. Co-authors: Gabriel Ménard, Michael D. Fryzuk, Howie Jong.

References begin on p.108

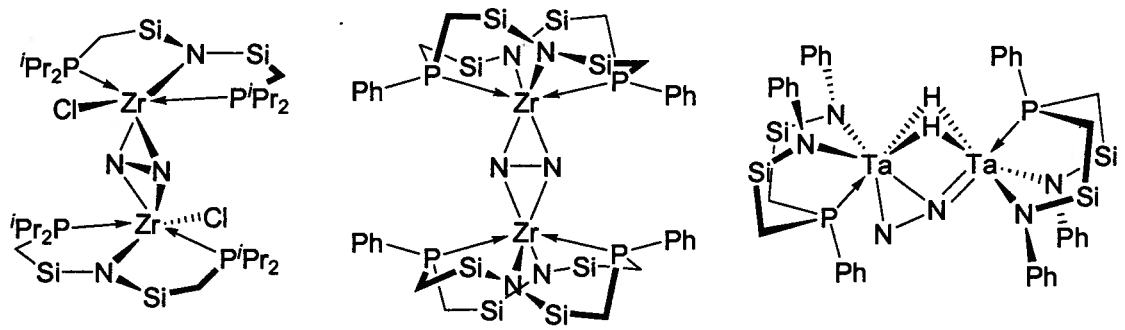

Figure 3.2. Some examples of N_2 activation in the Fryzuk group using the [PNP], [P_2N_2] or [NPN]-type ligand sets. Silyl methyl groups have been omitted for clarity.

Group 4 metal complexes of the [NPN] ligand have been synthesized and been shown to activate N_2. Both [NPN]$ZrCl_2$ and [NPN]$TiCl_2$ can be readily synthesized by metathesis of the lithiated [NPN] precursor and the respective metal halides. Interestingly, whereas the Zr complex can be reduced with KC_8 to yield the N_2 complex ([NPN]Zr(THF))$_2$(μ-η^2:η^2-N_2), the Ti analog underwent a rearrangement characterized by the formation of a P=N phosphinimide bond.[4] This new bond was formed from the P of the [NPN] ligand and the N of the activated N_2 moiety. This transformation led to complete cleavage of the N_2 unit.

The N-Si linkage of the [NPN] ligand is rather labile and has led to ligand decomposition or ligand rearrangement products. One such decomposition occurs when the side-on-end-on species ([NPN]Ta(μ-H))$_2$(μ-η^1:η^2-N_2), seen in Figure 3.2, is reacted with 9-BBN to produce the [{[NPN]Ta(H)}(μ-H)$_2$(μ-N_2-BC_8H_{14}){Ta[NPN]}] species shown in Scheme 3.1.[5] This complex is thermally unstable and undergoes ligand decomposition, by a set of proposed intermediates, promoted by the N-Si bond cleavage as shown in the scheme.

References begin on p.108

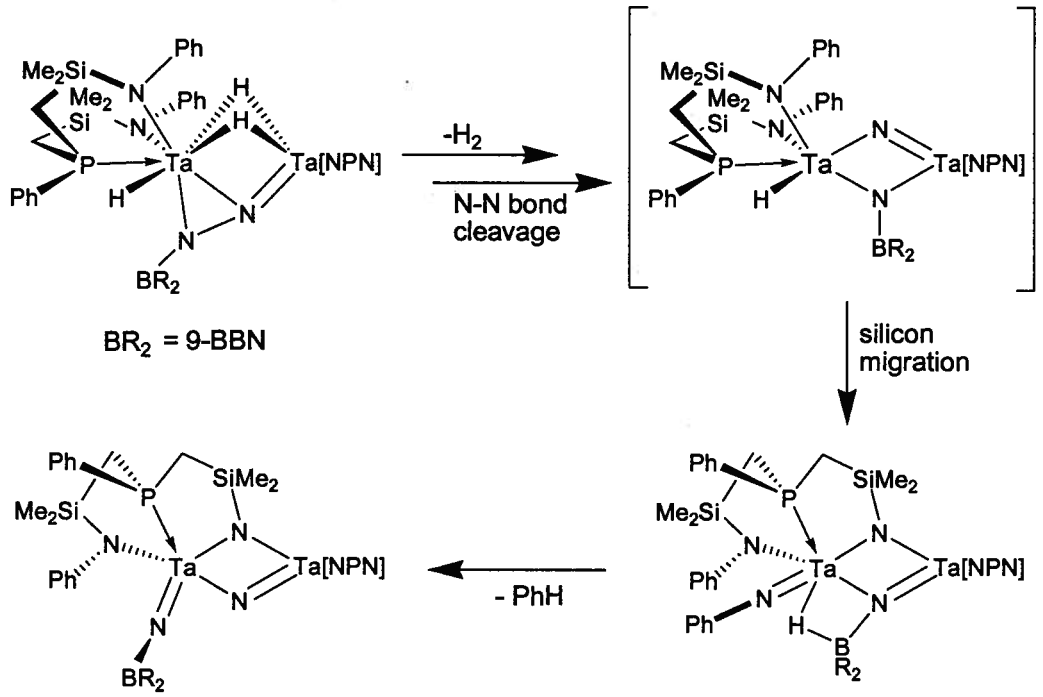

Scheme 3.1

The [NPN]* ligand (seen in Equation 3.1) was designed and synthesized recently in order to prevent such ligand rearrangements or decompositions encountered.[6] The Zr-chloride complex of this ligand, $[NPN]^*ZrCl_2$, was successfully shown to activate N_2 under reducing conditions.[7] Furthermore, the N_2 complexes, $\{[NPN]^*Zr(PMe_2R)\}(\mu\text{-}\eta^2:\eta^2\text{-}N_2)\{Zr[NPN]^*\}$ (R = Me or Ph), can slowly add H_2 to form the $\{[NPN]^*Zr(PMe_2R)\}(\mu\text{-}H)(\mu\text{-}\eta^2:\eta^2\text{-}N_2H)\{Zr[NPN]^*\}$ species as shown in Equation 3.1.

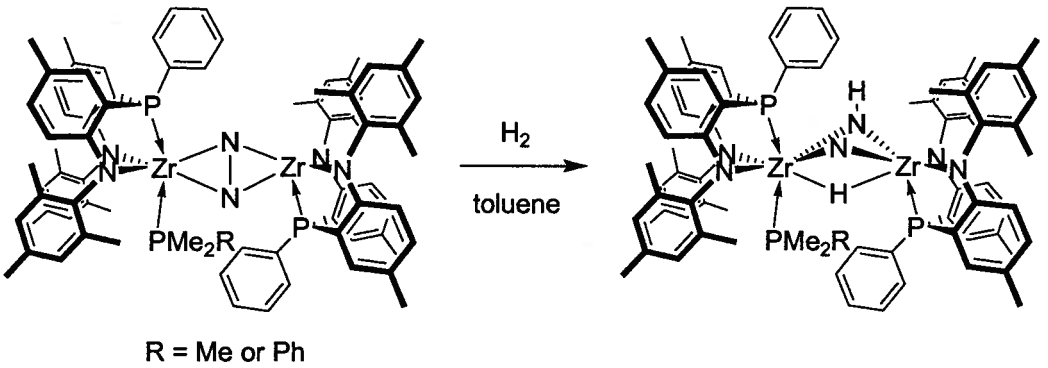

R = Me or Ph

Equation 3.1

References begin on p.108

As part of the ongoing investigation into early metal activation of N_2, the new $[NPN]^S$ ligand was synthesized as a variation to the $[NPN]^*$. The reason for synthesizing this five-membered bridged NPN ligand was to see whether changing the bond angles in the arene linker (from α to β, where β > α – see Figure 3.3) would affect the bond distances around the metal (M) centre. It was hoped that changing these angles would force a change in the P-M and/or N-M bond distances as shown in the figure. This could then open-up the area around the metal, thus making it more accessible for the coordination of N_2 and potentially leading to different chemistry in a Zr_2-N_2 complex.

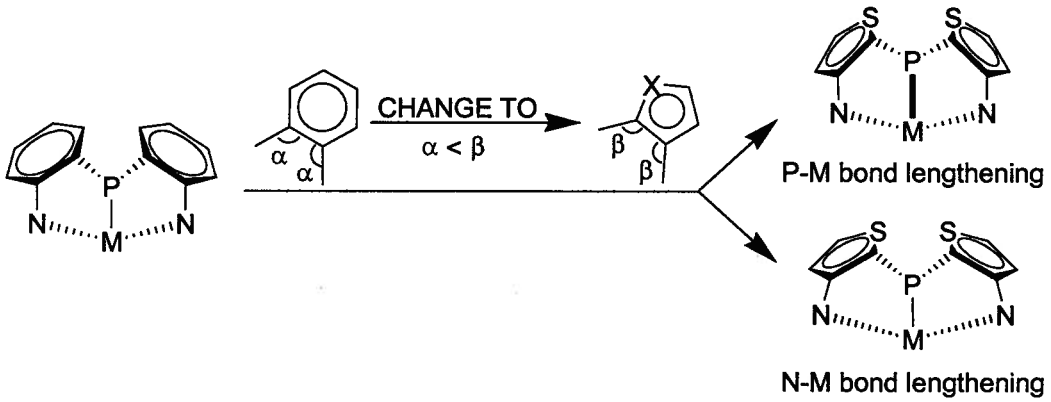

Figure 3.3. Anticipated bond length changes around the metal centre when changing the arene linker from a six-membered ring to a five-membered (M = metal, X = heteroatom, α,β represent angles).

As part of another investigation into early metal activation of N_2, the [OOO] ligand was synthesized as described in Chapter 2. The reason for the interest in this kind of ligand has to do with the many successes in using these types of ligands for N_2 activation. One such example was previously shown in Scheme 1.7.[8] In this case, a Nb-Nb dimer containing a trianionic linear-linked aryloxide ligand was reduced using lithium

References begin on p.108

triethylborohydride ($LiBHEt_3$) and incorporated N_2 to produce an N-N cleaved bridging species.

The synthesis of the new dianionic [OOO] ligand was designed mainly for group 4 metals; however, some group 5 metal chemistry was also attempted. The syntheses of Ti, Zr and Ta species were investigated. It was hoped that the incorporation bulky adamantyl groups would lead to novel early metal chemistry for the activation of N_2.

3.2 Results and Discussion

3.2.1 Attempted Syntheses of Ti[OOO] and Zr[OOO] Complexes

Initial attempts to synthesize a Ti[OOO] followed an analogous route to another similar ligand used in our laboratory, the [OPO] ligand ([OPO] = bis(3,5-*t*-butyl-2-phenoxy)phenylphosphine). The $[OPO]TiCl_2(THF)$ complex was synthesized by adding toluene to an intimate 1:1 mixture of $[OPO]:TiCl_4(THF)_2$.[9] Attempts to reproduce this to form a $[OOO]TiCl_2(THF)$ complex failed. Although the mixture did give the same dark red colour immediately upon addition of toluene as in the [OPO] reaction, the ^1H NMR spectrum clearly showed signs of multiple product formation. Specifically, several peaks could be seen in both the ^tBu and OMe diagnostic regions of the spectrum. Attempts to separate and isolate a single species from the product mixture failed.

Modifying this synthesis by adding a dilute solution of $[OOO]H_2$ (**2.9**) in toluene dropwise to a dilute solution of $TiCl_4(THF)_2$ in toluene at -78°C did not lead to the rapid formation of the dark red colour. However, after warming the solution overnight to room temperature, the solution was the same dark red colour the next day. The ^1H NMR spectrum of a sample of this mixture also revealed the formation of multiple products similar to the spectrum in the initial attempt. Heating this solution to 60°C for 2 hours

References begin on p.108

led to some changes in the ^{1}H NMR spectrum; however, no clean product formation seemed to occur. The same synthesis was also applied using the adduct-free $TiCl_4$ starting material. Unlike $TiCl_4(THF)_2$, adding the toluene solution of **2.9** to $TiCl_4$ at -78°C did lead to an immediate colour change to dark red. However, a more complicated ^{1}H NMR spectrum was ultimately obtained for this reaction.

Several attempts were also made to synthesize a Zr[OOO] complex. Salt metathesis is typically used in the synthesis of similar Zr[OPO][9] or Zr[OOO][10] compounds. The $[OOO]K_2(THF)_2$ (**3.1**) salt could be easily synthesized using 2.2 equivalents of KH and was characterized by ^{1}H and ^{13}C NMR spectroscopy and EI-MS. The ^{1}H NMR spectrum reveals that this ligand is in the U-conformation (*vide infra*). *In situ* formation of this salt followed by addition of this to a solution of $ZrCl_4(THF)_2$ in THF led to very broad peaks in the ^{1}H NMR spectrum of a sample after 6 hours of mixing at room temperature. This led to an inseparable mixture of products upon workup. In a similar attempt to the synthesis of a related Zr[OOO] complex,[10] the $[OOO]Li_2$ salt was prepared *in situ* and reacted at -78°C with a solution of $ZrCl_4$ in a toluene/THF solution. Once the solution reached room temperature, it was then heated to 60°C overnight. Again, very broad and indistinguishable peaks were obtained in the ^{1}H NMR spectrum and no single product could be isolated. The last attempt to synthesize a Zr[OOO] complex involved the aminolysis reaction of **2.9** with $Zr(NMe_2)_4$. The ^{1}H NMR spectrum again showed extremely broad peaks perhaps indicative of polymeric materials.

References begin on p.108

3.2.2 Synthesis of a "Half-On" [OOO(H)]$TaCl_4$ Complex

The synthesis of a Ta[OOO] compound was attempted using the analogous procedure for the synthesis of [OPO]$TaCl_3$ previously done in our laboratory.[9] Both **2.9** and $TaCl_5$ were intimately mixed in equal ratio and toluene was added to this all at once. After overnight stirring followed by workup, an orange powder was obtained in good yield (79%). The ^{1}H NMR spectrum of this solid in C_6D_6 surprisingly shows 4 peaks for the methylene linker protons each doublets with two having $^2J_{H\text{-}H}$ contants of 13.6 Hz and the other two having $^2J_{H\text{-}H}$ constants of 18.0 Hz. Furthermore, 3 separate ^{t}Bu peaks could be seen as well as a singlet representing an OH peak as confirmed by HMQC and HMBC experiments. It is important to note that linear-linked aryloxide ligands can adopt two separate conformations when attached to a metal centre or centres.[11] The U-conformation typically displays a more symmetric ^{1}H NMR pattern, whereas the S-conformation displays a less symmetric pattern. Both are shown in Figure 3.4.

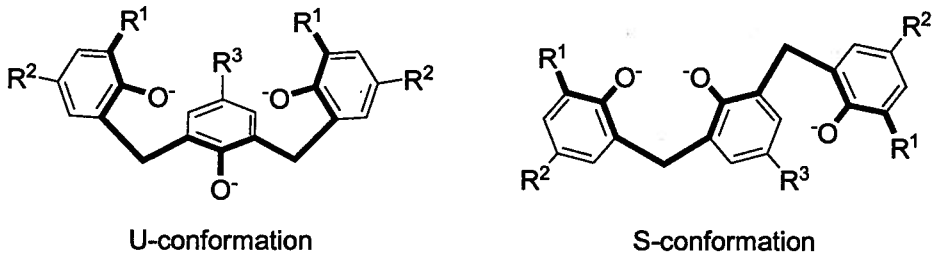

Figure 3.4. Typical conformations for linear-linked aryloxides ligated to metal centres.

The conformations depicted can also apply to dianionic (bearing a central OMe group) aryloxides. Thus, based on the ^{1}H NMR spectrum obtained, we propose that the [OOO] ligand has adopted a locked S-conformation and that it is only "half-on" the Ta centre, meaning that only one oxide group is linked to the metal centre whereas the

References begin on p.108

second remains as a pendant phenol group (this is in contrast to **3.1** which adopts the U-conformation). Due to the locked nature of the ligand, the OMe group is assumed to be coordinated to the Ta centre. The proposed formulation, as confirmed by EA, is therefore $[OOO(H)]TaCl_4$ and is denoted **3.2**. A similar result was previously reported for a potentially trianionic aryloxide ligand attached to a Nb centre and is shown in Equation 3.2.[12]

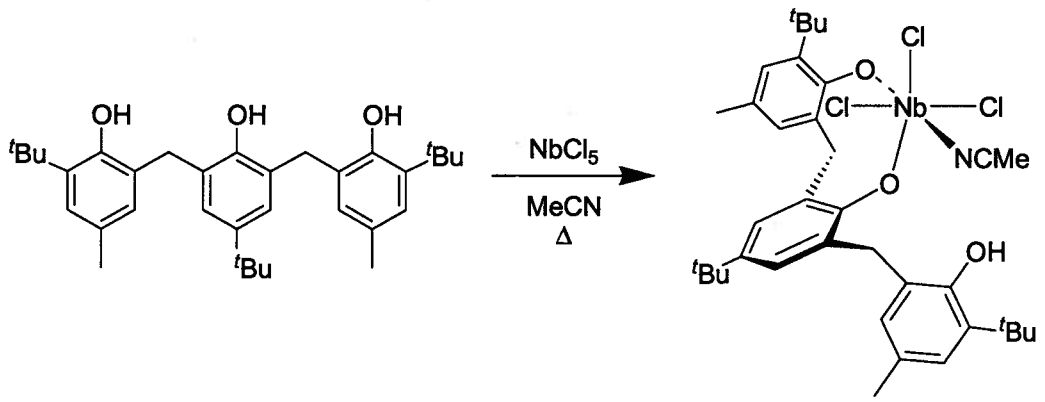

Equation 3.2

In this case, the ^1H NMR spectrum also displayed 4 inequivalent methylene protons in a locked fashion. Three separate ^tBu and 2 separate Me signals were also seen in this spectrum and the structure was unequivocally solved by single crystal X-ray diffraction which clearly shows the S-conformation for the ligand.

It is difficult to ascertain whether the $[OOO(H)]TaCl_4$ complex formed is in its monomeric or dimeric $([OOO(H)]TaCl_4)_2$ form, since the starting material $TaCl_5$ is a dimer, Ta_2Cl_{10}. EA cannot differentiate between the two and attempts to crystallize this compound have thus far failed. Although mass spectrometry could give a clue as to the structure of this complex, EI-MS analysis gave a misleading result. The result showed a mass spectrum consistent with a demethylated trioxide ligand as shown in Figure 3.5.

References begin on p.108

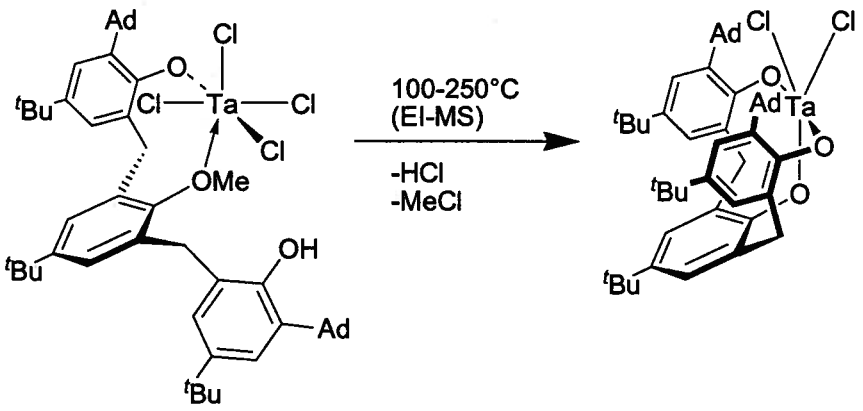

Ad = adamantyl

3.2

Figure 3.5. Proposed demethylation followed by deprotonation reactions promoted by the high temperatures used in the EI-MS.

Considering the NMR characterization of [OOO(H)]$TaCl_4$ clearly shows the presence of both a OMe and an OH group, and considering the formulation was confirmed by EA, it can be inferred that the demethylation and deprotonation reactions seen in the result of the EI-MS are simply the outcomes of the forcing conditions used in this analytical technique. Demethylation of a similar Zr dianionic linear-linked aryloxide under reducing conditions has previously been reported.[10] It has also been shown that the reaction of $TaCl_5$ with the related dimethoxy calixarene, *p*-^{t}Bu-calix[4]-$(OMe)_2(OH)_2$, leads to the singly demethylated [*p*-^{t}Bu-calix[4]-$(OMe)(O)_3TaCl_2$] species.[13] The synthesis involves refluxing a toluene solution for 36 hours. The demethylation is largely attributed to the strong Lewis acidity of the high valent metal centre. It is thus believed that a similar process occurs in the EI-MS analysis of **3.2**.

Inspired by the outcome of the EI-MS result, the first attempt to "close" the [OOO(H)]$TaCl_4$ (**3.2**) complex to make the [OOO]$TaCl_3$ species involved heating a

References begin on p.108

dilute toluene solution of **3.2** to reflux. After 2 hours, a sample was taken and analyzed by ^{1}H NMR. Although there was some change, no clear product formation could be seen. Furthermore, refluxing the solution overnight led to complete product decomposition as witnessed by the extremely broad peaks formed in the ^{1}H NMR spectrum. No clear sign of any major product could be found in this spectrum.

Several attempts were also made to deprotonate the phenol group of **3.2** using either 1.2 equivalents of KH, $KN(SiMe_3)_2$ or ^{n}BuLi. While the KH reaction produced no change, the reactions of $KN(SiMe_3)_2$ or ^{n}BuLi produced either no sign of the desired product or a mixture of products. As an alternative synthesis, the reaction of the potassium salt, $[OOO]K_2(THF)_2$ (**3.1**), with $TaCl_5$ was attempted. An immediate colour change to dark orange brown was observed. Subsequent ^{1}H NMR analysis revealed extremely broad peaks with multiple products obtained and no sign of the desired product.

3.2.3 Attempted Synthesis of $[NPN]^STaCl_3$: Formation of an Unexpected Product

Several attempts were made to synthesize a $Ta[NPN]^S$ compound by directly adding the proligand to an equimolar amount of $TaCl_5$. While there was an immediate colour change to dark orange/brown in each attempt, there was also generally a mixture of products obtained as evidenced by ^{1}H and $^{31}P\{^1H\}$ NMR spectroscopy.

As an initial attempt using salt metathesis to add the $[NPN]^S$ ligand to $TaCl_5$, the K salt of the $[NPN]^S$ ligand was synthesized *in situ* and added directly to a solution of $TaCl_5$. Removal of the THF solvent from the potassium salt synthesis was done since it is well known that $TaCl_5$ reacts with ethereal solvents due to its strong Lewis acidity. The reaction at room temperature leads to an immediate colour change to dark red. After

References begin on p.108

stirring overnight and subsequent workup, the $^{31}P\{^{1}H\}$ NMR spectrum displays one major new product with a peak considerably downfield at 34 ppm. Trace amounts of the proligand were also present at -55 ppm. The ^{1}H NMR spectrum indicates an unsymmetrical pattern with six different methyl peaks, attributed to the methyls on the mesityl rings, present in the aliphatic region. Also, 3 doublets and 1 doublet of doublets (due to H-H and P-H coupling) are also present representing the 4 distinct thiophene protons. The initial speculated structure to explain the inequivalent ^{1}H spectrum along with the single ^{31}P peak was a dimeric $([NPN]^{S}TaCl_3)_2$ complex of C_i symmetry.

The sample was analyzed by EI-MS and two strong molecular weight (MW) signals were obtained for mass-to-charge ratio (*m/e*) values of 538 ($[NPN]^{S}$) and 570 (minor). Mass spectral analysis of the compound did not initially provide more information considering the MW of the proposed dimeric compound is 1652 g/mol. A different technique was therefore needed since this mass exceeded the detection limit of the EI-MS. However, samples analyzed by MALDI-TOF analysis surprisingly confirmed the main molecular ion peak as being *m/e* 538.

Isolation of the product of this reaction was extremely difficult due to the apparent solubility of this compound in pentane and hexanes. This was surprising since a Ta complex bearing multiple phenyl rings on the ancillary ligand along with chloride ligands would be expected to be very insoluble in aliphatic non-polar solvents. Only very small quantities of dark red solid could be obtained at any given time. Fortunately, cooling a dark red pentane/hexanes solution of the product to -38°C yielded single clear crystals suitable for X-ray diffraction studies. To our great surprise, the solved structure of the

References begin on p.108

product (denoted **3.3**), consistent with NMR, EI-MS and MALDI-TOF results is shown in Figure 3.6.

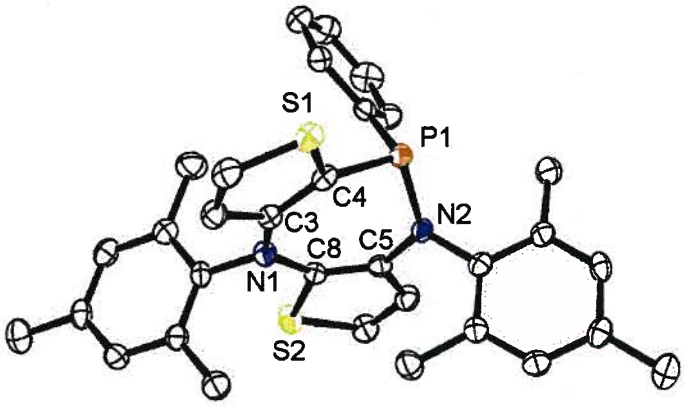

Figure 3.6. ORTEP drawing of the solid-state molecular structure of **3.3** (ellipsoids drawn at the 50% probability level). All hydrogen atoms have been omitted for clarity. Selected bond lengths (Å) and angles(°): P1-N2 1.7013(17), N2-C5 1.425(3), C5-C8 1.372(3), C8-N1 1.406(3), N1-C3 1.407(3), C3-C4 1.378(3), C4-P1 1.794(2), C4-P1-N2 103.09(9), P1-N2-C5 123.85(14), N2-C5-C8 128.39(18), C5-C8-N1 134.73(19), C8-N1-C3 127.32(18), N1-C3-C4 127.14(18), C3-C4-P1 131.99(16).

The reaction surprisingly leads to the clean oxidative ring-forming rearrangement as shown by **3.3**. Previous attempts to perform the same reaction with the $[P_2N_2]$ ligand using salt metathesis of the Li, Mg or Zn salts with $TaCl_5$ were attempted to produce a $[P_2N_2]TaCl_3$; however, none of these reactions proved successful.[14] Furthermore, the analogous reaction of the related $[NPN]^*K_2$ salt with $TaCl_5$ did not lead to any similar type of oxidative ring closing reactions.[15] It is important to note that this reaction is an oxidation reaction where the $TaCl_5$ is likely the oxidizing agent. This is shown in more details in Scheme 3.2.

References begin on p.108

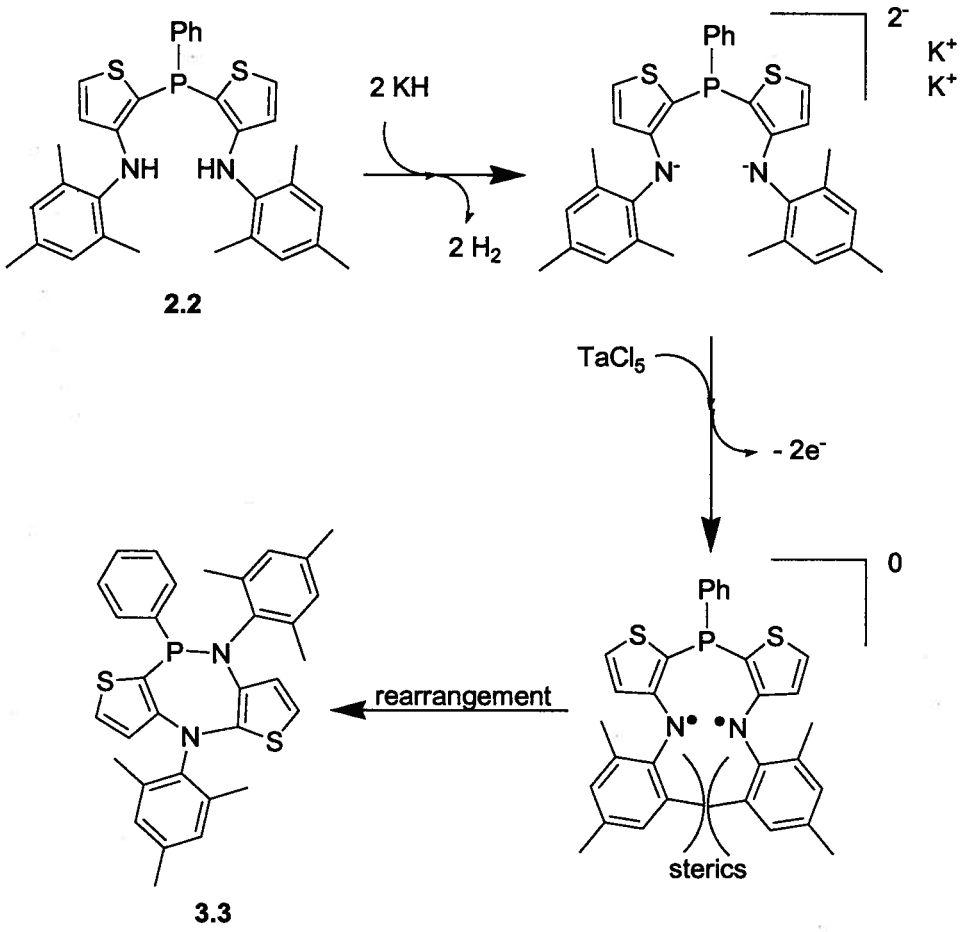

Scheme 3.2

In this scheme, it is proposed that the Ta centre is reduced. Previous experiments of alkali metal salt metathesis reactions with $TaCl_5$ have also been shown to produce low yields due to the competing reactions between nucleophilic displacement of chlorine ligands and reduction of the metal centre.[16] The proposed mechanism using $TaCl_5$ involves initial oxidation of the N-K bonds leading to K^+ and N• as shown in Scheme 3.2. Due to the steric bulk of the attached mesityl groups at the N• centres, the N-N bond formation step may be hindered. This can then lead to the rearrangement to form the less sterically crowded **3.3**.

References begin on p.108

In order to establish whether the Ta centre is the only 2 electron oxidizing agent capable of initiating this reaction, the identical reaction was performed using 1 equivalent of I_2. The rationale for using I_2 as the oxidizing agent was that the I_2 molecule would be reduced twice to produce the oxidized **3.3** species and 2 equivalents of KI. The results from this experiment clearly show that, among others, **3.3** is produced as evidenced in both the $^{31}P\{^1H\}$ and ^1H NMR spectra.

3.2.4 Syntheses of $[NPN]^SZr(NMe_2)_2$, $[NPN]^SZrCl_2$ and $[NPN]^SZrI_2$

The synthesis of $Zr[NPN]^S$ complexes can be easily undertaken starting from the $[NPN]^SH_2$ proligand (**2.2**). The $[NPN]^SZr(NMe_2)_2$ (**3.4**), $[NPN]^SZrCl_2$ (**3.5**) and $[NPN]^SZrI_2$ (**3.6**) complexes are all synthesized in high yields and all compounds have been isolated and fully characterized. The general synthetic steps for these syntheses are shown in Scheme 3.3.

References begin on p.108

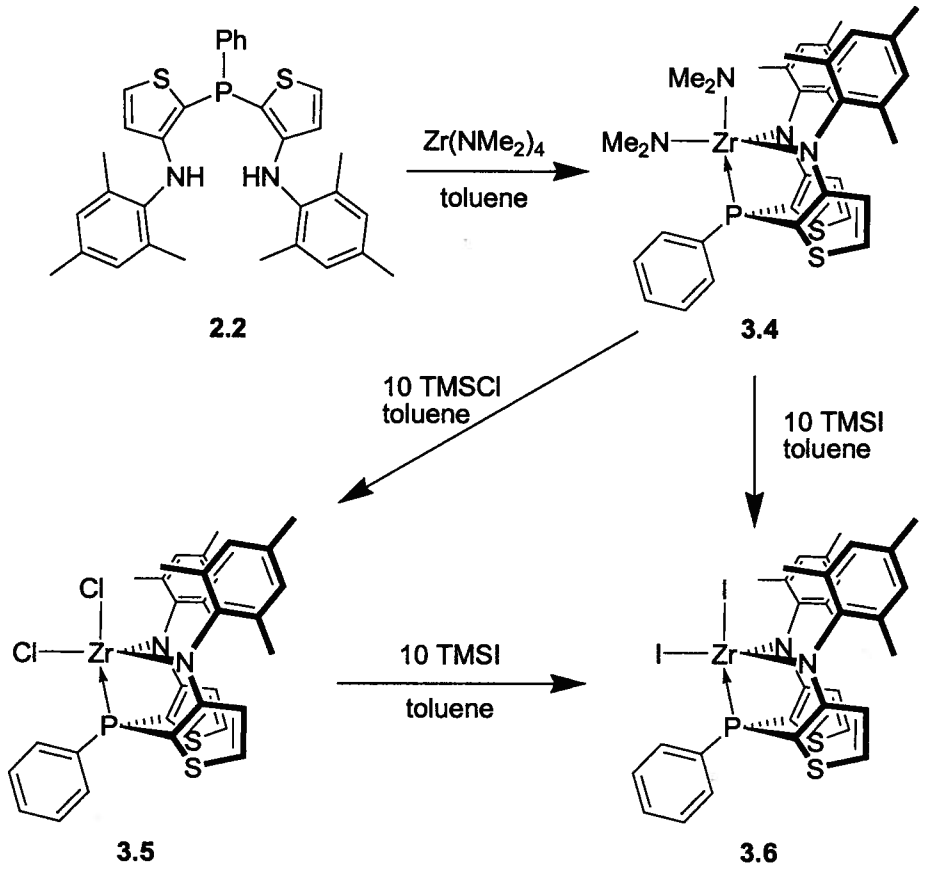

Scheme 3.3

The initial synthesis of $[NPN]^{S}Zr(NMe_2)_2$ (**3.4**) involves the aminolysis reaction of a 1:1 mixture of **2.2** and tetrakis(dimethylamido) zirconium, ($Zr(NMe_2)_4$). Addition of toluene leads to a yellow solution which after 1 hour can be worked-up to give an 80% yield of a yellow solid. The $^{31}P\{^1H\}$ NMR spectrum in C_6D_6 shows a new peak slightly more downfield than the proligand (-55.5 ppm) at -41 ppm. The ^1H NMR data shows 5 singlets in the aliphatic region, suggesting that the mesityl methyl groups are inequivalent due to hindered free rotation. This is also consistent with 2 separate *meta*-proton singlet peaks in the aromatic region. The thiophene peaks display the same pattern as in **2.2** of a doublet and a doublet of doublets (due to H-H and P-H coupling), the latter being significantly more upfield at 5.92 ppm than the former at 6.97 ppm. The solution NMR

References begin on p.108

data suggests a C_s symmetric trigonal bipyramidal complex with NMe_2 groups in both the equatorial and apical positions. These results are analogous to the related $[NPN]^*Zr(NMe_2)_2$ complex[6] and are also consistent with the solid state structure as shown in Figure 3.7.

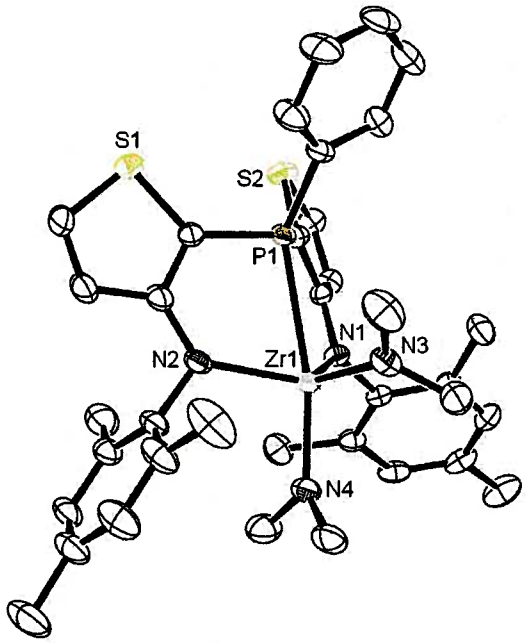

Figure 3.7. ORTEP drawing of the solid-state molecular structure of **3.4** (ellipsoids drawn at the 50% probability level). All hydrogen atoms have been omitted for clarity. Selected bond lengths (Å) and angles(°): Zr1-N1 2.1663(18), Zr1-N2 2.1464(19), Zr1-N3 2.022(2), Zr1-N4 2.0430(19), Zr1-P1 2.8410(6), N1-Zr1-N2 117.97(7), N3-Zr1-N4 99.19(8), N1-Zr1-P1 74.80(5), N2-Zr1-P1 72.24(5), N1-Zr1-N3 114.64(7), P1-Zr1-N3 88.78(6), P1-Zr1-N4 169.62(5).

As seen in Figure 3.7, the solid state structure is indeed trigonal bipyramidal but distorted. The $[NPN]^S$ ligand binds facially to the metal centre as is to be expected since the phosphine donor should prevent meridional coordination. The N1-Zr1-P1 and N2-

References begin on p.108

Zr1-P1 angles are noticeably smaller than 90° which makes the amide donors hinged out of the equatorial plane. Furthermore, the angles around N1 and N2 add up to 359.59° and 359.72° respectively, suggesting as expected sp^2 hybridization at the amide donors.

The $[NPN]^SZrCl_2$ (**3.5**) complex can be readily synthesized from **3.4** using an excess of trimethylsilyl chloride (TMSCl) in toluene. The pure yellow product is easily obtained upon workup in 80% yield. The $^{31}P\{^1H\}$ NMR spectrum in C_6D_6 shows a singlet at -36 ppm. Similar to compound **3.4**, 3 peaks in the aliphatic region for 3 separate methyl groups on the mesityl rings are present, thus suggesting hindered rotation. The solution NMR data suggests a C_s symmetric trigonal bipyramidal complex. Although a symmetric C_{2v} bridged dimer $([NPN]^SZrCl)_2(\mu\text{-}Cl)_2$ is possible in solution and cannot be ruled out, the solid state structure clearly shows the monomeric structure as seen in Figure 3.8.

References begin on p.108

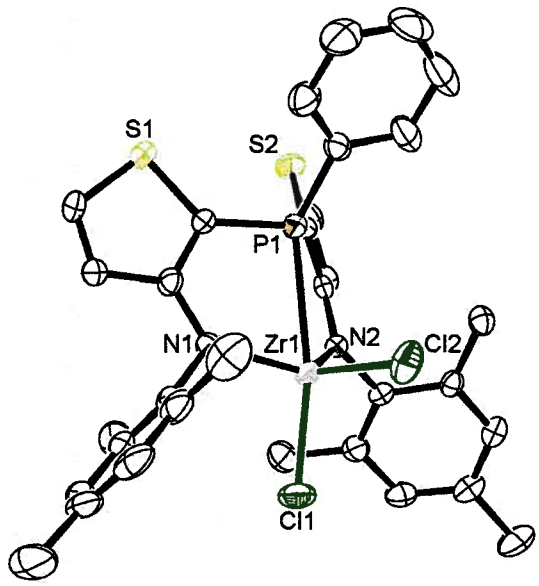

Figure 3.8. ORTEP drawing of the solid-state molecular structure of **3.5** (ellipsoids drawn at the 50% probability level). All hydrogen atoms have been omitted for clarity. Selected bond lengths (Å) and angles(°): Zr1-N1 2.072(3), Zr1-N2 2.070(3), Zr1-Cl1 2.3773(12), Zr1-Cl2 2.3909(16), Zr1-P1 2.8352(12), N1-Zr1-N2 121.28(11), Cl1-Zr1-Cl2 101.27(5), N1-Zr1-P1 72.64(8), N2-Zr1-P1 72.90(8), N1-Zr1-Cl2 115.28(9), P1-Zr1-Cl2 91.88(5), P1-Zr1-Cl1 166.84(4).

The solid state structure displayed in Figure 3.8 is in large part analogous to the one shown in Figure 3.7. The structure is again distorted trigonal bipyramidal with the amide donors hinged out of the equatorial plane. One of the expected differences in changing from NMe_2 ligands to less bulky Cl ligands is the N1-Zr1-N2 angle which increases slightly from approximately 118° to 121°, respectively. The Zr-N (average 2.09 Å for **3.4** and 2.07 Å for **3.5**), Zr-Cl (average 2.38 Å) and Zr-P (2.84 Å) bonds in both **3.4** and **3.5** are typical.[17,18]

References begin on p.108

The iodide complex, $[NPN]^{S}ZrI_2$ (**3.6**), can also be synthesized in high yield using an excess of trimethylsilyl iodide (TMSI). As shown in Scheme 3.3, this compound can be synthesized via 2 different routes. The cleanest route to this synthesis is by using **3.4** as the starting material and treating it with excess TMSI. After 3 hours, a pure orange product, **3.6**, is obtained following workup in 82% yield. The $^{31}P\{^{1}H\}$ NMR spectrum in C_6D_6 shows a singlet at -35 ppm, slightly shifted from the -36 ppm peak for the dichloride, **3.5**. The ^{1}H NMR data is analogous to the one for **3.5** and also suggests a C_s symmetric trigonal bipyramidal complex. The solid state structure, seen in Figure 3.9, shows this type of structure. As in both **3.4** and **3.5**, the structure is again distorted trigonal bipyramidal with the amide donors hinged out of the equatorial plane. Furthermore, the Zr-N (average 2.07 Å), Zr-I (average 2.78 Å) and Zr-P (2.84 Å) bonds are also typical in this complex.[17,18,19]

References begin on p.108

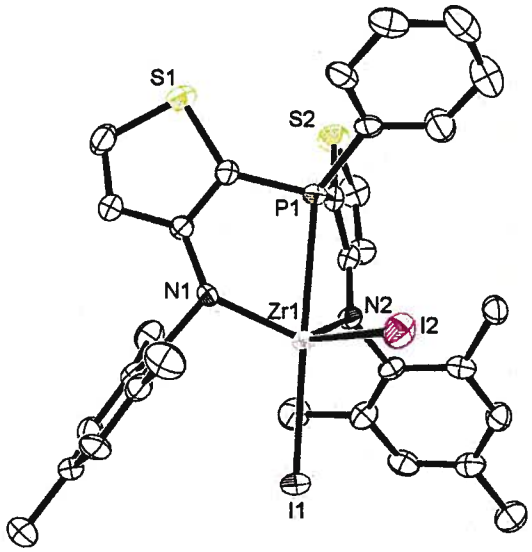

Figure 3.9. ORTEP drawing of the solid-state molecular structure of **3.6** (ellipsoids drawn at the 50% probability level). All hydrogen atoms have been omitted for clarity. Selected bond lengths (Å) and angles(°): Zr1-N1 2.054(4), Zr1-N2 2.081(5), Zr1-I1 2.7812(8), Zr1-I2 2.7757(15), Zr1-P1 2.8357(16), N1-Zr1-N2 116.80(17), I1-Zr1-I2 95.51(3), N1-Zr1-P1 70.08(12), N2-Zr1-P1 73.56(12), N1-Zr1-I2 114.40(12), P1-Zr1-I2 85.27(4), P1-Zr1-I1 177.40(4).

The $[NPN]^{S}ZrI_2$ complex can also be readily synthesized from the dichloride species $[NPN]^{S}ZrCl_2$. The reaction is performed in an analogous way using TMSI, but a longer reaction time of approximately 15 hours is required. The yield is 88%. Although this may seem like the highest yielding route, the overall yield is lower since this is a two step procedure. Finally, this complex can also be synthesized using a one-pot protocol. Mixing $[NPN]^{S}H_2$ (**2.2**) with $Zr(NMe_2)_4$ in toluene for 1 hour, followed by the direct addition of excess TMSI yields the desired product. The overall yield is 73%. Although this route provides the highest overall yield, this reaction is often complicated by the

References begin on p.108

appearance of intractable impurities requiring an extra filtration step. The NMR analysis also tends to show trace impurities. Thus, although this method is convenient, it generally does not yield the purest product. The optimal method for synthesizing **3.6** is, therefore, by the first method described.

3.2.5 Advances Toward the Synthesis of a $([NPN]^{S}Zr)_2$-N_2 Complex

In Chapter 1, several examples were given for the successful activation of N_2. Figure 3.2 also shows some of these successful examples in the Fryzuk group using different ligand systems. Most reductions in our group are performed with strong alkali metal reducing agents, particularly KC_8 or Na/Hg amalgam. Both these reducing agents are said to have reduction potentials similar to the free metals at E^o = -2.931 V and E^o = -2.71 V, respectively.[20]

It should be noted that no reduction experiments were attempted with the "half-on" $[OOO(H)]TaCl_4$ species since the free O-H group was considered to be potentially problematic. Standard reduction conditions involve the vacuum transfer addition of the dry solvent, usually THF, to an intimate mixture of the metal-halide complex and the reducing agent at -196°C in a thick-walled Kontes-sealed reaction vessel. The mixture is then pressurized with N_2 and allowed to thaw to -78°C, thus raising the pressure in the vessel, and is maintained at this temperature for 4-5 hours with rapid mixing. The vessel is then left on the bath overnight and allowed to slowly warm to room temperature.

Initial reduction experiments focused on the $[NPN]^{S}ZrCl_2$ (**3.5**) species using 2 equivalents of KC_8 in THF, similar to the successful reduction performed on the $[NPN]^{*}ZrCl_2$ system.[7] Several attempts were made to reduce this species to obtain an N_2 compound; however, the $^{31}P\{^1H\}$ and ^1H NMR spectra always showed the formation of

References begin on p.108

multiple products with some $[NPN]^SH_2$ proligand and no clear signs of an N_2-containing compound. Furthermore, attempts to isolate a single product failed. EI-MS analysis confirmed only the presence of the $[NPN]^SH_2$ proligand with no sign of any higher molecular weight species. The reduction of this species was also tried in a similar fashion with sodium naphthalenide and the results were also inconclusive.

As an alternative to dichloride starting materials, diiodide metal complexes have been shown to sometimes yield better results.[21] For this reason, $[NPN]^SZrI_2$ (**3.6**) was synthesized as detailed above. A wide range of different reaction conditions, including changing the pressure, the solvent, the reaction times, the working gas, or the reducing agent were attempted.

Several attempts were initially made using the standard reduction procedure with 2 equivalents of KC_8 in THF. The reaction mixtures were generally dark green/brown the next day which is in sharp contrast to the bright blue-green solutions reported for the reduction of $[NPN]^*ZrCl_2$ under the same conditions.[7] Both $^{31}P\{^1H\}$ and ^1H NMR spectra showed the presence of a wide range of products with very broad peaks in both cases. The proligand, $[NPN]^SH_2$, was also present. Attempts to isolate any single product failed. EI-MS analysis confirmed only the presence of $[NPN]^SH_2$ with trace signs of higher molecular weight species, none of which indicate an N_2 complex. Three peaks were consistently seen in the $^{31}P\{^1H\}$ spectra at -30 ppm, -15 ppm and +50 ppm. Unfortunately, these products are all unlikely to be N_2 complexes since these same peaks are seen in the analogous reduction performed under vacuum.

Changing the solvent system from THF to toluene generally gave a larger mixture of products. Interestingly, none of the products in the $^{31}P\{^1H\}$ NMR spectrum from the

References begin on p.108

toluene reduction reactions seem to correlate with the peaks seen when THF was used. Broad and multiple peaks were seen in the spectra and attempts to isolate a single compound failed. The toluene reactions generally also led to incomplete reaction of the starting material even when the reaction was left stirring at room temperature for 3 days.

Changing the working gas from N_2 to H_2 in THF also led to a wide range of product formation. There was no evidence of H_2 activation in the ^{1}H NMR spectrum as there were no signs of hydride signals typically found outside the normal regions of the spectrum. Scans from +50 ppm to -50 ppm showed no unusual signals outside the typical boundaries.

Another approach to activate N_2 with $[NPN]^SZrI_2$ involved changing the reducing agent to a milder one. Reduction using 1.1 equivalent of Mg powder (E^o = -2.372 V)[20] led to the formation of a small amount of new product; however, the major peak was the starting material. Reduction using 10 equivalents Mg powder led to an unexpected new main product. Although both $^{31}P\{^1H\}$ and ^{1}H NMR spectra are analogous to the $[NPN]^SZrI_2$ starting material, closer inspection clearly shows that a new species was formed. The $^{31}P\{^1H\}$ peak is slightly shifted from -35 ppm for the starting material to -30 ppm for the new product. All ^{1}H NMR peaks display the same pattern as in the starting material except they are all slightly shifted. Four small new peaks could be seen in the ^{1}H NMR spectrum and included diagnostic triplets at 3.44 ppm and 0.72 ppm integrating for 2 and 3 protons, respectively. Two multiplets, each integrating for 2 protons, could also be seen in the 1.22 ppm and 1.01 ppm regions. Mass spectral analysis confirmed the product to be $[NPN]^SZrI(OBu)$ (**3.7**). Cleavage of THF under reducing conditions is not uncommon.[22,23] It has been seen in our laboratory for the reduction of a

References begin on p.108

Zr-carbene complex, $[NCN]ZrCl_2$, with KC_8 in THF to yield the [NCN]ZrCl(OBu) species.[24]

The result found for the Mg reaction served to confirm at least one of the common products found in the reductions of $[NPN]^SZrCl_2$ or $[NPN]^SZrI_2$ in THF with KC_8 either under N_2 or under vacuum. Thus, the -30 ppm ($^{31}P\{^1H\}$) signal seen as a significant peak in all the reductions performed with either of these compounds when THF is used as the solvent, was confirmed to be the $[NPN]^SZrX(OBu)$ (X = Cl or I) species by ^1H NMR spectroscopy. The $[NPN]^SZrI(OBu)$ (**3.7**) species produced is, as expected, not seen when toluene is used as the solvent; however, there are signs indicative of the activation of toluene in the ^1H NMR spectrum in the 3-5 ppm region. The result from the Mg reduction prompted us to attempt a reduction using a different ethereal solvent, diethyl ether.

The reduction of $[NPN]^SZrI_2$ in Et_2O with 2.2 equivalents of KC_8 was performed using the same standard procedure as with the THF reactions. After warming to room temperature overnight, the solution was blue-green the next day. $^{31}P\{^1H\}$ NMR analysis in Et_2O of the crude reaction mixture clearly showed the formation of a single major product at -23.5 ppm, with minor impurities. It should be noted that a signal in this approximate region has never been seen for any of the previous reductions mentioned above. Removal of the Et_2O to isolate a solid proved slightly problematic as doing so led to significant broadening of the major peak, potentially a sign of decomposition as seen when coordinated THF is removed from the related $\{[NPN]^*Zr(THF)\}_2(\mu\text{-}\eta^2\text{:}\eta^2\text{-}N_2)$ complex.[7] Therefore, the ether adduct of this complex is thought to not be isolable (see Figure 3.10).

References begin on p.108

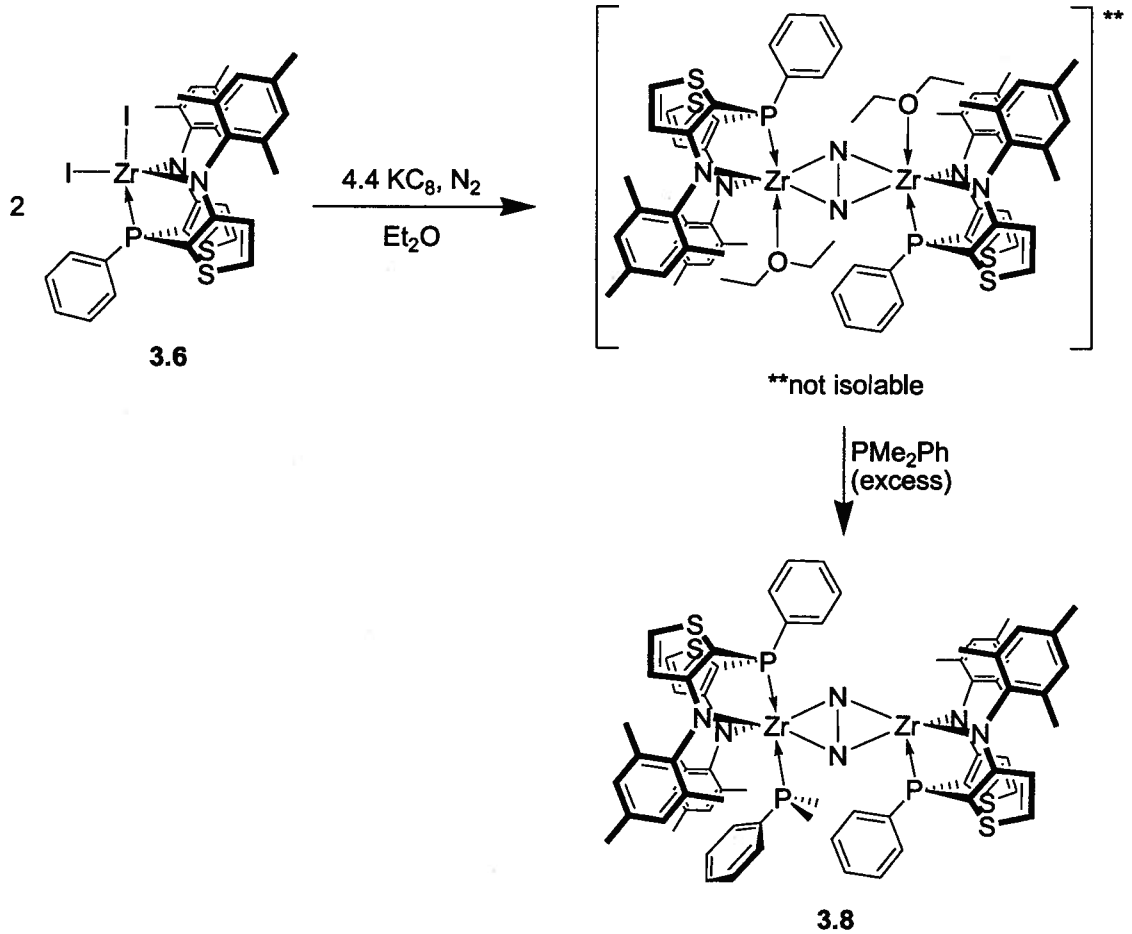

Figure 3.10. Proposed formation of complex **3.8** from the reduction of **3.6** in Et_2O using KC_8. The proposed Et_2O adduct is not isolable likely due to the volatility of the coordinated Et_2O molecules. The complex can be isolated using PMe_2Ph to form **3.8**.

Further characterization and simultaneous isolation was undertaken, as shown in Figure 3.10, by adding excess dimethylphenylphosphine (PMe_2Ph) to an Et_2O solution of this new compound. Removal of the Et_2O followed by a pentane wash led to the isolation of a green powder. The $^{31}P\{^1H\}$ NMR spectrum of this complex is very analogous to the spectra observed for the dinitrogen species $\{[NPN]^*Zr(PMe_2R)\}(\mu\text{-}\eta^2\text{:}\eta^2\text{-}N_2)\{Zr[NPN]^*\}$ (R = Me or Ph), previously shown in Equation 3.1.[7] This pattern is shown in Figure 3.11.

References begin on p.108

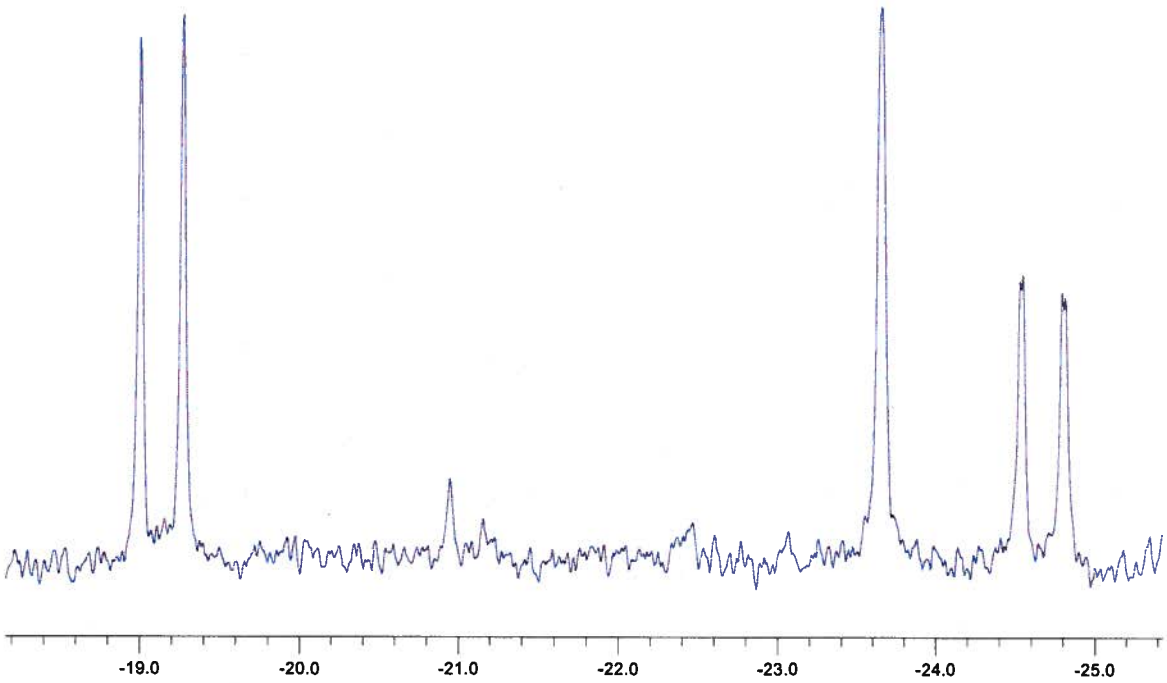

Figure 3.11. $^{31}P\{^{1}H\}$ NMR spectrum (C_6D_6) of the proposed complex **3.8**. Both doublets have $J_{P\text{-}P}$ = 105.4 Hz.

In this spectrum, the major peaks are two coupled doublets ($J_{P\text{-}P}$ = 105.4 Hz), respectively at -19.1 ppm and -24.7 ppm, and a singlet at -23.7 ppm. This pattern results from the two coupling phosphines on the same metal centre (P from $[NPN]^S$ and P from PMe_2Ph) and the lone phosphine forming a singlet from the $[NPN]^S$ on the adjacent metal centre. This same pattern emanates in the $^{31}P\{^{1}H\}$ NMR for **8** shown below.[7] The ^{1}H NMR spectrum of **3.8** also shows a pattern consistent with C_s symmetry as seen with **8**. Attempts are currently underway to obtain a solid state structure of this new compound by X-ray diffraction. Considering the NMR evidence obtained thus far, which is strikingly similar to the one obtained for **8**, it is believed that the new complex is a similar

References begin on p.108

analog to **8** represented by **3.8**. It is not yet possible to determine for certainty whether the N_2 moiety is coordinated in a side-on or an end-on fashion.

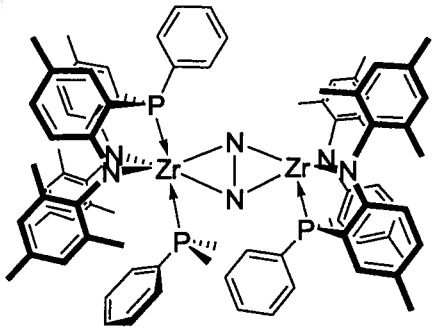

8

3.3 Conclusions

In this chapter, many attempts were made to form a Ti or Zr complex of the [OOO] (**2.9**) ligand. All attempts proved unsuccessful; however, a Ta complex could be obtained. The new "half-on" [OOO(H)]$TaCl_4$ (**3.2**) complex features a mono-deprotonated ligand attached to the metal centre and locked in the S-conformation. Attempts to "close" this ligand to the U-conformation and form the desired [OOO]$TaCl_3$ complex were unsuccessful.

In the attempted synthesis of a related $[NPN]^{S}TaCl_3$ complex, an unexpected product was obtained. The addition of 1 equivalent of $[NPN]^{S}K_2$, formed *in situ*, to 1 equivalent of $TaCl_5$ leads to an immediate colour change to dark red. One major new product is seen in the NMR analyses. This product was confirmed by single crystal X-ray diffraction to be the oxidative ring-forming rearrangement product **3.3** as shown in Figure 3.6. Preliminary experiments suggest that the $TaCl_5$ is not the only oxidizing agent that can perform this reaction as the same product is seen when I_2 is used.

References begin on p.108

The syntheses of $[NPN]^{S}Zr(NMe_2)_2$, $[NPN]^{S}ZrCl_2$ and $[NPN]^{S}ZrI_2$ complexes were all undertaken with relative ease and high yields were obtained. These complexes were fully characterized and their solid state structures shown in Figures 3.7-3.9, respectively. The attempted reduction reactions of $[NPN]^{S}ZrCl_2$ using either KC_8 or sodium naphthalenide to form an N_2 complex generally led to a mixture of products. No single compound could be isolated from these mixtures. The reduction of $[NPN]^{S}ZrI_2$ using KC_8 in THF at different pressures also led to unidentifiable products. Using H_2 as the working gas or changing the solvent from THF to toluene also led to unsuccessful reductions. Changing the reducing agent from KC_8 to Mg powder did lead to a single product identified by $^{31}P\{^1H\}$ and ^1H NMR spectroscopy and EI-MS to be the THF ring-opened product $[NPN]^{S}ZrI(OBu)$ (**3.7**). This prompted us to attempt a reduction using a different ethereal solvent, diethyl ether.

The reduction of $[NPN]^{S}ZrI_2$ using 2.2 equivalents of KC_8 in Et_2O led to a characteristic blue-green solution. Isolation of this product was done by forming the PMe_2Ph adduct thus yielding the characteristic $^{31}P\{^1H\}$ NMR spectrum as seen in Figure 3.11. The ^1H NMR spectrum corroborates the proposed N_2 structure depicted by **3.8**. Both spectra are also analogous to the ones previously obtained for complex **8**, shown above. These preliminary results are highly indicative of an N_2 complex. Attempts are currently underway to characterize this complex in more detail.

The change in reactivity from the similar compounds $[NPN]^{*}ZrCl_2$ to $[NPN]^{S}ZrX_2$ (X = Cl or I) is surprising as the structures are very similar. Whereas the $[NPN]^{*}ZrCl_2$ complex cleanly reduces N_2 in THF using KC_8, the analogous reaction of $[NPN]^{S}ZrX_2$ (X = Cl or I) leads to a large mixture of products. Only when using Et_2O,

References begin on p.108

which is less prone to activation than THF, does the reaction give a clean product. As proposed in the beginning of this chapter (Figure 3.3), it was expected that introducing a five-membered linker instead of the six-membered would likely elongate the Zr-P, Zr-N or both bond distances. In comparing the six-membered $[NPN]^{*}ZrCl_2$ to the five-membered $[NPN]^{S}ZrCl_2$, all bond distances and angles are similar except for the Zr-P bond lengths and the N1-Zr-N2 bond angles (where N1 and N2 represent the amide donors of the respective [NPN] ligands). The Zr-P bond lengths are 2.72 Å and 2.84 Å respectively for $[NPN]^{*}ZrCl_2$[6] and $[NPN]^{S}ZrCl_2$ (and $[NPN]^{S}ZrI_2$). The N1-Zr-N2 bond angles are 114° and 121° respectively (117° for $[NPN]^{S}ZrI_2$). While no trend yet exists to explain the effects of the Zr-P bond lengths or the N1-Zr-N2 bond angles on the activation of N_2 under reducing conditions, it is possible that one or both of these changes cause the $[NPN]^{S}ZrX_2$ (X = Cl or I) complexes to be much more reactive toward THF than the similar $[NPN]^{*}ZrCl_2$ system. Further investigations are currently underway.

3.4 Experimental Section

3.4.1 General Considerations

Except where noted, experimental procedures follow those outlined in Chapter 2. Mass spectrometry (MALDI-TOF) was performed at the Department of Chemistry of the University of British Columbia.

3.4.2 Starting Materials and Reagents

$TiCl_4(THF)_2$,[25] $ZrCl_4(THF)_2$,[25] and KC_8[26] were prepared according to literature procedures. Sodium naphthalenide was prepared and titrated according to a literature procedure.[27] $TaCl_5$ and I_2 were purchased from Aldrich and sublimed prior to use. KH

References begin on p.108

was purchased from Aldrich as a 30% wt. dispersion in mineral oil. It was isolated as a solid by filtering on a glass frit, washing with copious dry hexanes and drying. $KN(SiMe_3)_2$ was purchased from Aldrich and recrystallized from toluene prior to use. $TiCl_4$ was purchased from Aldrich and distilled by trap-to-trap distillation prior to use. ^nBuLi was titrated against diphenylacetic acid using the known literature procedure.[28] TMSCl and TMSI were purchased from Aldrich and used without further purification. $Zr(NMe_2)_4$, $ZrCl_4$ and Mg powder were purchased from Strem and used without further purification.

Synthesis of [OOO]K_2(THF)$_2$ (3.1). To an intimate mixture of **2.9** (0.5 g, 0.66 mmol) and 2.2 equivalents of KH (0.058 g, 1.45 mmol) was added THF (20 mL). The solution was allowed to stir overnight and the next day was filtered on a glass frit with celite. The THF was gently removed to obtain a white solid (0.55 g, 85%). Due to the moisture sensitivity of this compound, satisfactory EA could not be obtained. Integration of the ^1H NMR spectrum gives precisely 2 THF molecules for this salt.

^1H NMR (400 MHz, C_6D_6): δ 7.42 (d, J = 2.4 Hz, 2H), 7.32 (d, J = 2.4 Hz, 2H), 7.23 (s, 2H), 4.58 (d, J = 13.2 Hz, 2H), 3.71 (s, 3H), 3.42-3.35 (overlapping doublet and THF, 10H), 2.47-2.44 (m, 6H), 2.24-2.20 (m, 12H), 1.91 (bs, 12H), 1.52 (s, 18H), 1.39-1.36 (*THF*) (m, 8H), 0.94 (s, 9H).

^{13}C NMR (100 MHz, C_6D_6): δ 166.3, 153.9, 147.3, 138.3, 136.1, 130.7, 130.5, 126.6, 122.8, 122.0, 67.6, 62.0, 41.5, 38.2, 38.0, 34.18, 34.15, 33.7, 32.6, 31.1, 29.9, 25.6.

EI-MS (m/z): 832 $[M - 2{\bullet}THF]^+$, 817 $[M - 2{\bullet}THF - CH_3]^+$.

References begin on p.108

Synthesis of "Half-On" [OOO(H)]$TaCl_4$ (3.2). To an intimate mixture of $TaCl_5$ (0.227 g, 0.63 mmol) and **2.9** (0.500 g, 0.66 mmol) was added toluene (20 mL) all at once. The solution turned orange within a few minutes and was stirred overnight. The reaction mixture was taken to dryness to obtain an orange residue. Upon addition of minimal pentane, an orange precipitate formed that was collected on a frit, washed with minimal pentane and dried (0.540 g, 0.5 mmol, 79%).

^{1}H NMR (400 MHz, C_6D_6): δ 7.55 (d, J = 2.4 Hz, 1H), 7.49 (d, J = 2.4 Hz, 1H), 7.35 (d, J = 2.4 Hz, 1H), 7.14-7.12 (m, 2H), 6.94 (d, J = 2.4 Hz, 1H), 5.03 (*OH*) (s, 1H), 4.99 (d, ^2J = 13.6 Hz, 1H), 4.62 (d, ^2J = 18.0 Hz, 1H), 4.21 (s, 3H), 4.01 (d, ^2J = 18.0 Hz, 1H), 3.26 (d, ^2J = 13.6 Hz, 1H), 2.36 (bs, 6H), 2.11-2.07 (m, 9H), 1.94 (bs, 3H), 1.83-1.74 (m, 9H), 1.58-1.55 (m, 3H), 1.39 (s, 9H), 1.38 (s, 9H), 0.88 (s, 9H).

^{13}C NMR (100 MHz, C_6D_6): δ 157.6, 153.9, 151.7, 151.6, 149.1, 144.6, 143.0, 136.9, 135.2, 132.0, 130.9, 127.2, 126.1, 126.0 (2 overlapping carbons), 124.3, 123.7, 123.2, 73.3, 42.0, 41.1, 38.4, 37.6, 37.4, 36.8, 34.8, 34.6, 34.5, 33.3, 32.8, 31.9, 31.6, 30.8, 29.6, 29.3.

Anal. Calcd for $C_{53}H_{71}Cl_4O_3Ta$: C, 59.00; H, 6.63. Found: C, 59.24; H, 6.86.

EI-MS (m/z): 990 $[M - HCl - MeCl]^+$, 975 $[M - HCl - MeCl - CH_3]^+$

Synthesis of 3.3. $[NPN]^SK_2$ was synthesized *in situ* by adding THF (75 mL) to an intimate mixture of **2.2** (0.5 g, 0.92 mmol) and 2.05 equivalents of KH (0.076 g, 1.90 mmol). The mixture was allowed to stir for 3 hours. The THF was removed *in vacuo* and the orange residue was dissolved in toluene (30 mL). In a separate flask, $TaCl_5$ (0.331 g, 0.92 mmol) was mixed in 35 mL toluene. The $[NPN]^SK_2$ solution was added dropwise to this by cannula transfer. The pale yellow $TaCl_5$ solution immediately turned

References begin on p.108

very dark red. After mixing overnight, the solution was filtered on celite and the toluene removed *in vacuo*. Attempts to isolate a pure solid were generally unsuccessful. $^{31}P\{^1H\}$ and ^1H NMR spectra of the crude reaction mixture indicate one major product. Dissolving the crude residue in a pentane/hexanes mixture and cooling to -38C led to the formation of clear single crystals suitable for X-ray diffraction. The structure was solved and is shown in Figure 3.6. It also matches the crude NMR spectra as well as the mass spectral results.

^1H NMR (400 MHz, C_6D_6): δ 7.70-7.66 (m, 2H), 7.13-7.07 (m, 2H), 7.03-6.99 (m, 1H), 6.82 (bs, 1H), 6.78 (bs, 1H), 6.75 (bs, 1H), 6.71 (bs, 1H), 6.61-6.58 (m, 1H), 6.30 (d, J = 6.0 Hz, 1H), 5.89 (d, J = 6.0 Hz, 1H), 5.84 (d, J = 5.6 Hz, 1H), 2.53 (s, 3H), 2.27 (s, 3H), 2.14 (s, 3H), 2.11 (s, 3H), 2.06 (s, 3H), 1.47 (s, 3H).

$^{31}P\{^1H\}$ NMR (161 MHz, C_6D_6): δ 33.9.

EI-MS (m/z): 538 $[M]^+$, 523 $[M - CH_3]^+$.

Synthesis of $[NPN]^SZr(NMe_2)_2$ (3.4). $Zr(NMe_2)_4$ (0.989 g, 3.70 mmol) and **2.2** (2.00 g, 3.70 mmol) were mixed together and toluene (40 mL) was added to obtain a lemon yellow solution that was stirred for 1 hour. The reaction mixture was taken to dryness to obtain a yellow residue. Upon addition of minimal hexanes, a bright yellow precipitate formed that was collected on a frit and dried (2.11 g, 2.95 mmol, 80%). Slow cooling to -35°C of a concentrated Et_2O solution of the compound yielded single crystals suitable for X-ray crystallography.

^1H NMR (400 MHz, C_6D_6): δ 7.86-7.81 (m, 2H), 7.15-7.10 (m, 2H), 7.05-7.01 (m, 1H), 6.97 (d, J = 5.2 Hz, 2H), 6.89 (bs, 2H), 6.87 (bs, 2H), 5.92 (dd, $J_{H\text{-}H}$ = 5.2 Hz, $J_{P\text{-}H}$ = 4.0 Hz, 2H), 2.99 (s, 6H), 2.36 (s, 6H), 2.26 (s, 6H), 2.25 (s, 6H), 2.17 (s, 6H).

References begin on p.108

$^{31}P\{^1H\}$ NMR (161 MHz, C_6D_6): δ -41.4.

^{13}C NMR (100 MHz, C_6D_6): δ 168.6 (d, J = 138.8 Hz), 146.4 (d, J = 8.4 Hz), 135.31, 135.29, 134.9, 133.8, 133.7, 133.4, 131.9 (d, J = 53.2 Hz), 129.7, 129.2, 128.7 (d, J = 36.8 Hz), 120.1 (d, J = 41.6 Hz), 99.4 (d, J = 84.0 Hz), 43.0, 42.8 (d, J = 18.8 Hz), 20.9, 19.3, 19.2.

Satisfactory EA values for this compound could not be obtained due to persistent residual solvents.

EI-MS (m/z): 716 $[M]^+$, 672 $[M - NMe_2]^+$.

Synthesis of $[NPN]^SZrCl_2$ (3.5). To a stirred yellow toluene solution (85 mL) of **3.4** (2.55 g, 3.56 mmol) was added trimethylsilyl chloride (4.52 mL, 35.6 mmol) dropwise. The clear yellow solution was stirred for 5 hours. The reaction mixture was taken to dryness to obtain a yellow powder that was collected on a frit, washed with pentane (3 × 5 mL), and dried (2.0 g, 2.85 mmol, 80%). Slow evaporation of an Et_2O solution of the compound yielded single crystals suitable for X-ray crystallography.

^1H NMR (400 MHz, C_6D_6): δ 7.89-7.84 (m, 2H), 7.07-7.04 (m, 2H), 7.00-6.96 (m, 1H), 6.88 (bs, overlapping singlet and doublet, 4H), 6.74 (bs, 2H), 5.72 (dd, J_{H-H} = 5.2 Hz, J_{P-H} = 3.2 Hz, 2H), 2.46 (s, 6H), 2.36 (s, 6H), 2.08 (s, 6H).

$^{31}P\{^1H\}$ NMR (161 MHz, C_6D_6): δ -36.2

^{13}C NMR (100 MHz, C_6D_6): δ 166.6 (d, J = 145.2 Hz), 140.7 (d, J = 13.6 Hz), 137.6, 137.4, 136.4, 135.8, 131.6 (d, J = 53.2 Hz), 131.2, 130.7 (d, J = 8.8 Hz), 130.6, 130.5, 129.3 (d, J = 42.4 Hz), 118.5 (d, J = 46.0 Hz), 105.8 (d, J = 127.6 Hz), 21.0, 19.3, 19.1.

Anal. Calcd for $C_{32}H_{31}Cl_2N_2PS_2Zr$: C, 54.84; H, 4.46; N, 4.00. Found: C, 54.69; H, 4.65; N, 3.88.

References begin on p.108

EI-MS (m/z): 700 $[M]^+$.

Synthesis of $[NPN]^SZrI_2$ (3.6) from $[NPN]^SZr(NMe_2)_2$ (3.4). To a stirred yellow toluene solution (50 mL) of **3.4** (1.60 g, 2.23 mmol) was added trimethylsilyl iodide (3.18 mL, 22.3 mmol) dropwise. The solution rapidly turned orange and was stirred for 3 hours. The reaction mixture was taken to dryness to obtain an orange powder that was collected on a frit, washed with pentane (3 × 5 mL), and dried (1.61 g, 1.82 mmol, 82%). Slow evaporation of an Et_2O solution of the compound yielded single crystals suitable for X-ray crystallography.

Synthesis of $[NPN]^SZrI_2$ (3.6) from $[NPN]^SZrCl_2$ (3.5). To a stirred yellow toluene solution (50 mL) of **3.5** (0.9 g, 1.28 mmol) was added trimethylsilyl iodide (1.83 mL, 12.8 mmol) dropwise. The solution turned orange and was stirred overnight. The reaction mixture was taken to dryness to obtain an orange powder that was collected on a frit, washed with pentane (3 × 5 mL), and dried (1.00 g, 1.13 mmol, 88%).

Synthesis of $[NPN]^SZrI_2$ (3.6) from $[NPN]^SH_2$ (2.2) and $Zr(NMe_2)_4$ – One-pot synthesis. $Zr(NMe_2)_4$ (0.495 g, 1.85 mmol) and **2.2** (1.00 g, 1.85 mmol) were mixed together and toluene (40 mL) was added to obtain a lemon yellow solution that was stirred for 1 hour. Trimethylsilyl iodide (2.63 mL, 18.5 mmol) was added dropwise to the yellow solution. The solution rapidly turned orange and was stirred for 3 hours. The reaction mixture was taken to dryness to obtain an orange powder that was collected on a frit with celite. The solids were washed on the celite with pentane (3 × 10 mL). The product was then extracted from the celite by washing it with excess toluene into an empty round bottom. Removal of the toluene *in vacuo* produced 1.20 g (1.36 mmol, 73%) of product.

References begin on p.108

^{1}H NMR (400 MHz, C_6D_6): δ 7.81-7.76 (m, 2H), 7.10-7.05 (m, 2H), 7.02-6.98 (m, 1H), 6.85 (bs, overlapping singlet and doublet, 4H), 6.78 (bs, 2H), 5.69 (dd, J_{H-H} = 5.2 Hz, J_{P-H} = 3.6 Hz, 2H), 2.60 (s, 6H), 2.25 (s, 6H), 2.09 (s, 6H).

^{31}P{^{1}H} NMR (161 MHz, C_6D_6): δ -35.3

^{13}C NMR (100 MHz, C_6D_6): δ 167.0 (d, J = 144.4 Hz), 138.9 (d, J = 14.0 Hz), 138.6, 137.9, 136.9, 136.6, 132.0, 131.6 (d, J = 48.0 Hz), 130.95, 130.92, 130.8 (d, J = 9.6 Hz), 129.1 (d, J = 44.4 Hz), 118.3 (d, J = 46.8 Hz), 106.6 (d, J = 118.4 Hz), 21.2, 20.8, 20.4.

Anal. Calcd for $C_{32}H_{31}I_2N_2PS_2Zr$: C, 43.49; H, 3.54; N, 3.17. Found: C, 43.39; H, 3.72; N, 3.08.

EI-MS (m/z): 882 $[M]^+$, 755 $[M - I]^+$.

3.4.3 General Procedure for the Reduction Reactions

The general procedure is given for the reduction of $[NPN]^SZrI_2$ using 2.2 equivalents of KC_8 in Et_2O. All other reduction reactions described in this chapter follow a similar protocol unless specified below. $[NPN]^SZrI_2$ (0.362 g, 0.41 mmol) and KC_8 (0.122 g, 0.90 mmol) were mixed together in a 400-mL thick-walled Kontes-sealed reaction vessel (bomb) and shaken to mix thoroughly. Et_2O (10 mL) was vacuum-transferred to the mixture at -196°C. The vessel was filled with N_2 gas at -196°C, sealed, warmed to -78°C using a dry ice/acetone bath and kept at this temperature for 4-5 hours. Once the mixture had melted, it was stirred vigorously. The bomb was kept behind a blast shield at all times. After the 4-5 hours at -78°C, the bomb was allowed to warm to room temperature gradually overnight in the bath. The next day, the bomb was depressurized by first cooling to -196°C, opening the seal to N_2 and allowing the bomb to warm to room temperature.

References begin on p.108

Reduction with Mg powder – Synthesis of $[NPN]^{S}ZrI(OBu)$ (3.7). This reduction can either be performed using the standard protocol or can be done at room temperature under 1 atmosphere of N_2. THF (10 mL) was added to a mixture of $[NPN]^{S}ZrI_2$ (**3.6**) (0.200 g, 0.23 mmol) and Mg powder (0.055 g, 2.3 mmol). The solution gradually turned red/pale brown overnight. The solution was brought to dryness and then filtered on a glass pad using THF. The THF is then removed and the sample was analyzed by $^{31}P\{^1H\}$, ^1H NMR and EI-MS.

^1H NMR (400 MHz, C_6D_6): δ 8.32-8.27 (m, 2H), 7.21-7.16 (m, 2H), 7.06-7.02 (m, 1H), 6.94 (d, J = 5.2 Hz, 2H), 6.84 (bs, 4H), 5.79 (dd, J_{H-H} = 5.2 Hz, J_{P-H} = 3.6 Hz, 2H), 3.44 (t, J = 7.2 Hz, 2H), 2.48 (s, 6H), 2.18 (s, 6H), 2.09 (s, 6H), 1.27-1.18 (m, 2H), 1.04-0.98 (m, 2H), 0.72 (t, J = 7.2 Hz, 3H).

$^{31}P\{^1H\}$ NMR (161 MHz, C_6D_6): δ -30.4

EI-MS (m/z): 828 $[M]^+$, 701 $[M - I]^+$.

Reduction of $[NPN]^{S}ZrI_2$ with KC_8 in Et_2O – Possible formation of 3.8. The procedure follows the general procedure given. The blue-green solution was filtered on a glass frit to remove all residual graphite. The solution was concentrated and excess PMe_2Ph (0.2 mL, 1.4 mmol) was added to the solution and stirred for one hour. The Et_2O was removed *in vacuo* and pentane (10 mL) was added. The mixture was stirred for 30 minutes and was then filtered on a glass frit. The green solids were collected, washed with minimal pentane and hexanes and dried.

^1H NMR (400 MHz, C_6D_6): δ 8.08-8.03 (m, 2H), 7.96-7.91 (m, 2H), 7.37-6.65 (overlapping aromatic signals, 23H), 5.99 (dd, J_{H-H} = 5.2 Hz, J_{P-H} = 3.6 Hz, 2H), 5.58 (dd,

References begin on p.108

J_{H-H} = 5.2 Hz, J_{P-H} = 3.6 Hz, 2H), 2.31 (s, 6H), 2.18 (s, 6H), 2.15 (s, 6H), 2.00 (s, 6H), 1.72 (s, 6H), 1.56 (s, 6H), 0.78 (d, J_{P-H} = 6.0 Hz, 6H).

$^{31}P\{^{1}H\}$ NMR (161 MHz, C_6D_6): δ -19.1 (d, J_{P-P} = 105.4 Hz), -23.7, -24.7 (d, J_{P-P} = 105.4 Hz).

References begin on p.109

3.5 References

[1] Vidyaratne, I.; Crewdson, P.; Lefebvre, E.; Gambarotta, S. *Inorg. Chem.* **2007**, *46*, 8836.

[1] Laplaza, C. E.; Johnson, M. J. A.; Peters, J. C.; Odom, A. L.; Kim, E.; Cummins, C. C.; George, G. N.; Pickering, I. J. *J. Am. Chem. Soc.* **1996**, *118*, 8623.

[1] Hirotsu, M.; Fontaine, P. P.; Zavalij, P. Y.; Sita, L. R. *J. Am. Chem. Soc.* **2007**, *129*, 12690.

[1] Morello, L.; Yu, P.; Carmichael, C. D.; Patrick, B. O.; Fryzuk, M. D. *J. Am. Chem. Soc.* **2005**, *127*, 12796.

[1] Fryzuk, M. D.; MacKay, B. A.; Johnson, S. A.; Patrick, B. O. *Angew. Chem. Int. Ed.* **2002**, *41*, 3709.

[1] MacLachlan, E. A.; Fryzuk, M. D. *Organometallics*, **2005**, *24*, 1112.

[1] MacLachlan, E. A.; Hess, F. M.; Patrick, B. O.; Fryzuk, M. D. *J. Am. Chem. Soc.* **2007**, *129*, 10895.

[1] Kawaguchi, H.; Matsuo, T. *Angew. Chem. Int. Ed.* **2002**, *41*, 2792.

[1] Carmichael, C. D. *Donor Atom Substitutions in Amidophosphine Ligands: Early Transition Metal Complexes of Arsine and Aryloxide Containing Ligands*; PhD thesis, University of British Columbia: Vancouver, 2005.

[1] Matsuo, T.; Kawaguchi, H. *Inorg. Chem.* **2007**, *46*, 8426.

[1] Matsuo, T.; Kawaguchi, H. *Chem. Lett.* **2004**, *33*, 640.

[1] Matsuo, T.; Kawaguchi, H. *Inorg. Chem.* **2002**, *41*, 6090.

[1] Castellano, B.; Solari, E.; Floriani, C.; Re, N.; Chiesi-Villa, A.; Rizzoli, C. *Chem. Eur. J.* **1999**, *5*, 722.

[1] Johnson, S. A. *Ligand Design and the Synthesis of Reactive Organometallic Complexes of Tantalum for Dinitrogen Activation*; PhD thesis, University of British Columbia: Vancouver, 2000.

[1] Hess, F. M.; Fryzuk, M. D. *unpublished results.*

[1] Freundlich, J. S.; Schrock, R. R.; Davis, W. M. *Organometallics*. **1996**, *15*, 2777.

[1] Skinner, M. E. G.; Li, Y.; Mountford, P. *Inorg. Chem.* **2002**, *41*, 1110.

[1] Chien, P-S; Liang, L-C. *Inorg. Chem.* **2005**, *44*, 5147.

[1] King, W. A.; Di Bella, S.; Gulino, A.; Lanza, G.; Fragalà, I. L.; Stern, C. L.; Marks, T. J. *J. Am. Chem. Soc.* **1999**, *121*, 355.

[1] Vanysek, P. In *CRC Handbook of Chemistry and Physics, 87 Edition*; Lide, D. R., Ed.; CRC Press: Boca Raton, FL, 2006.

[1] Fryzuk, M. D.; Corkin, J. R.; Patrick, B. O. *Can. J. Chem.* **2003**, *81*, 1376.

[1] Sobota, P.; Janas, Z. *J. Organomet. Chem.* **1983**, *243*, 35.

[1] Miller, R. L.; Toreki, R.; LaPointe, R. E.; Wolczanski, P. T.; Van Duyne, G. D.; Roe, D. C. *J. Am. Chem. Soc.* **1993**, *115*, 5570.

[1] Spencer, L. P. *Early Transition Metal Complexes Supported by Amidophosphine and Amidocarbene Ligands*; PhD thesis, University of British Columbia: Vancouver, 2006.

[1] Manzer, L. E. *Inorg. Synth.* **1982**, *21*, 135.

[1] Bergbreiter, D. E.; Killough, J. M. *J. Am. Chem. Soc.* **1978**, *100*, 2126.

[1] Adam, W.; Arce, J. *J. Org. Chem.* **1972**, *37*, 507.

[1] Kofron, W. G.; Baclawski, L. M. *J. Org. Chem.* **1976**, *41*, 1879.

CHAPTER 4

Thesis Summary and Future Work

4.1 Thesis Summary

This thesis describes the synthesis of a new diamidophosphine ligand, $[NPN]^S$, as well as a new dianionic linear-linked aryloxide ligand, [OOO]. The synthesis of the $[NPN]^SH_2$ proligand led to some surprising results. In fact, as shown in the retrosynthetic analysis in Scheme 2.1, the phosphine coupling reaction was expected to yield the phosphine in the 4- positions of the thiophene rings. However, the phosphine actually bonds to the 2- positions of the rings. Reactions using different ratios of ^{t}BuLi along with either $PhPCl_2$ or CF_3COOD as quenching agents were performed in order to obtain some insight into the reaction mechanism. The results suggest that lithium-bromine exchange is the predominant reaction, but is in competition with the deprotonation of the N-H and/or the 2- position protons. As described in Chapter 2, the 4- position C-Li bond does not seem to react favourably with $PhPCl_2$ to produce the expected regiochemistry in the product. Inter- or intramolecular proton transfer to the 4- position, along with competitive deprotonation reactions, are believed to promote the formation of the required 2,N-dilithiated species which ultimately reacts predominantly with $PhPCl_2$ to form the $[NPN]^SH_2$ proligand.

The $[NPN]^S$ ligand was synthesized as a variation to the recently synthesized $[NPN]^*$ ligand in our group.[1] Both the $[NPN]^S$ and $[NPN]^*$ ligands have bridging aryl rings between the phosphine and amide donors; however, the $[NPN]^S$ ligand was synthesized to monitor the effects a five-membered aryl linker would have on the

References begin on p.116

activation of N_2 compared to the six-membered $[NPN]^*$ version. Several Zr species bearing the $[NPN]^S$ ligand were synthesized. Reduction of the $[NPN]^SZrI_2$ complex under several different reaction conditions was investigated. Whereas reduction using the same standard conditions (KC_8 reducing agent and THF as solvent) as with the $[NPN]^*ZrCl_2$ complex[2] failed to produce an N_2 complex, the reduction of $[NPN]^SZrI_2$ using KC_8 and Et_2O as solvent produced very promising signs of an N_2 complex. Although this could point to a difference in reactivity between both complexes, this cannot be ascertained for certain at this point since the reduction of $[NPN]^*ZrCl_2$ using Et_2O as solvent has yet to be attempted. Indeed, reductions performed in Et_2O are rare since THF and toluene are the typical solvent mediums used for N_2 activation.[2,3,4,5]

Attempts to synthesize a $Ta[NPN]^S$ complex failed; however, the formation of a new major product was observed when the $[NPN]^SK_2$ salt reacted *in situ* with an equimolar amount of $TaCl_5$. This product was crystallographically characterized and was shown to have no Ta in its structure. Instead, the K salt was oxidized, likely by Ta, and underwent a rearrangement to form a seven-membered ring containing a P-N bond. Similar reactivity was observed when I_2 was used as the oxidant.

Finally, the synthesis of the new [OOO] ligand was undertaken as an extension of the work done with early metals bearing linear-linked aryloxide ligands.[6] Previous work by other groups has shown that some of these complexes can activate N_2.[5] Attempts to synthesize Ti and Zr complexes with the [OOO] ligand failed; however, a "half-on" $[OOO(H)]TaCl_4$ complex, containing a pendant phenol, could be successfully synthesized. Attempts to "close" this system by coordinating the pendant OH group and

References begin on p.116

forming a [OOO]$TaCl_3$ species failed. No attempts to reduce this species to form an N_2 complex were undertaken.

4.2 Future Work

In section 3.2.5, convincing evidence emerged to suggest that a Zr_2-N_2 complex had been formed from the reduction of $[NPN]^S ZrI_2$ using KC_8 as reducing agent in Et_2O. Preliminary results show that the PMe_2Ph adduct seems to be formed analogous to the established $\{[NPN]^* Zr(PMe_2Ph)\}(\mu\text{-}\eta^2\text{:}\eta^2\text{-}N_2)\{Zr[NPN]^*\}$ species. Efforts are currently underway to confirm this structure. The $([NPN]^* Zr)_2$-N_2 complexes and several of its adducts have been shown to react with H_2 or other reagents to produce new N-H[2] or N-E[7] bonds (E = Si, C). These results are undoubtedly very important considering one of the fundamental goals in N_2 activation chemistry is to use N_2 as a feedstock for the synthesis of organonitrogen molecules. As described in Chapter 1, the formation of new N-H bonds also carries much importance in the field of N_2 activation. Thus, the proposed new N_2 complex containing the $[NPN]^S$ ligand will be reacted with H_2 and other reagents in order to establish whether the reactivity of this complex is different from the $([NPN]^* Zr)_2$-N_2 complexes.

As hypothesized in the introductory section of Chapter 3, either the N-M or P-M bonds were expected to elongate by changing the aryl linker of the NPN moiety from a six-membered to a five-membered ring. In fact with Zr complexes, it was shown that the Zr-P bond actually became longer when changing the NPN ligand from $[NPN]^*$ to $[NPN]^S$, whereas the Zr-N bond lengths did not change noticeably. Although yet unclear, it is possible that this subtle bond length difference plays a significant role in the

References begin on p.116

noticeable difference in reactivity observed when reducing the $[NPN]^{S}ZrX_2$ (X = Cl or I) species compared to the $[NPN]^{*}ZrCl_2$ complex.

A longer, rigid 4-bond aryl spacer between the amide and phosphine donors would be expected to elongate the P-M bond length even more. This could be done using the commercially available 2,5-dibromothiophene and mesitylaniline in a synthesis outlined in Figure 4.1, similar to the synthesis of the $[NPN]^{S}H_2$ (**2.2**) proligand. The effects of having a potentially very long P-M bond in a metal complex with this new ligand could then be monitored, particularly with respect to N_2 activation.

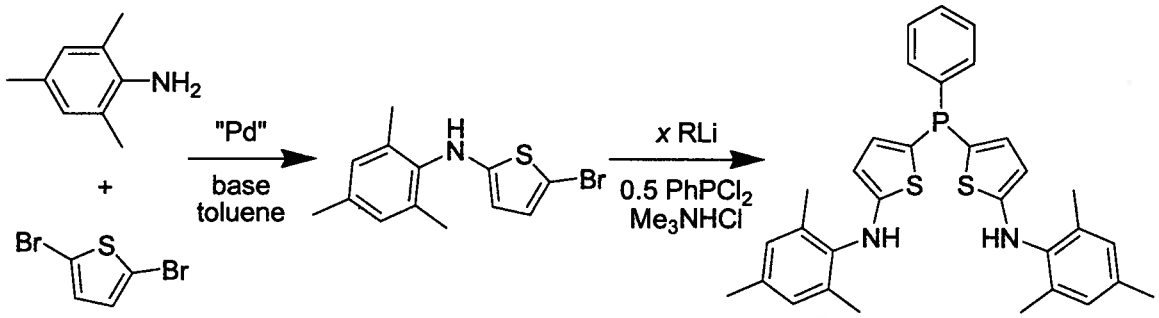

Figure 4.1. Proposed synthesis for a new $[NPN]^{S}$-type ligand with a 4-bond, rigid aryl spacer. The Pd catalyst, base and equivalents and nature of RLi remain vague as optimal conditions for this synthesis would have to be established in more detail.

The $[OOO]H_2$ proligand has proven difficult to coordinate to group 4 metals such as Zr and Ti; however, some success was obtained with Ta. As described in Chapter 3, the ^{1}H NMR spectrum of the "half-on" $[OOO(H)]TaCl_4$ shows 4 distinct methylene doublet signals as well as 3 separate ^{t}Bu signals characteristic of a locked S-conformation for this type of ligand. In comparison, the $[OOO]K_2(THF)_2$ (**3.1**) salt displays only 2 separate methylene doublets and 2 ^{t}Bu signals (in a 2:1 ratio). This therefore suggests that the K salt is locked in the more symmetric U-conformation (see Figure 3.4).

References begin on p.116

A comparison of the ionic radii of both K^+ and Ta^{5+} reveals that K^+ is much larger. In fact, with a coordination number (CN) of 6 for both K^+ and Ta^{5+}, the ionic radii are 1.38Å and 0.64Å respectively (K^+ with a CN of 4 has an ionic radius of 1.37Å).[8] This information could suggest that the $[OOO]H_2$ proligand requires a large metal centre to be bound in the U-conformation.

Our laboratory has recently begun to explore the chemistry of U for N_2 activation. U(III) species are attractive for N_2 chemistry since they contain 3 possible electrons (from U(III) to U(VI)) which can be used to reduce N_2. Some progress has recently been made using U(III) complexes to activate N_2.[9] U is attractive for the [OOO] ligand since it is much larger than Ta and other early transition metals. In fact, U^{3+} with a CN of 6 has an ionic radius of 1.03Å.[8] U(III) complexes of [OOO] are an interesting target since the chemistry of linear-linked aryloxide ligands with U is very limited and mainly focuses on higher valent U(VI) species.[6]

Several U(III) starting materials can be readily synthesized such as $U(N(SiMe_3)_2)_3$,[10] UI_3[9] and $UI_3(THF)_4$.[11] Thus, preliminary reactions using either the $[OOO]K_2(THF)_2$ (**3.1**) salt or the $[OOO]H_2$ (**2.9**) proligand with some of these starting materials are currently underway to determine whether U(III) complexes can be formed. However, it should be noted that uranium's high Lewis acidity may cause many unwanted reactions such as removal of the methyl from the methoxy group. This was shown to happen for the demethylation of calixarenes in the presence of highly Lewis acidic metals as previously discussed in section 3.2.2. Finally, forming a U(III) complex with [OOO] may also prove problematic considering U tends to be in either a higher oxidation state or form *ate* complexes with oxide ligands.[12,13]

References begin on p.116

4.3 References

[1] MacLachlan, E. A.; Fryzuk, M. D. *Organometallics*, **2005**, *24*, 1112.

[2] MacLachlan, E. A.; Hess, F. M.; Patrick, B. O.; Fryzuk, M. D. *J. Am. Chem. Soc.* **2007**, *129*, 10895.

[3] Fryzuk, M. D.; Love, J. B.; Rettig, S. J.; Young, V. G. *Science*. **1997**, *275*, 1445.

[4] Bernskoetter, W. H.; Lobkovsky, E.; Chirik, P. J. *J. Am. Chem. Soc.* **2005**, *127*, 14051.

[5] Kawaguchi, H.; Matsuo, T. *Angew. Chem. Int. Ed.* **2002**, *41*, 2792.

[6] Matsuo, T.; Kawaguchi, H. *Chem. Lett.* **2004**, *33*, 640.

[7] MacLachlan, E. A. *Group 4 Complexes of an Arene-Bridged Diamidophosphine Ligand for Nitrogen Activation*; PhD thesis, University of British Columbia: Vancouver, 2006.

[8] *CRC Handbook of Chemistry and Physics, 87 Edition*; Lide, D. R., Ed.; CRC Press: Boca Raton, FL, 2006.

[9] Cloke, F. G. N.; Hitchcock, P. B. *J. Am. Chem. Soc.* **2002**, *124*, 9352.

[10] Andersen, R. A. *Inorg. Chem.* **1979**, *18*, 1507.

[11] Clark, D. L.; Sattelberger, A. P.; Bott, S. G.; Vrtis, R. N. *Inorg. Chem.* **1989**, *28*, 1771.

[12] Kaltsoyannis, N.; Scott, P. *The f elements*; Oxford University Press: New York, 1999.

[13] Cotton, S. *Lanthanide and Actinide Chemistry*; John Wiley & Sons Ltd: West Sussex, 2006.

References begin on p.116

APPENDIX

X-ray Crystal Structure Data and Analysis

A.1 X-ray Crystal Structure Data

Table A.1. Crystal Data and Structure Refinement for **2.1** and dibromo-[NPN]^{S}H$_2$ (**2.4**).

compound	**2.1**	**2.4**
formula	$C_{13}H_{14}BrNS$	$C_{32}H_{31}Br_2N_2PS_2$
FW	296.22	698.50
T, K	173	173
cryst. sys.	orthorhombic	monoclinic
space group	Pbcn	P2/c
a, Å	19.1120(16)	22.805(2)
b, Å	7.1497(6)	7.2671(7)
c, Å	18.9027(15)	20.1594(19)
α, °	90	90
β, °	90	115.710(4)
γ, °	90	90
V, Å^3	2583.0(4)	3010.2(5)
Z	8	4
ρ_{calc}, g/cm^3	1.523	1.541
abs. coeff., mm^{-1}	3.317	2.910
F(000)	1200	1416
cryst. size, mm	0.38 x 0.22 x 0.18	0.5 x 0.18 x 0.06
radiation	Mo	Mo
θ range, °	2.13 – 27.53	2.02 – 22.72
total no. of reflns	26235	14780
no. of unique reflns	2976	3982
completeness to	θ = 27.53°, 99.9%	θ = 22.72°, 98.5%
max and min. trans.	0.5504 and 0.4049	0.8398 and 0.6255
gof	1.009	1.037
final R indices [I > 2sigma(I)]	R1 = 0.0265, wR2 = 0.0603	R1 = 0.0243, wR2 = 0.0561
R indices (all data)	R1 = 0.0401, wR2 = 0.0655	R1 = 0.0322, wR2 = 0.0588
largest diff. peak and hole, e/Å^3	0.350 and -0.285	0.247 and -0.277

References begin on p.121

Table A.2. Crystal Data and Structure Refinement for **3.3** and $[NPN]^{S}Zr(NMe_2)_2$ (**3.4**) (co-crystallized with ½ Et_2O)

compound	**3.3**	**3.4**
formula	$C_{32}H_{31}N_2PS_2$	$C_{38}H_{48}N_4O_{0.50}PS_2Zr$
FW	538.68	755.11
T, K	173	173
cryst. sys.	monoclinic	monoclinic
space group	P2(1)/n	C2/c
a, Å	14.8600(6)	34.159(4)
b, Å	11.3228(5)	14.2705(16)
c, Å	16.7549(6)	15.7812(18)
α, °	90	90
β, °	100.159(2)	101.325(5)
γ, °	90	90
V, $Å^3$	2774.93(19)	7543.0(14)
Z	4	8
ρ_{calc}, g/cm^3	1.289	1.330
abs. coeff., mm^{-1}	0.274	0.478
F(000)	1136	3160
cryst. size, mm	0.28 x 0.08 x 0.08	0.38 x 0.21 x 0.085
radiation	Mo	Mo
θ range, °	1.69 – 25.05	1.55 – 27.71
total no. of reflns	17740	37771
no. of unique reflns	4915	8721
completeness to	θ = 25.05°, 100.0%	θ = 27.71°, 98.4%
max and min. trans.	0.9843 and 0.7306	0.96018 and 0.79899
gof	1.001	1.017
final R indices [I > 2sigma(I)]	R1 = 0.0373, wR2 = 0.0807	R1 = 0.0350, wR2 = 0.0713
R indices (all data)	R1 = 0.0632, wR2 = 0.0904	R1 = 0.0608, wR2 = 0.0804
largest diff. peak and hole, e/$Å^3$	0.252 and -0.256	0.467 and -0.466

References begin on p.121

Table A.3. Crystal Data and Structure Refinement for $[NPN]^{S}ZrCl_2$ (**3.5**) and $[NPN]^{S}ZrI_2$ (**3.6**).

compound	**3.5**	**3.6**
formula	$C_{32}H_{31}Cl_2N_2PS_2Zr$	$C_{32}H_{31}I_2N_2PS_2Zr$
FW	700.80	883.70
T, K	173	173
cryst. sys.	monoclinic	monoclinic
space group	P2(1)/n	P2(1)/c
a, Å	8.578(5)	9.425(5)
b, Å	19.944(5)	19.464(5)
c, Å	18.983(5)	18.223(5)
α, °	90	90
β, °	92.685(5)	98.305(5)
γ, °	90	90
V, $Å^3$	3244(2)	3308(2)
Z	4	4
ρ_{calc}, g/cm^3	1.435	1.774
abs. coeff., mm^{-1}	0.706	2.398
F(000)	1432	1720
cryst. size, mm	0.5 x 0.11 x 0.08	0.31 x 0.24 x 0.08
radiation	Mo	Mo
θ range, °	1.48 – 25.70	2.09 – 27.84
total no. of reflns	28937	31906
no. of unique reflns	6164	7697
completeness to	θ = 25.70°, 99.8%	θ = 27.84°, 97.9%
max and min. trans.	0.9451 and 0.7837	0.8254 and 0.4884
gof	0.979	0.955
final R indices [I > 2sigma(I)]	R1 = 0.0403, wR2 = 0.0726	R1 = 0.0440, wR2 = 0.0689
R indices (all data)	R1 = 0.0919, wR2 = 0.0880	R1 = 0.1121, wR2 = 0.0861
largest diff. peak and hole, $e/Å^3$	0.481 and -0.395	0.665 and -0.673

References begin on p.121

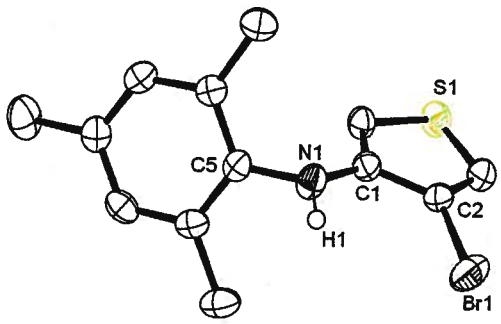

Figure A.1. ORTEP drawing of the solid-state molecular structure of **2.1** (ellipsoids drawn at the 50% probability level). All hydrogen atoms, except the N-H bonds, have been omitted for clarity. Selected bond lengths (Å) and angles(°): C5-N1 1.425(2), N1-H1 0.76(2), N1-C1 1.385(2), C2-Br1 1.883(2), C1-N1-C5 120.19(16), C1-N1-H1 114.7(18), C5-N1-H1, 113.8(18), C1-C2-Br1 121.89(15).

A.2 X-ray Crystal Structure Analysis

Selected crystals were coated in oil, mounted on a glass fiber, and placed under an N_2 stream. Measurements for compounds were made on a Bruker X8 Apex II diffractometer or a Rigaku AFC-7 diffractometer, both with graphite-monochromated Mo Kα radiation (λ = 0.71073 Å). The data were collected at a temperature of 173 ± 1 K. Data were collected and integrated using the Bruker SAINT software package.[1] Data were corrected for absorption effects using the multi-scan technique (SADABS)[2] and for Lorentz and polarization effects. Neutral atom scattering factors were taken from Cromer and Waber.[3] Anomalous dispersion effects were included in F_{calc};[4] the values for $\Delta f''$ and $\Delta f'''$ were those of Creagh and McAuley.[5] The values for the mass attenuation coefficients are those of Creagh and Hubbell.[6] All refinements were performed using the SHELXTL crystallographic software package of Bruker-AXS. The structure was solved by direct methods. All non-hydrogen atoms were refined anisotropically using SHELXL-

References begin on p.121

97. Except where noted, hydrogen atoms were included in fixed positions. Structures were solved and refined using the WinGX software package version 1.70.01.

A.3 References

[1] SAINT. Version 6.02. Bruker AXS Inc., Madison, Wisconsin, USA. (1999).

[2] SADABS. Bruker Nonius area detector scaling and absorption correction - V2.05, Bruker AXS Inc., Madison, Wisconsin, USA.

[3] Cromer, D. T.; Waber, J. T. *International Tables for X-ray Crystallography, Vol. IV*; The Kynoch Press: Birmingham, England, 1974, Table 2.2 A.

[4] Ibers, J. A.; Hamilton, W. C. *Acta Crystallogr.* **1964**, *17*, 781.

[5] Creagh, D. C.; McAuley, W.J. *International Tables for Crystallography, Vol C*; Wilson, A. J. C., ed., Kluwer Academic Publishers: Boston, 1992, Table 4.2.6.8, pp. 219-222.

[6] Creagh, D. C.; Hubbell, J.H. *International Tables for Crystallography, Vol C*; Wilson, A.J.C, ed., Kluwer Academic Publishers: Boston, 1992, Table 4.2.4.3, pp. 200-206.

References begin on p.121